NORSAR Scientific Report No. 2-2006

Semiannual Technical Summary

1 January - 30 June 2006

Frode Ringdal (ed.)

Kjeller, August 2006

REPORT DOCUMENTATION PAGE

Form Approved
OMB No. 0704-0188

1. REPORT DATE *(DD-MM-YYYY)*	2. REPORT TYPE	3. DATES COVERED *(From - To)*
15-08-2006	Semiannual Technical Summary	1 January - 30 June 2006

4. TITLE AND SUBTITLE
Semiannual Technical Summary, 1 January - 30 June 2006

5a. CONTRACT NUMBER
F08650-01-C-0055 & FA2521-06-C-8003

5b. GRANT NUMBER

5c. PROGRAM ELEMENT NUMBER
NDC Support / R&D

6. AUTHOR(S)
Frode Ringdal (Ed.)

5d. PROJECT NUMBER
T/0155 & T/6110

5e. TASK NUMBER
SOW Task 4.2 & 4.3

5f. WORK UNIT NUMBER
CDRL sequence nos. A001-A004

7. PERFORMING ORGANIZATION NAME(S) AND ADDRESS(ES)
Stiftelsen NORSAR
Post Box 53
NO-2027 Kjeller
Norway

8. PERFORMING ORGANIZATION REPORT NUMBER
Scientific Report No. 2-2006

9. SPONSORING/MONITORING AGENCY NAME(S) AND ADDRESS(ES)
AFTAC/TTS, 1030 South Highway A1A MS 1000, Patrick AFB, FL 32925-3002

Army Space and Missile Defense Command , 1515 Wilson Blvd., Suite 720
Arlington, VA 22209

10. SPONSOR/MONITOR'S ACRONYM(S)
AFTAC/TTS & USASMDC

11. SPONSOR/MONITOR'S REPORT NUMBER(S)

12. DISTRIBUTION/AVAILABILITY STATEMENT
Approved for public release; distribution unlimited

13. SUPPLEMENTARY NOTES

14. ABSTRACT

This report describes the activities carried out at NORSAR under Contract No. F08650-01-C-0055 (T/0155) during 1 January - 28 February and Contract No. FA2521-06-C-8003 (T/6110) for the period 1 March- 30 June 2006. Descriptions of relevant research activities funded through other contracts are also included. In addition, this report provides summary information on operation and maintenance (O&M) activities at the Norwegian National Data Center (NDC) during the same period. Research activities described in this report are largely funded by the United States Government, and the United States also covers the cost of transmission of selected data to the US NDC.

(cont.)

15. SUBJECT TERMS
NORSAR, Norwegian Seismic Array

16. SECURITY CLASSIFICATION OF:			17. LIMITATION OF ABSTRACT	18. NUMBER OF PAGES	19a. NAME OF RESPONSIBLE PERSON
a. REPORT	b. ABSTRACT	c. THIS PAGE			SSgt Joshua W. Bricker, AFTAC/TTS
U	U	U	SAR	74	19b. TELEPHONE NUMBER *(Include area code)* (321) 494-9471

Reset

Standard Form 298 (Rev. 8/98)
Prescribed by ANSI Std. Z39.18

Abstract (cont.)

The O&M activities, including operation of transmission links within Norway and to Vienna, Austria are being funded jointly by the CTBTO/PTS and the Norwegian Government, with the understanding that the funding of O&M activities for primary stations in the International Monitoring System (IMS) will gradually be transferred to the CTBTO/PTS. The O&M statistics presented in this report are included for the purpose of completeness, and in order to maintain consistency with earlier reporting practice.

The NOA Detection Processing system has been operated throughout the period with an uptime of 100%. A total of 2,306 seismic events have been reported in the NOA monthly seismic bulletin during the reporting period. On-line detection processing and data recording at the NDC of data from ARCES, FINES, SPITS and HFS data have been conducted throughout the period. Processing statistics for the arrays for the reporting period are given.

A summary of the activities at the Norwegian NDC and relating to field installations during the reporting period is provided in Section 4. Norway is now contributing primary station data from two seismic arrays: NOA (PS27) and ARCES (PS28), one auxiliary seismic array SPITS (AS72), and one auxiliary three-component station (AS73). These data are being provided to the IDC via the global communications infrastructure (GCI). Continuous data from the three arrays are in addition being transmitted to the US NDC. The performance of the data transmission to the US NDC has been satisfactory during the reporting period.

Summaries of four scientific and technical contributions are presented in Chapter 6 of this report.

Section 6.1 is entitled “Processing of low-magnitude seismic events near Novaya Zemlya”. It contains an analysis of recordings from the SPITS array for three seismic events near Novaya Zemlya during March 2006. The increase in sampling rate from 40 Hz to 80 Hz for the upgraded SPITS array has for the first time given an opportunity to analyze the high-frequency wave propagation across the Barents Sea. The best filter band for detection appears to be either 5-10 Hz or 10-20 Hz. However, the most remarkable feature is the strong SNR observed even at the highest frequency filter band analyzed (20-36 Hz). The strong energy at these high frequencies is especially remarkable taking into account that the epicentral distance being more than 1000 km. While such a frequency band would not be used for detection purposes, the high frequency data could be very important for signal characterization. We also discuss the improvement in Sn-phase detection at SPITS resulting from the inclusion of five new three-component seismometers in the upgraded array.

Section 6.2 is entitled “Infrasound observations of two recent meteor impacts in Norway”. During the summer of 2006, a large number of people observed sound and light phenomena from two meteor impacts in Norway. The first event was on 7 June at about 00:07 GMT in northern Norway (Finnmark). The explosion was recorded on several seismic and infrasonic stations in northern Scandinavia. By combining all observations and using them as input to a traditional event location program (HYPOSAT) a presumed location of the meteor explosion could be determined. To locate the event, we used two different procedures, one based on backazimuths only and the second using backazimuths and arrival times. The two locations turned out to be consistent within less than 5 km.

The second event was on 14 July at about 08:18 GMT in southern Norway (Oslo Fjord area). The explosion of this meteor was heard in Rygge and at least 2 fragments were found on the

ground in the Rygge - Moss area. On the traces of the short period sensors of the large NORSAR array, a signal was detected crossing the array from south to north with sound velocity. We were able to read onset times on short term average (STA) traces for 28 of the NORSAR seismometers, and used these times as input parameters for HYPOSAT. Although the resulting event location estimate has a fairly large error ellipse, it is sufficiently precise to be confidently connected with the observed meteor explosion and the area where its fragments were found.

Section 6.3 is entitled "Improvements to SPITS regional S-phase detection; coherent beamforming of rotated horizontal components". As mentioned earlier, the number of three-component sites at the SPITS array was increased from one to six, during the recent refurbishment of the SPITS array. This new array configuration opened for the possibility to redefine and tune the automatic data processing recipes of the SPITS array, including redefinition of the detection beam deployment, procedures for fk-analysis and the rules for fully automatic single array event location. This contribution describes the details of the new beam deployment, and presents some examples of the improvements achieved.

For a test period of 58 full days, we have run automatic multi-array phase association and event location using the Generalized Beamforming (GBF) approach. Focusing on the Barents Sea area, north of 70^{o} latitude, we have searched for events where the SPITS and the ARCES arrays both have defining P- and S-phase detections. We found 36 such events of this type during the actual time period, compared with only 17 such events detected using the old SPITS detection recipe for the same time period. A striking improvement is documented for the three recent events near Novaya Zemlya (also discussed in Section 6.1), where S-phase signals at SPITS are now detected on the horizontal coherent beams and associated with the P- and S-phases at ARCES and the P-phase at SPITS.

Section 6.4 is entitled "The exploitation of repeating seismic events to measure and correct erroneous timing at the KBS station, Spitsbergen, during February and March 2006". The background for this study was the observation of a timing error at the KBS station between February 17, 2006, and March 22, 2006, resulting from a temporary technical fault. The operators of the station were alerted to the problem rapidly and took the necessary corrective steps. Scientists at NORSAR only became aware of a synchronization problem when attempting to locate an interesting seismic event at Novaya Zemlya on 5 March 2006 using KBS phase determinations in addition to ARCES and SPITS observations. Successive, strategic attempts to locate the event using a fixed set of phase determinations indicated that anomalous P- and S-arrival times at KBS were almost certainly to blame for the large observed residuals in the location estimates. It was demonstrated that if both P- and S- phases had arrived at KBS approximately 8 seconds later than indicated on the seismograms, the phase determinations would be consistent with P- and S- arrivals from the SPITS and ARCES seismic arrays.

Mining-induced seismicity at the Barentsburg coal mine, close to the SPITS and KBS stations, results in signals at both sites which are very similar from event to event. Many such events occurred during the period in which the timing at KBS was erroneous. The frequency of these repeating events was sufficiently high during this period for the KBS timing error to be measured by comparing the time separating the correlating patterns in the subsequent waveforms at the two different stations. Based upon numerous waveform correlation calculations, we can state with a high level of confidence that the time-stamp on the KBS data at the time of the March 5, 2006, seismic event at Novaya Zemlya was approximately 8.07 seconds earlier than real-time. The corrected arrival time estimates allow for a very well-defined location estimate for the Novaya Zemlya event.

Although the rockbursts at the Barentsburg mine are a convenient source of repeating signals for our timing verification, they are by no means unique and there are most likely such sources in the vicinity of many seismic stations. Their identification could provide us with a wide range of means with which to verify or control instrumental timing. There are probably many more on the island of Spitsbergen; they have simply yet to be identified. In situations where seismologists discover sources of repeating seismic signals, we would advocate the documentation and publication of these sources (preferably with reference to specific events and with details about the signal repetition) such that the signals can subsequently be exploited to verify instrumental timing.

1 January - 28 February 2006

AFTAC Project Authorization	:	T/0155/PKO
ARPA Order No.	:	4138 AMD # 53
Program Code No.	:	0F10
Name of Contractor	:	Stiftelsen NORSAR
Effective Date of Contract	:	1 Feb 2001
Contract Expiration Date	:	28 February 2006
Amount of Contract	:	$ 2,933,442.48

1 March - 30 June 2006

AFTAC Project Authorization	:	T/6110
Purchase Request No.	:	F3KTK85290A1
Name of Contractor	:	Stiftelsen NORSAR
Effective Date of Contract	:	1 March 2006
Contract Expiration Date	:	30 September 2006
Amount of Contract	:	$ 94,126.97

Project Manager	:	Frode Ringdal +47 63 80 59 00
Title of Work	:	The Norwegian Seismic Array (NORSAR) Phase 3
Period Covered by Report	:	1 January - 30 June 2006

Part of the research presented in this report was supported by the Army Space and Missile Defense Command and was monitored by AFTAC, Patrick AFB, FL32925, under contract no. F08650-01-C-0055 (1 Jan - 28 Feb 06). Other activities were supported and monitored by AFTAC, Patrick AFB, FL32925, under contract no. FA2521-06-C-8003 (1 Mar - 30 Jun 06). Other sponsors are acknowledged where appropriate.

The operational activities of the seismic field systems and the Norwegian National Data Center (NDC) are currently jointly funded by the Norwegian Government and the CTBTO/PTS, with the understanding that the funding of IMS-related activities will gradually be transferred to the CTBTO/PTS.

NORSAR Contribution No. 980

Table of Contents

Page

1 Summary

This report describes the activities carried out at NORSAR under Contract No. F08650-01-C-0055 during 1 January - 28 February 2006, and under Contract No. FA2521-06-C-8003 for the period 1 March - 30 June 2006. Description of relevant research activities funded through other contracts are also included. In addition, this report provides summary information on operation and maintenance (O&M) activities at the Norwegian National Data Center (NDC) during the same period. Research activities described in this report are largely funded by the United States Government, and the United States also covers the cost of transmission of selected data to the US NDC. The O&M activities, including operation of transmission links within Norway and to Vienna, Austria are being funded jointly by the CTBTO/PTS and the Norwegian Government, with the understanding that the funding of O&M activities for primary stations in the International Monitoring System (IMS) will gradually be transferred to the CTBTO/PTS. The O&M statistics presented in this report are included for the purpose of completeness, and in order to maintain consistency with earlier reporting practice.

The seismic arrays operated by the Norwegian NDC comprise the Norwegian Seismic Array (NOA), the Arctic Regional Seismic Array (ARCES) and the Spitsbergen Regional Array (SPITS). This report presents statistics for these three arrays as well as for additional seismic stations which through cooperative agreements with institutions in the host countries provide continuous data to the NORSAR Data Processing Center (NDPC). These additional stations include the Finnish Regional Seismic Array (FINES) and the Hagfors array in Sweden (HFS).

The NOA Detection Processing system has been operated throughout the period with an uptime of 100%. A total of 2,306 seismic events have been reported in the NOA monthly seismic bulletin during the reporting period. On-line detection processing and data recording at the NDC of data from ARCES, FINES, SPITS and HFS data have been conducted throughout the period. Processing statistics for the arrays for the reporting period are given.

A summary of the activities at the Norwegian NDC and relating to field installations during the reporting period is provided in Section 4. Norway is now contributing primary station data from two seismic arrays: NOA (PS27) and ARCES (PS28), one auxiliary seismic array SPITS (AS72), and one auxiliary three-component station (AS73). These data are being provided to the IDC via the global communications infrastructure (GCI). Continuous data from the three arrays are in addition being transmitted to the US NDC. The performance of the data transmission to the US NDC has been satisfactory during the reporting period.

So far among the Norwegian stations, the NOA and the ARCES array (PS27 and PS28 respectively), the radionuclide station at Spitsbergen (RN49) and the auxiliary seismic station on Jan Mayen (AS73) have been certified. Provided that adequate funding continues to be made available (from the PTS and the Norwegian Ministry of Foreign Affairs), we envisage continuing the provision of data from these and other Norwegian IMS-designated stations in accordance with current procedures. The IMS infrasound station at Karasjok (IS37) is expected to be built in the fall of 2006, provided that the local authorities grant the permissions required for the establishment of the station.

Summaries of four scientific and technical contributions are presented in Chapter 6 of this report.

Section 6.1 is entitled “Processing of low-magnitude seismic events near Novaya Zemlya”. It contains an analysis of recordings from the SPITS array for three seismic events near Novaya

Zemlya during March 2006. The increase in sampling rate from 40 Hz to 80 Hz for the upgraded SPITS array has for the first time given an opportunity to analyze the high-frequency wave propagation across the Barents Sea. The best filter band for detection appears to be either 5-10 Hz or 10-20 Hz. However, the most remarkable feature is the strong SNR observed even at the highest frequency filter band analyzed (20-36 Hz). The strong energy at these high frequencies is especially remarkable taking into account that the epicentral distance being more than 1000 km. While such a frequency band would not be used for detection purposes, the high frequency data could be very important for signal characterization.

The difficulties in detecting Sn phases at SPITS has been noted in previous Semiannual Reports. As also discussed in Section 6.3, the inclusion of five new three-component seismometers in the upgraded SPITS array was motivated by the need to improve S-phase detection at SPITS, and by the early observations of large S-phase amplitudes on the horizontal components of the originally installed 3-C sensor. We show, for each of the three events, Sn beams steered towards the epicenter using the rotated (transverse) components, as well as more conventional Pn and Sn beams from the vertical components. Although there are some differences in signal-to-noise ratios of the three events, the general interpretation of the three figures is similar: The two beams based upon vertical components show clear Pn and Sn phases, but the Sn phase could be difficult to detect by a power detector due to the strong preceding coda from the Pn-phase. In contrast, the beam trace rotated in the transverse direction shows almost no sign of the Pn phase, whereas the Sn phase is quite strong. Clearly, the detection of Sn-phases could be greatly improved by augmenting the beam deployment with several steered beams, rotated so as to provide transverse components, toward the grid points in the beam deployment system.

Section 6.2 is entitled “Infrasound observations of two recent meteor impacts in Norway”. During the summer of 2006, a large number of people observed sound and light phenomena from two meteor impacts in Norway. The first impact was on 7 June at about 00:07 GMT in northern Norway (Finnmark) and the second impact was on 14 July at about 08:18 GMT in southern Norway (Oslo Fjord area). The observations indicate that the first event was larger than the second. Fragments of the meteors have up to now only been found for the second event in Rygge and Moss.

The first explosion, in northern Norway, was recorded on several seismic and infrasonic stations in northern Scandinavia. By combining all observations and using them as input to a traditional event location program (HYPOSAT) a presumed location of the meteor explosion could be determined. To locate the event, we used two different procedures: First, the BAZ observations from the arrays (ARCES, Apatity, Jämtön, and Lycksele) were used, and secondly, these BAZ observations were supplemented with arrival times of the infrasonic signals at nearby stations (KIF, TRO, and ARCES), modelling the atmosphere as propagation medium of the infrasonic waves by a simple halfspace with a constant velocity of 0.33 km/s. These locations turned out to be consistent within less than 5 km.

The second explosion, which occurred about five weeks later, was observed in the border region between southern Norway and Sweden. The explosion of the meteor was heard in Rygge and at least 2 fragments were found on the ground in the Rygge - Moss area. We searched nearby seismic stations for corresponding signals. No related signal could be found in records of the broadband station KONO and of the Hagfors array in Southern Sweden. However, on the traces of the short period sensors of the large NORSAR array, a signal was detected crossing the array from south to north with sound velocity. Unfortunately the signal

itself is quite incoherent so that no standard tool to analyze array data could be applied. Nevertheless, we were able to read onset times on short term average (STA) traces for 28 of the NORSAR seismometers, and used these times as input parameters for HYPOSAT, again using a halfspace model with a constant velocity of 0.33 km/s. Although the resulting event location estimate has a fairly large error ellipse, it is sufficiently precise to be confidently connected with the observed meteor explosion and the area where its fragments were found.

Section 6.3 is entitled "Improvements to SPITS regional S-phase detection; coherent beamforming of rotated horizontal components". As mentioned earlier, the number of three-component sites at the SPITS array was increased from one to six, during the recent refurbishment of the SPITS array. This new array configuration opened for the possibility to redefine and tune the automatic data processing recipes of the SPITS array, including redefinition of the detection beam deployment, procedures for fk-analysis and the rules for fully automatic single array event location. This contribution describes the details of the new beam deployment, and presents some examples of the improvements achieved.

When using the horizontal components for S-phase detection, it is preferable to decompose the energy into SH and SV components. This is because explosion-type sources are expected to radiate S energy mostly of SV type, whereas many earthquakes (however, depending on the radiation pattern) may dominantly radiate SH energy. Therefore, in the new beam deployment, all horizontal beams are coherently stacked for radial and transverse components after rotating the original north-south and east-west components with respect to the actual backazimuth (BAZ) of the beam. A total of 999 beams are defined, out of which 221 are radial component, and 222 are transverse component coherent horizontal beams. The higher sampling rate of the upgraded SPITS array also made it possible to include a high frequency 12-24 Hz filter in the detection processing.

Following the implementation of horizontal coherent beams in the new detection process, corresponding modifications had to be included for the subsequent automatic f-k analysis. We have now run the new SPITS processing setup for 58 consecutive days. This resulted in an average of 2945 detections per day, which is about twice as many as the number of detections found when using the old processing recipe (average of 1655 per day).

For this same time period we have run automatic multi-array phase association and event location using the Generalized Beamforming (GBF) approach. Focusing on the Barents Sea area, north of 70^{o} latitude, we have searched for events where the SPITS and the ARCES arrays both have defining P- and S-phase detections. We found 36 such events of this type during the actual time period, compared with only 17 such events detected using the old SPITS detection recipe for the same time period. A striking improvement is documented for the three recent events near Novaya Zemlya (also discussed in Section 6.1), where S-phase signals at SPITS are now detected on the horizontal coherent beams and associated with the P- and S-phases at ARCES and the P-phase at SPITS.

Section 6.4 is entitled "The exploitation of repeating seismic events to measure and correct erroneous timing at the KBS station, Spitsbergen, during February and March 2006". The background for this study was the observation of a timing error at the KBS station between February 17, 2006, and March 22, 2006, resulting from a temporary technical fault. The operators of the station were alerted to the problem rapidly and took the necessary corrective steps. Scientists at NORSAR only became aware of a synchronization problem when attempting to locate an interesting seismic event at Novaya Zemlya on 5 March 2006 using KBS phase deter-

minations in addition to ARCES and SPITS observations. Successive, strategic attempts to locate the event using a fixed set of phase determinations indicated that anomalous P- and S-arrival times at KBS were almost certainly to blame for the large observed residuals in the location estimates. It was demonstrated that if both P- and S- phases had arrived at KBS approximately 8 seconds later than indicated on the seismograms, the phase determinations would be consistent with P- and S- arrivals from the SPITS and ARCES seismic arrays.

Mining-induced seismicity at the Barentsburg coal mine, close to the SPITS and KBS stations, results in signals at both sites which are very similar from event to event. Many such events occurred during the period in which the timing at KBS was erroneous. The frequency of these repeating events was sufficiently high during this period for the KBS timing error to be measured by comparing the time separating the correlating patterns in the subsequent waveforms at the two different stations. Based upon numerous waveform correlation calculations, we can state with a high level of confidence that the time-stamp on the KBS data at the time of the March 5, 2006, seismic event at Novaya Zemlya was approximately 8.07 seconds earlier than real-time. The corrected arrival time estimates allow for a very well-defined location estimate for the Novaya Zemlya event.

Although the rockbursts at the Barentsburg mine are a convenient source of repeating signals for our timing verification, they are by no means unique and there are most likely such sources in the vicinity of many seismic stations. Their identification could provide us with a wide range of means with which to verify or control instrumental timing. There are probably many more on the island of Spitsbergen; they have simply yet to be identified. In situations where seismologists discover sources of repeating seismic signals, we would advocate the documentation and publication of these sources (preferably with reference to specific events and with details about the signal repetition) such that the signals can subsequently be exploited to verify instrumental timing.

Frode Ringdal

2 Operation of International Monitoring System (IMS) Stations in Norway

2.1 PS27 — Primary Seismic Station NOA

The mission-capable data statistics were 100%, the same as for the previous reporting period. The net instrument availability was 98.343%.

There were no outages of all subarrays at the same time in the reporting period.

Monthly uptimes for the NORSAR on-line data recording task, taking into account all factors (field installations, transmissions line, data center operation) affecting this task were as follows:

2006		Mission Capable	Net instrument availability
January	:	100%	98.626%
February	:	100%	98.412%
March	:	100%	98.322%
April	:	100%	98.347%
May	:	100%	97.671%
June	:	100%	98.698%

B. Kr. Hokland

NOA Event Detection Operation

In Table 2.1.1 some monthly statistics of the Detection and Event Processor operation are given. The table lists the total number of detections (DPX) triggered by the on-line detector, the total number of detections processed by the automatic event processor (EPX) and the total number of events accepted after analyst review (teleseismic phases, core phases and total).

	Total DPX	Total EPX	Accepted Events		Sum	Daily
			P-phases	Core Phases		
Jan	12,067	897	197	66	263	8.5
Feb	11,043	926	265	55	320	11.4
Mar	11,523	1,109	314	79	393	12.7
Apr	10,901	1,053	451	127	578	19.3
May	5,817	820	290	102	392	12.6
Jun	6,283	775	306	54	360	12.0
	57,634	5,580	1,823	483	2,306	12.75

Table 2.1.1. *Detection and Event Processor statistics, 1 January - 30 June 2006.*

NOA detections

The number of detections (phases) reported by the NORSAR detector during day 001, 2006, through day 181, 2006, was 57,634, giving an average of 318 detections per processed day (181 days processed).

B. Paulsen

U. Baadshaug

2.2 PS28 — Primary Seismic Station ARCES

The mission-capable data statistics were 99.997%, as compared to 99.287% for the previous reporting period. The net instrument availability was 97.983%.

The main outages in the period are presented in Table 2.2.1.

Day	Period
06/02	18.46 - 18.54

Table 2.2.1. *The main interruptions in recording of ARCES data at NDPC, 1 January - 30 June 2006.*

Monthly uptimes for the ARCES on-line data recording task, taking into account all factors (field installations, transmission lines, data center operation) affecting this task were as follows:

2006		Mission Capable	Net instrument availability
January	:	100%	97.905
February	:	99.980%	99.686%
March	:	100%	99.582%
April	:	100%	99.959%
May	:	100%	95.037%
June	:	100%	95.891%

B.Kr. Hokland

Event Detection Operation

ARCES detections

The number of detections (phases) reported during day 001, 2006, through day 181, 2006, was 178,381, giving an average of 986 detections per processed day (181 days processed).

Events automatically located by ARCES

During days 001, 2006, through 181, 2006, 8728 local and regional events were located by ARCES, based on automatic association of P- and S-type arrivals. This gives an average of 48.2 events per processed day (181 days processed). 55% of these events are within 300 km, and 82% of these events are within 1000 km.

U. Baadshaug

2.3 AS72 — Auxiliary Seismic Station Spitsbergen

The mission-capable data for the period were 100%, the same as for the previous reporting period. The net instrument availability was 95.431%.

There were no outages of all instruments at the same time in the reporting period.

Monthly uptimes for the Spitsbergen on-line data recording task, taking into account all factors (field installations, transmissions line, data center operation) affecting this task were as follows:

2006		Mission Capable	Net instrument availability
January	:	100%	93.490%
February	:	100%	90.082%
March	:	100%	92.384%
April	:	100%	99.664%
May	:	100%	97.038%
June	:	100%	99.686%

B.Kr. Hokland

Event Detection Operation

Spitsbergen array detections

The number of detections (phases) reported from day 001, 2006, through day 181, 2006, was 307,835, giving an average of 1701 detections per processed day (181 days processed).

Events automatically located by the Spitsbergen array

During days 001, 2006, through 181, 2006, 23,054 local and regional events were located by the Spitsbergen array, based on automatic association of P- and S-type arrivals. This gives an average of 127.4 events per processed day (181 days processed). 71% of these events are within 300 km, and 88% of these events are within 1000 km.

U. Baadshaug

2.4 AS73 — Auxiliary Seismic Station at Jan Mayen

The IMS auxiliary seismic network includes a three-component station on the Norwegian island of Jan Mayen. The station location given in the protocol to the Comprehensive Nuclear-Test-Ban Treaty is 70.9˚N, 8.7˚W.

The University of Bergen has operated a seismic station at this location since 1970. A so-called Parent Network Station Assessment for AS73 was completed in April 2002. A vault at a new location (71.0^{o}N, 8.5^{o}W) was prepared in early 2003, after its location had been approved by the PrepCom. New equipment was installed in this vault in October 2003, as a cooperative effort between NORSAR and the CTBTO/PTS. Continuous data from this station are being transmitted to the NDC at Kjeller via a satellite link installed in April 2000. Data are also made available to the University of Bergen.

The station was certified by the CTBTO/PTS on 12 June 2006.

J. Fyen

2.5 IS37 — Infrasound Station at Karasjok

The IMS infrasound network will include a station at Karasjok in northern Norway. The coordinates given for this station are 69.5˚N, 25.5˚E. These coordinates coincide with those of the primary seismic station PS28.

A site survey for this station was carried out during June/July 1998 as a cooperative effort between the CTBTO/PTS and NORSAR. The site survey led to a recommendation on the exact location of the infrasound station. There was, however, a strong local opposition against establishing the station at the recommended location, and an alternative site has been identified. The appropriate application forms have been sent to the local authorities to obtain the permissions needed to establish the station at this alternative location. Station installation is expected to take place in the fall of 2006, provided that such permissions are granted by mid-August 2006 at the latest.

A site preparation proposal has been submitted to the PTS. Due to scarce vegetation, possible high winds and difficult arctic operating conditions, the PTS has accepted our proposal to build 9 elements.

J. Fyen

2.6 RN49 — Radionuclide Station on Spitsbergen

The IMS radionuclide network includes a station on the island of Spitsbergen. This station is also among those IMS radionuclide stations that will have a capability of monitoring for the presence of relevant noble gases upon entry into force of the CTBT.

A site survey for this station was carried out in August of 1999 by NORSAR, in cooperation with the Norwegian Radiation Protection Authority. The site survey report to the PTS contained a recommendation to establish this station at Platåberget, near Longyearbyen. The infrastructure for housing the station equipment was established in early 2001, and a noble gas detection system, based on the Swedish “SAUNA” design, was installed at this site in May 2001, as part of PrepCom’s noble gas experiment. A particulate station (“ARAME” design) was installed at the same location in September 2001. A certification visit to the particulate sta-

tion took place in October 2002, and the particulate station was certified on 10 June 2003. Both systems underwent substantial upgrading in May/June 2006. The equipment at RN49 is being maintained and operated in accordance with a contract with the CTBTO/PTS.

S. Mykkeltveit

3 Contributing Regional Seismic Arrays

3.1 NORES

NORES has been out of operation since lightning destroyed the station electronics on 11 June 2002.

J. Torstveit

3.2 Hagfors (IMS Station AS101)

Data from the Hagfors array are made available continuously to NORSAR through a cooperative agreement with Swedish authorities.

The mission-capable data statistics were 100%, as compared to 99.993% for the previous reporting period. The net instrument availability was 100%.

There were no outages of all instruments in the reporting period.

Monthly uptimes for the Hagfors on-line data recording task, taking into account all factors (field installations, transmissions line, data center operation) affecting this task were as follows:

2006		Mission Capable	Net instrument availability
January	:	100%	100%
February	:	100%	100%
March	:	100%	100%
April	:	100%	99.999%
May	:	100%	100%
June	:	100%	100%

B.Kr. Hokland

Hagfors Event Detection Operation

Hagfors array detections

The number of detections (phases) reported from day 001, 2006, through day 181, 2006, was 135,642, giving an average of 749 detections per processed day (181 days processed).

Events automatically located by the Hagfors array

During days 001, 2006, through 181, 2006, 3915 local and regional events were located by the Hagfors array, based on automatic association of P- and S-type arrivals. This gives an average of 21.6 events per processed day (181 days processed). 78% of these events are within 300 km, and 93% of these events are within 1000 km.

U. Baadshaug

3.3 FINES (IMS station PS17)

Data from the FINES array are made available continuously to NORSAR through a cooperative agreement with Finnish authorities.

The mission-capable data statistics were 99.998%, as compared to 100% for the previous reporting period. The net instrument availability was 97.125%.

Monthly uptimes for the FINES on-line data recording task, taking into account all factors (field installations, transmissions line, data center operation) affecting this task were as follows:

2006		Mission Capable	Net instrument availability
January	:	99.989%	98.282%
February	:	100%	95.238%
March	:	100%	95.181%
April	:	100%	95.238%
May	:	99.999%	98.710%
June	:	100%	99.948%

B.Kr. Hokland

FINES Event Detection Operation

FINES detections

The number of detections (phases) reported during day 001, 2006, through day 181, 2006, was 49,793, giving an average of 275 detections per processed day (181 days processed).

Events automatically located by FINES

During days 001, 2006, through 181, 2006, 2745 local and regional events were located by FINES, based on automatic association of P- and S-type arrivals. This gives an average of 15.2 events per processed day (181 days processed). 81% of these events are within 300 km, and 88% of these events are within 1000 km.

U. Baadshaug

3.4 Regional Monitoring System Operation and Analysis

The Regional Monitoring System (RMS) was installed at NORSAR in December 1989 and has been operated at NORSAR from 1 January 1990 for automatic processing of data from ARCES and NORES. A second version of RMS that accepts data from an arbitrary number of arrays and single 3-component stations was installed at NORSAR in October 1991, and regular operation of the system comprising analysis of data from the 4 arrays ARCES, NORES, FINES and

GERES started on 15 October 1991. As opposed to the first version of RMS, the one in current operation also has the capability of locating events at teleseismic distances.

Data from the Apatity array was included on 14 December 1992, and from the Spitsbergen array on 12 January 1994. Detections from the Hagfors array were available to the analysts and could be added manually during analysis from 6 December 1994. After 2 February 1995, Hagfors detections were also used in the automatic phase association.

Since 24 April 1999, RMS has processed data from all the seven regional arrays ARCES, NORES, FINES, GERES (until January 2000), Apatity, Spitsbergen, and Hagfors. Starting 19 September 1999, waveforms and detections from the NORSAR array have also been available to the analyst.

Phase and event statistics

Table 3.5.1 gives a summary of phase detections and events declared by RMS. From top to bottom the table gives the total number of detections by the RMS, the number of detections that are associated with events automatically declared by the RMS, the number of detections that are not associated with any events, the number of events automatically declared by the RMS, and finally the total number of events worked on interactively (in accordance with criteria that vary over time; see below) and defined by the analyst.

New criteria for interactive event analysis were introduced from 1 January 1994. Since that date, only regional events in areas of special interest (e.g, Spitsbergen, since it is necessary to acquire new knowledge in this region) or other significant events (e.g, felt earthquakes and large industrial explosions) were thoroughly analyzed. Teleseismic events of special interest are also analyzed.

To further reduce the workload on the analysts and to focus on regional events in preparation for Gamma-data submission during GSETT-3, a new processing scheme was introduced on 2 February 1995. The GBF (Generalized Beamforming) program is used as a pre-processor to RMS, and only phases associated with selected events in northern Europe are considered in the automatic RMS phase association. All detections, however, are still available to the analysts and can be added manually during analysis.

	Jan 06	Feb 06	Mar 06	Apr 06	May 06	Jun 06	Total
Phase detections	122,608	129,031	130,794	116,939	157,735	141,959	799,066
- Associated phases	4,013	4,338	4,547	4,349	5,212	4,794	27,253
- Unassociated phases	118,595	124,693	126,247	112,590	152,523	137,165	771,813
Events automatically declared by RMS	876	838	860	767	894	998	5,233
No. of events defined by the analyst	43	56	71	49	80	59	358

Table 3.5.1. RMS phase detections and event summary 1 January - 30 June 2006.

U. Baadshaug

B. Paulsen

4 NDC and Field Activities

4.1 NDC Activitities

NORSAR functions as the Norwegian National Data Center (NDC) for CTBT verification. Six monitoring stations, comprising altogether 129 field sensors, will be located on Norwegian territory as part of the future IMS as described elsewhere in this report. The four seismic IMS stations are all in operation today, and all of them are currently providing data to the CTBTO on a regular basis. PS27, PS28, AS73 and RN49 are all certified. The infrasound station in northern Norway is planned to be established within next year. Data recorded by the Norwegian stations is being transmitted in real time to the Norwegian NDC, and provided to the IDC through the Global Communications Infrastructure (GCI). Norway is connected to the GCI with a frame relay link to Vienna.

Operating the Norwegian IMS stations continues to require increased resources and additional personnel both at the NDC and in the field. Strictly defined procedures as well as increased emphasis on regularity of data recording and timely data transmission to the IDC in Vienna have led to increased reporting activities and implementation of new procedures for the NDC. The NDC carries out all the technical tasks required in support of Norway's treaty obligations. NORSAR will also carry out assessments of events of special interest, and advise the Norwegian authorities in technical matters relating to treaty compliance.

Verification functions; information received from the IDC

After the CTBT enters into force, the IDC will provide data for a large number of events each day, but will not assess whether any of them are likely to be nuclear explosions. Such assessments will be the task of the States Parties, and it is important to develop the necessary national expertise in the participating countries. An important task for the Norwegian NDC will thus be to make independent assessments of events of particular interest to Norway, and to communicate the results of these analyses to the Norwegian Ministry of Foreign Affairs.

Monitoring the Arctic region

Norway will have monitoring stations of key importance for covering the Arctic, including Novaya Zemlya, and Norwegian experts have a unique competence in assessing events in this region. On several occasions in the past, seismic events near Novaya Zemlya have caused political concern, and NORSAR specialists have contributed to clarifying these issues.

International cooperation

After entry into force of the treaty, a number of countries are expected to establish national expertise to contribute to the treaty verification on a global basis. Norwegian experts have been in contact with experts from several countries with the aim of establishing bilateral or multilateral cooperation in this field. One interesting possibility for the future is to establish NORSAR as a regional center for European cooperation in the CTBT verification activities.

NORSAR event processing

The automatic routine processing of NORSAR events as described in NORSAR Sci. Rep. No. 2-93/94, has been running satisfactorily. The analyst tools for reviewing and updating the solu-

tions have been continually modified to simplify operations and improve results. NORSAR is currently applying teleseismic detection and event processing using the large-aperture NOA array as well as regional monitoring using the network of small-aperture arrays in Fennoscandia and adjacent areas.

Communication topology

Norway has implemented an independent subnetwork, which connects the IMS stations AS72, AS73, PS28, and RN49 operated by NORSAR to the GCI at NOR_NDC. A contract has been concluded and VSAT antennas have been installed at each station in the network. Under the same contract, VSAT antennas for 6 of the PS27 subarrays have been installed for intra-array communication. The seventh subarray is connected to the central recording facility via a leased land line. The central recording facility for PS27 is connected directly to the GCI (Basic Topology). All the VSAT communication is functioning satisfactorily. As of 10 June 2005, AS72 and RN49 are connected to NOR_NDC through a VPN link.

Jan Fyen

4.2 Status Report: Provision of data from Norwegian seismic IMS stations to the IDC

Introduction

This contribution is a report for the period January - June 2006 on activities associated with provision of data from Norwegian seismic IMS stations to the International Data Centre (IDC) in Vienna. This report represents an update of contributions that can be found in previous editions of NORSAR's Semiannual Technical Summary. It is noted that as of 30 June 2006, three of the four Norwegian seismic stations providing data to the IDC have been formally certified.

Norwegian IMS stations and communications arrangements

During the reporting interval 1 January - 30 June 2006, Norway has provided data to the IDC from the four seismic stations shown in Fig. 4.2.1. PS27 —NOA is a 60 km aperture teleseismic array, comprised of 7 subarrays, each containing six vertical short period sensors and a three-component broadband instrument. PS28 — ARCES is a 25-element regional array with an aperture of 3 km, whereas AS72 — Spitsbergen array (station code SPITS) has 9 elements within a 1-km aperture. AS73 — JMIC has a single three-component broadband instrument.

The intra-array communication for NOA utilizes a land line for subarray NC6 and VSAT links based on TDMA technology for the other 6 subarrays. The central recording facility for NOA is located at the Norwegian National Data Center (NOR_NDC).

Continuous ARCES data are transmitted from the ARCES site to NOR_NDC using a 64 kbits/s VSAT satellite link, based on BOD technology.

Continuous SPITS data were transmitted to NOR_NDC via a VSAT terminal located at Platåberget in Longyearbyen (which is the site of the IMS radionuclide monitoring station RN49 installed during 2001) up to 10 June 2005. The central recording facility (CRF) for the SPITS array has been moved to the University of Spitsbergen (UNIS). A 512 bps SHDSL link has been established between UNIS and NOR_NDC. Data from the array elements to the CRF

are transmitted via a 2.4 Ghz radio link (Wilan VIP-110). Both AS72 and RN49 data are now transmitted to NOR_NDC over this link using VPN technology.

A minimum of seven-day station buffers have been established at the ARCES and SPITS sites and at all NOA subarray sites, as well as at the NOR_NDC for ARCES, SPITS and NOA.

The NOA and ARCES arrays are primary stations in the IMS network, which implies that data from these stations is transmitted continuously to the receiving international data center. Since October 1999, this data has been transmitted (from NOR_NDC) via the Global Communications Infrastructure (GCI) to the IDC in Vienna. Data from the auxiliary array station SPITS — AS72 have been sent in continuous mode to the IDC during the reporting period. AS73 — JMIC is an auxiliary station in the IMS, and the JMIC data have been available to the IDC throughout the reporting period on a request basis via use of the AutoDRM protocol (Kradolfer, 1993; Kradolfer, 1996). In addition, continuous data from all three arrays is transmitted to the US_NDC.

Uptimes and data availability

Figs. 4.2.2 and 4.2.3 show the monthly uptimes for the Norwegian IMS primary stations ARCES and NOA, respectively, for the period 1 January - 30 June 2006, given as the hatched (taller) bars in these figures. These barplots reflect the percentage of the waveform data that is available in the NOR_NDC data archives for these two arrays. The downtimes inferred from these figures thus represent the cumulative effect of field equipment outages, station site to NOR_NDC communication outage, and NOR_NDC data acquisition outages.

Figs. 4.2.2 and 4.2.3 also give the data availability for these two stations as reported by the IDC in the IDC Station Status reports. The main reason for the discrepancies between the NOR_NDC and IDC data availabilities as observed from these figures is the difference in the ways the two data centers report data availability for arrays: Whereas NOR_NDC reports an array station to be up and available if at least one channel produces useful data, the IDC uses weights where the reported availability (capability) is based on the number of actually operating channels.

Use of the AutoDRM protocol

NOR_NDC's AutoDRM has been operational since November 1995 (Mykkeltveit & Baadshaug, 1996). The monthly number of requests by the IDC for JMIC data for the period January - June 2006 is shown in Fig. 4.2.4.

NDC automatic processing and data analysis

These tasks have proceeded in accordance with the descriptions given in Mykkeltveit and Baadshaug (1996). For the period January - June 2006, NOR_NDC derived information on 425 supplementary events in northern Europe and submitted this information to the Finnish NDC as the NOR_NDC contribution to the joint Nordic Supplementary (Gamma) Bulletin, which in turn is forwarded to the IDC. These events are plotted in Fig. 4.2.5.

Data access for the station NIL at Nilore, Pakistan

NOR_NDC continued to provide access to the seismic station NIL at Nilore, Pakistan, through a VSAT satellite link between NOR_NDC and Pakistan's NDC in Nilore.

Current developments and future plans

NOR_NDC is continuing the efforts towards improving and hardening all critical data acquisition and data forwarding hardware and software components, so as to meet the requirements related to operation of IMS stations.

The NOA array was formally certified by the PTS on 28 July 2000, and a contract with the PTS in Vienna currently provides partial funding for operation and maintenance of this station. The ARCES array was formally certified by the PTS on 8 November 2001, and a contract with the PTS is in place which also provides for partial funding of the operation and maintenance of this station. Provided that adequate funding continues to be made available (from the PTS and the Norwegian Ministry of Foreign Affairs), we envisage continuing the provision of data from all Norwegian seismic IMS stations without interruption to the IDC in Vienna.

U. Baadshaug
S. Mykkeltveit
J. Fyen

References

Kradolfer, U. (1993): Automating the exchange of earthquake information. *EOS, Trans., AGU*, 74, 442.

Kradolfer, U. (1996): AutoDRM — The first five years, *Seism. Res. Lett.*, 67, 4, 30-33.

Mykkeltveit, S. & U. Baadshaug (1996): Norway's NDC: Experience from the first eighteen months of the full-scale phase of GSETT-3. *Semiann. Tech. Summ., 1 October 1995 - 31 March 1996*, NORSAR Sci. Rep. No. 2-95/96, Kjeller, Norway.

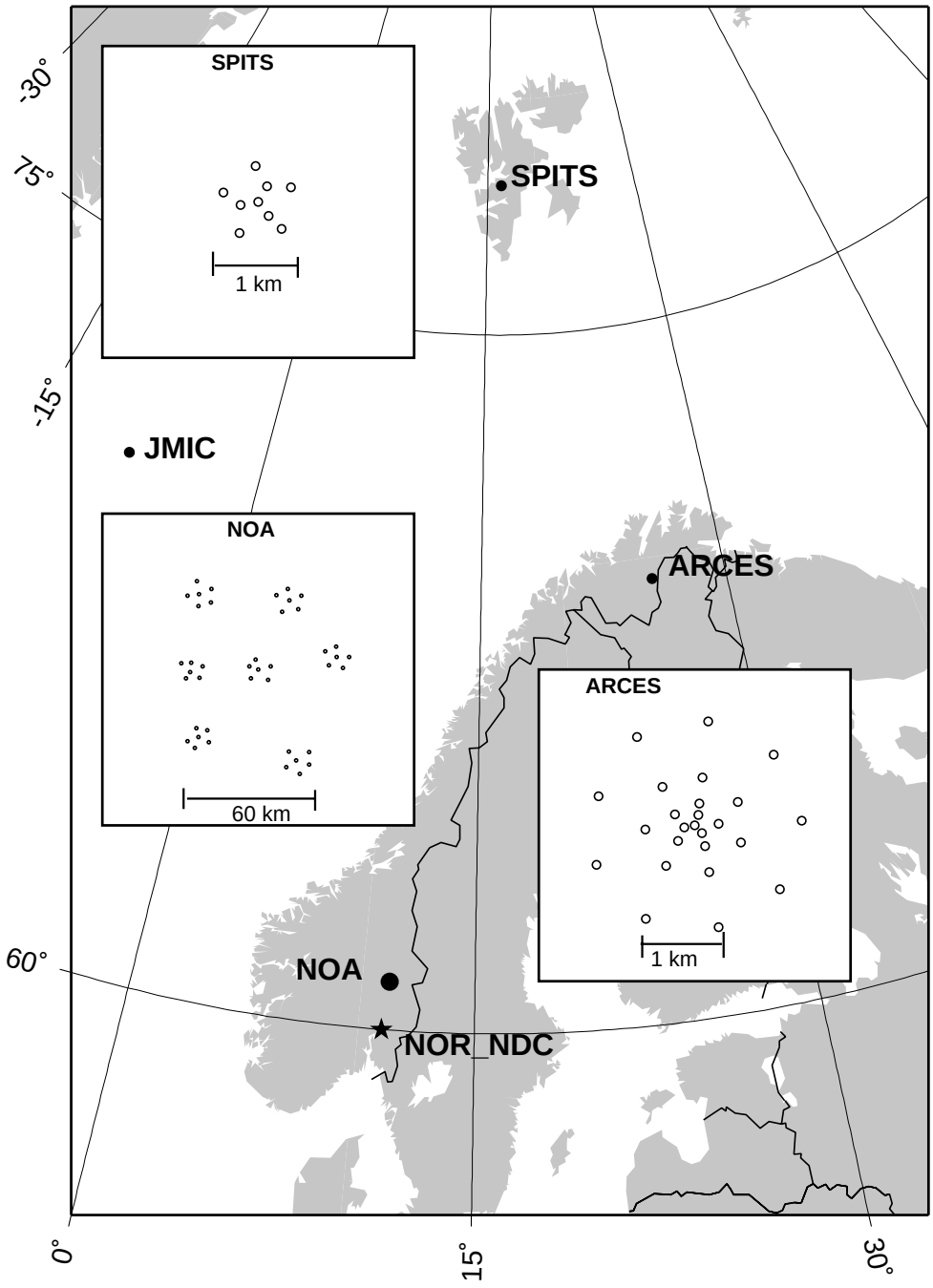

Fig. 4.2.1. The figure shows the locations and configurations of the three Norwegian seismic IMS array stations that provided data to the IDC during the period January - June 2006. The data from these stations and the JMIC three-component station are transmitted continuously and in real time to the Norwegian NDC (NOR_NDC). The stations NOA and ARCES are primary IMS stations, whereas SPITS and JMIC are auxiliary IMS stations.

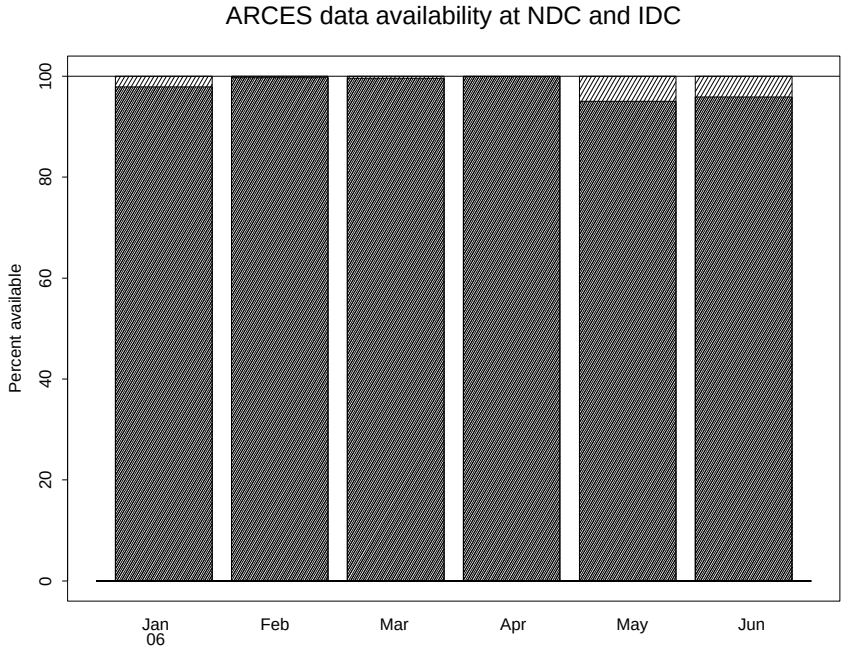

Fig. 4.2.2. The figure shows the monthly availability of ARCES array data for the period January - June 2006 at NOR_NDC and the IDC. See the text for explanation of differences in definition of the term "data availability" between the two centers. The higher values (hatched bars) represent the NOR_NDC data availability.

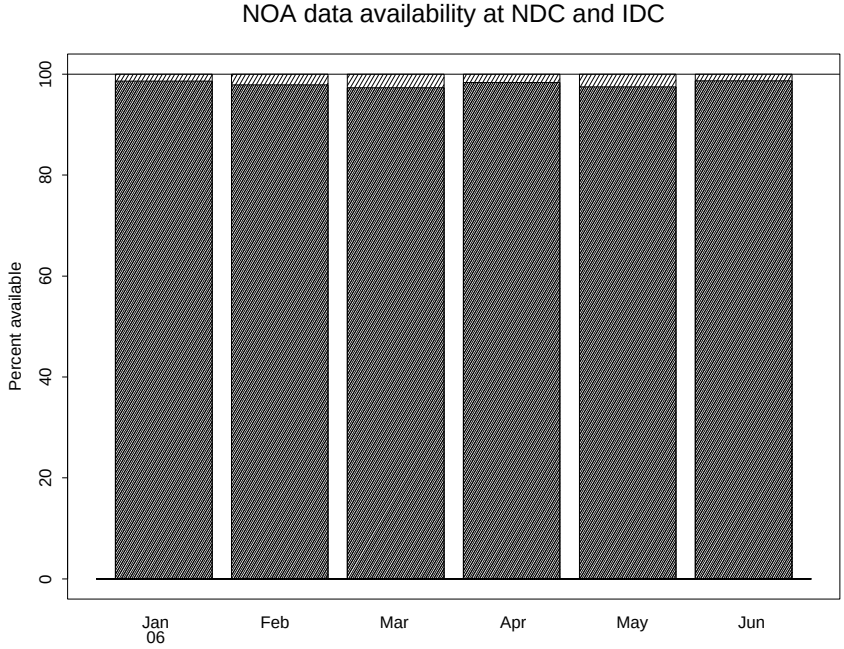

Fig. 4.2.3. The figure shows the monthly availability of NORSAR array data for the period January - June 2006 at NOR_NDC and the IDC. See the text for explanation of differences in definition of the term "data availability" between the two centers. The higher values (hatched bars) represent the NOR_NDC data availability.

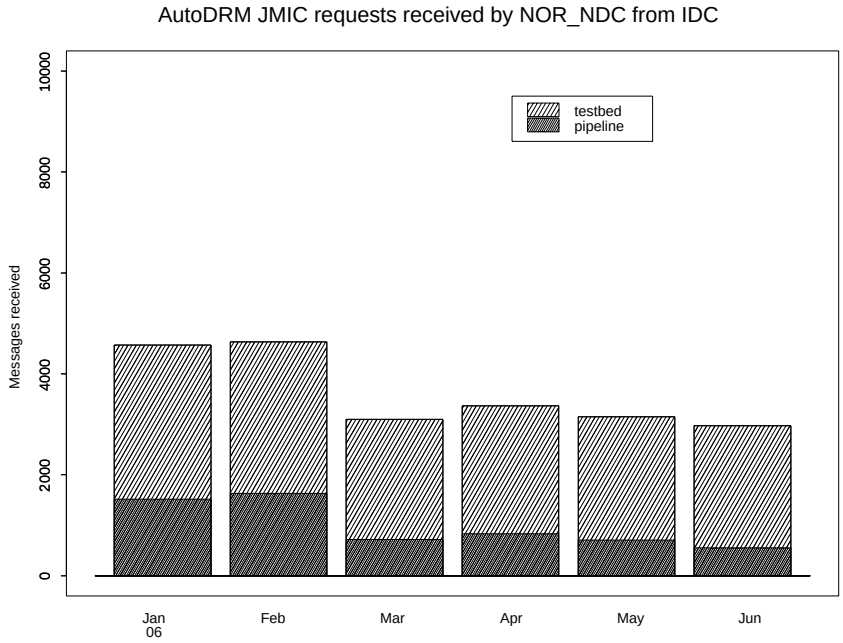

Fig. 4.2.4. The figure shows the monthly number of requests received by NOR_NDC from the IDC for JMIC waveform segments during January - June 2006.

Reviewed Supplementary events

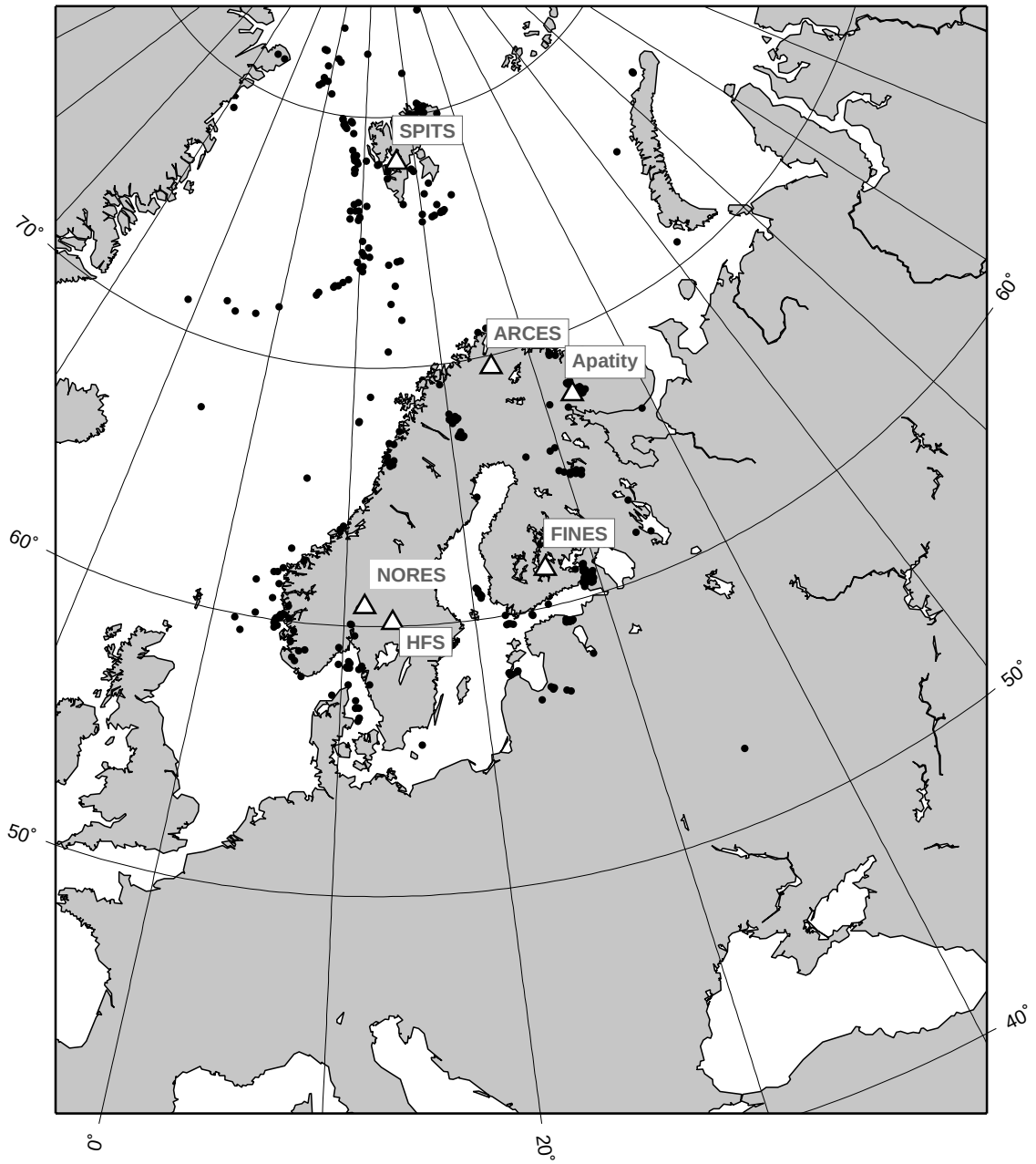

Fig. 4.2.5. The map shows the 425 events in and around Norway contributed by NOR_NDC during January - June 2006 as supplementary (Gamma) events to the IDC, as part of the Nordic supplementary data compiled by the Finnish NDC. The map also shows the main seismic stations used in the data analysis to define these events.

4.3 Field Activities

The activities at the NORSAR Maintenance Center (NMC) at Hamar currently include work related to operation and maintenance of the following IMS seismic stations: the NOA teleseismic array (PS27), the ARCES array (PS28) and the Spitsbergen array (AS72). Some work has also been carried out in connection with the seismic station on Jan Mayen (AS73), the radionuclide station at Spitsbergen (RN49), and preparations for the infrasound station at Karasjok (IS37). NORSAR also acts as a consultant for the operation and maintenance of the Hagfors array in Sweden (AS101).

NORSAR carries out the field activities relating to IMS stations in a manner generally consistent with the requirements specified in the appropriate IMS Operational Manuals, which are currently being developed by Working Group B of the Preparatory Commission. For seismic stations these specifications are contained in the Operational Manual for Seismological Monitoring and the International Exchange of Seismological Data (CTBT/WGB/TL-11/2), currently available in a draft version.

All regular maintenance on the NORSAR field systems is conducted on a one-shift-per-day, five-day-per-week basis. The maintenance tasks include:

- Operating and maintaining the seismic sensors and the associated digitizers, authentication devices and other electronics components.
- Maintaining the power supply to the field sites as well as backup power supplies.
- Operating and maintaining the VSATs, the data acquisition systems and the intra-array data transmission systems.
- Assisting the NDC in evaluating the data quality and making the necessary changes in gain settings, frequency response and other operating characteristics as required.
- Carrying out preventive, routine and emergency maintenance to ensure that all field systems operate properly.
- Maintaining a computerized record of the utilization, status, and maintenance history of all site equipment.
- Providing appropriate security measures to protect against incidents such as intrusion, theft and vandalism at the field installations.

Details of the daily maintenance activities are kept locally. As part of its contract with CTBTO/PTS NORSAR submits, when applicable, problem reports, outage notification reports and equipment status reports. The contents of these reports and the circumstances under which they will be submitted are specified in the draft Operational Manual.

P.W. Larsen
K.A. Løken

5 Documentation Developed

Gibbons, S.J. (2006): The exploitation of repeating seismic events to measure and correct erroneous timing at the KBS station, Spitsbergen, during February and March 2006. **In:** Semiannual Technical Summary, 1 January - 30 June 2006, NORSAR Sci. Rep. 2-2006, Kjeller, Norway.

Gibbons, S.J. & F. Ringdal (2006): The detection of low magnitude seismic events using array-based waveform correlation. Geophys. J. Inter., 165, 149-166.

Gibbons, S.J., M. Bøttger-Sørensen, D.B. Harris & F. Ringdal (2006): The detection and location of low magnitude earthquakes in northern Norway using multi-channel waveform correlation. Submitted to Phys. Earth Planet. Sci.

Gibbons, S.J. (2006): On the identification and documentation of timing errors: An example at the KBS station, Spitsbergen. Seis. Res. Lett., 77, 555-567.

Ringdal, F. (2006): Semiannual Technical Summary, 1 July - 31 December 2005. NORSAR Sci. Rep. 1-2006, Kjeller, Norway, January 2006.

Ringdal, F.& S.J. Gibbons (2006): Processing of low-magnitude seismic events near Novaya Zemlya. **In:** Semiannual Technical Summary, 1 January - 30 June 2006, NORSAR Sci. Rep. 2-2006, Kjeller, Norway.

Schweitzer, J. & T. Kværna (2006): Infrasound observations of two recent meteor impacts in Norway. **In:** Semiannual Technical Summary, 1 January - 30 June 2006, NORSAR Sci. Rep. 2-2006, Kjeller, Norway.

Schweitzer, J. & T. Kværna (2006): Improvements to SPITS regional S-phase detection; coherent beamforming of rotated horizontal components. **In:** Semiannual Technical Summary, 1 January - 30 June 2006, NORSAR Sci. Rep. 2-2006, Kjeller, Norway.

Stevens, J.L., S.J. Gibbons, N. Rimer, H. Xu, C. Lindholm, F. Ringdal, T. Kværna & J.R. Murphy (2006): Analysis and simulation of chemical explosions in nonspherical cavities in granite. J. Geophys. Res., 111.

6 Summary of Technical Reports / Papers Published

6.1 Processing of low-magnitude seismic events near Novaya Zemlya

Sponsored by US Army Space and Missile Defence Command, Contract No. W9113M-05-C-0224

Introduction

The regional processing system at the NORSAR Data Center, as described in detail by Ringdal and Kværna (2004), comprises the following steps:

- Automatic single array processing, using a suite of bandpass filters in parallel and a beam deployment that covers both P and S type phases for the region of interest.
- An STA/LTA detector applied independently to each beam, with broadband f-k analysis for each detected phase in order to estimate azimuth and phase velocity.
- Single-array phase association for initial location of seismic events, and also for the purpose of chaining together phases belonging to the same event, so as to prepare for the subsequent multiarray processing.
- Multi-array event detection, using the Generalized Beamforming (GBF) approach (Ringdal and Kværna, 1989; Kværna et. al., 1999) to associate phases from all stations in the regional network and thereby provide automatic network locations for events in all of northern Europe. The resulting automatic event list is made available on the Internet (www.norsar.no).
- Interactive analysis of selected events, resulting in a reviewed regional seismic bulletin, which includes hypocentral information, magnitudes and selected waveform plots. This reviewed bulletin is also available on the Internet.

Experience over the past several years has demonstrated that the automated event list generated by the GBF procedure is nearly "complete", in the sense that it provides an exhaustive search of all possible detected phase combinations that could correspond to real events. The reviewed bulletin is more selective, since our current resources do not allow a complete analysis of all real seismic events that are associated through the automatic algorithms. An important topic of current research is to develop methods to enable the analyst to easily select events from areas of particular interest, and focus on these events in the interactive analysis.

A major enhancement to the monitoring network has been the recent upgrade of the Spitsbergen seismic array, which has included installation of five new three-component seismometers as well as an upgrading of the sampling rate from 40 to 80 Hz. In another contribution in this isssue, Schweitzer and Kværna (2006) describe some recent processing improvements in the Spitsbergen on-line detection system that have been made to take advantage of these enhancements.

Detection of small seismic events near Novaya Zemlya

Over the years, the regional processing system at NORSAR has detected a number of small seismic events on or near Novaya Zemlya. As estimated by Ringdal (1997), the threshold of the array network to confidently detect and locate seismic events in this region is about magnitude

2.5. The two regional arrays Spitsbergen and ARCES are by far the most sensitive monitoring stations, but occasionally other stations will contribute to improved location accuracy for detected events.

Table 6.1.1 lists small seismic events in the Novaya Zemlya region, located outside the nuclear test site and detected over the years by the NORSAR regional processing system. During March 2006, three such events occurred, as listed in the table. These events, which we denote as 2006-064, 2006-073 and 2006-089 were all very small, with magnitudes of 2.7, 2.2 and 2.3 respectively. Figure 6.1.1 shows the location and associated error ellipse of each of these three events. In this paper, we discuss the detection performance and signal characteristics of these three events in some detail.

We first comment briefly upon the performance of the automatic Generalized Beamforming (GBF) system in operation at NORSAR. At the time these events occurred, all three events were well defined by the automatic process (Table 6.1.2), and could thus easily be reviewed by the analyst, with appropriate editing and correction of phase readings. This performance is quite impressive, taking into account the low magnitudes of these events and the considerable epicentral distance (about 1000 km or more to the nearest array). Nevertheless, there are some features that point to the need for further enhancement. In particular, we note that event 2006-073 has no Sn phase detection at the Spitsbergen array but, even so, the event location is quite good. Event 2006-089 has an ARCES Lg phase which is clearly erroneous. Lg phases are never detected at ARCES (or Spitsbergen) for Novaya Zemlya events, because of the blockage effect caused by the thick sedimentary layers in the Barents Sea.

As discussed by Schweitzer and Kværna (2006), the main improvement to the on-line processing systems in operation at NORSAR that has been made possible with the upgraded Spitsbergen array is the ability to improve the detection of Sn-phases. The difficulties in detecting Sn phases at Spitsbergen has been noted in previous Semiannual Reports, and is one of the main reasons behind the inclusion of additional three-component sensors in the current upgrade. We will return to a discussion of possible ways to make optimal use of the horizontal components for Sn-phase detection later in this paper.

We also comment briefly upon the locations shown in Figure 6.1.1. The locations have been made using the two arrays Spitsbergen and ARCES only. The Spitsbergen channel SPB5_BHZ was not used in direction estimates for the 2006-073 event since the time-stamp is demonstrably incorrect at this time. The estimated epicenters are all offshore, but the error ellipses indicate that coastal or inland locations cannot be entirely excluded, even for the event on 30 March. The point here is that accurate location error ellipses are extremely difficult to calculate, since they require knowledge of both the earth model error and the reading errors for the arrival time picks. While we believe that the Barents model is quite reliable, the time picks are subject to a considerable uncertainty, especially in view of the emergent nature of many of the signals. For small seismic events, with low signal-to-noise ratios, the uncertainty in time picks is very difficult to quantify.

High frequency spectral characteristics

The increase in sampling rate from 40 to 80 Hz at the Spitsbergen array enables us for the first time to study high frequency characteristics of the signals recorded at this site. Many studies

have emphasized the outstanding quality of high-frequency seismic recordings at this array, e.g. several contributions in previous Semiannual Reports, as well as a publication by Bowers et. al. (2001). We are now in a position to verify some of these projections.

Figure 6.1.2 shows Spitsbergen spectrograms for the 2006-064 event. We have chosen the three-component instrument at array site B1 for this display, and the vertical component is shown along with the rotated longitudinal and transverse components. The most noticeable feature is the high SNR of the P-phase for this small (m_b=2.7) event. In fact, the SNR on the array beam is above 100, indicating that even an event at this site more than an order of magnitude smaller could have been detected. This should not, however, be extrapolated to a general statement about detection thresholds for the Spitsbergen array, since the SNR to a large extent depends upon path-specific focussing effects. Nevertheless, the amount of high-frequency energy is remarkable, taking into account that the epicentral distance is as large as 1100 km. We note that the vertical and radial components have significant P-wave energy even above 20 Hz. The transverse component shows (not unexpectedly) a small P-wave and a much larger S-wave, indicating that the use of transverse components could be useful in detecting S-phases.

This type of spectrogram is also quite useful in studying the data quality as recorded by individual seismometers. As an example, Figure 6.1.3 shows Spitsbergen spectrograms for six individual seismometers (vertical components) for the 2006-089 event. We have chosen the center seismometer and the five seismometers in the B-ring. We note that three seismometers (A0, B2 and B5) have significant and nearly constant noise in the frequency interval 25-30 Hz. The source of this noise, which occurs periodically over extended time intervals, is not known. Furthermore, the seismometer B4 has strong noise at 10 Hz and below. The reaons for these abnormal noise conditions and possibilities for their mitigation are being investigated.

The 2006-089 event shown in Figure 6.1.3 had a magnitude of 2.3 and is thus considerably smaller than the 2006-064 event which was shown in Figure 6.1.2. In addition, the distance to the Spitsbergen array is somewhat greater in this case (1300 km versus 1100 km for the 2006-064 event). Consequently, the signal-to-noise ratio is not quite as large as for the earlier event. Nevertheless, we see that for the best sites signal frequencies well above 20 Hz are recorded. At two of the sites (B4 and B5) the signal is masked by noise. For the site B5, a 20 Hz low-pass filter would give a satisfactory signal-to-noise ratio. The site B4 has too strong noise to be useful for detection purposes, and this site is currently masked out in the on-line detection process. Nevertheless, B4 can be useful for slowness estimation of larger signals.

We would like at this point to give some additional comments about the advantage of high-frequency recordings. Figure 6.1.4 and 6.1.5 show Spitsbergen seismometer B1 filtered in various passbands for events 2006-064 and 2006-089. The event 2006-064 is the largest one, and consequently has stronger signals than 2006-089. Nevertheless, the signal-to-noise ratios are high for all of the filter bands for both of the events. The best filter band for detection appears to be either 5-10 Hz or 10-20 Hz. However, the most remarkable feature is the strong SNR even at the highest frequencies (20-36 Hz). While such a frequency band would not be used for detection purposes, the high frequency data could be very important for signal characterization, as discussed by Bowers et. al. (2001).

Sn-phase detection at the Spitsbergen array

As mentioned earlier, the inclusion of 6 three-component seismometers in the upgraded Spitsbergen array has made possible improved processing of Sn-phases. Figures 6.1.6-6.1.8 show, for each of the three events, Sn beams steered towards the epicenter using the rotated (transverse) components, as well as more conventional Pn and Sn beams from the vertical components.

In each figure, the top trace is a beam steered to the epicenter with a P-wave velocity, and using a typical detection filter (3-16 Hz). The middle trace is an "optimum" beam designed to detect the S-wave. It represents the beams of the transverse components of the six three-component seismometers in the array, filtered in the band 2-4 Hz and steered to the epicenter with an S-phase velocity. The bottom trace shows, for comparison, an Sn-beam of vertical sensors using the same (2-4 Hz) filter.

Although there are some differences in signal-to-noise ratios of the three events, the general interpretation of the three figures is similar: The two beams based upon vertical components (the top and bottom trace of each figure) show clear Pn and Sn phases, but the Sn phase could be difficult to detect by a power detector due to the strong preceding coda from the Pn-phase. In contrast, the middle trace, which uses only the horizontal components, rotated in the transverse direction, shows almost no sign of the Pn phase, whereas the Sn phase is quite strong. Clearly, the detection of Sn-phases could be greatly improved by augmenting the beam deployment with several steered beams, rotated so as to provide transverse components, toward the grid points in the beam deployment system.

Discussion

This analysis has reconfirmed our previous estimates of the detection capability of the regional array network in northern Europe, indicating that the network is capable of detecting seismic events at Novaya Zemlya down to about magnitude 2.5 (Ringdal, 1997). The automatic detection and location of the three seismic events in March 2006 near Novaya Zemlya have shown that the GBF process in operation at NORSAR works well. Nevertheless, some possibilities for improvements have been noted, in particular the potential for improved Sn-phase detection by the Spitsbergen array, using the recently installed three-component seismometers. An enhanced detection processing system for the Spitsbergen array is discussed in another contribution in this issue (Schweitzer and Kværna, 2006).

The new Spitsbergen array configuration has shown excellent recordings of high-frequency data from Novaya Zemlya events. For the first time, we have been able to verify that significant signal energy at frequencies above 20 Hz can be recorded for events near Novaya Zemlya, at an epicentral distance exceeding 1000 km. This is a quite remarkable observation, and supports the projections made by Bowers et. al. (2001) in their paper discussing the level of deterrence to possible CTBT violations in the Novaya Zemlya region provided by data from the Spitsbergen array.

References

Bowers, D., P. D. Marshall, and A. Douglas (2001). The level of deterrence provided by data from the SPITS seismometer array to possible violations of the Comprehensive Test Ban in the Novaya Zemlya region, *Geophys. J. Int.*, 146, pp. 425-438.

Kværna, T., J. Schweitzer, L. Taylor and F. Ringdal (1999): Monitoring of the European Arctic using Regional Generalized Beamforming. *Semiannual Technical Summary 1 October 1998 - 31 March 1999*, NORSAR Sci. Rep. 2-98/99, Kjeller, Norway.

Marshall, P.D., R.C. Stewart and R.C. Lilwall (1989): The seismic disturbance on 1986 August 1 near Novaya Zemlya: a source of concern? *Geophys. J.*, 98, 565-573.

Ringdal, F., 1997. Study of low-magnitude seismic events near the Novaya Zemlya nuclear test site. *Bull. Seism. Soc. Am.*, **87**, 1563-1575

Ringdal, F., and T. Kværna (1989). A multi-channel processing approach to real time network detection, phase association, and threshold monitoring, *Bull. seism. Soc. Am.*, **79**, pp. 1927-1940.

Ringdal, F., and T. Kværna (2004). Some aspects of regional array processing at NORSAR. Semiannual Technical Summary, 1 July – 31 December 2003, NORSAR Sci. Rep. **1-2004**, 34-44.

Schweitzer, J. and T. Kværna (2006): Upgrading the Spitsbergen on-line data processing system. *Semiannual Technical Summary 1 January - 30 June 2006*, NORSAR Sci. Rep. 2-2006, Kjeller, Norway.

Frode Ringdal
Steven J. Gibbons

Table 6.1.1: List of seismic events in or near Novaya Zemlya (1980-2006) located outside the test site

Date/time	Location	m_b	Comment
01.08.1986/ 13.56.38	72.945 N, 56.549 E	4.3	Located by Marshall et.al. (1989)
31.12.1992/ 09.29.24	73.600 N 55.200 E	2.7	Located by NORSAR
23.02.1995/ 21.50.00	71.856 N, 55.685 E	2.5	Located by NORSAR
13.06.1995/ 19.22.38	75.170 N, 56.740 E	3.5	Located by NORSAR
13.01.1996/ 17.17.23	75.240 N, 56.660 E	2.4	Approximately co-located with preceding event
16.08.1997/ 02.11.00	72.510 N, 57.550 E	3.5	Located by NORSAR
16.08.1997/ 06.19.10	72.510 N, 57.550 E	2.6	Co-located with preceding event
23.02.2002/ 01.21.14	74.047 N, 57.671 E	3.0	Located by NORSAR
27.07.2002 18.20.45	73.720N 56.870E	2.0	Located by NORSAR
10.11.2002 11.04.47	70.880N 47.401E	2.0	Located by NORSAR
08.10.2003/ 23.07.10	75.645N, 63.345E	2.5	Located by NORSAR
05.03.2006/ 23.17.36	76.800N, 66.040E	2.7	Located by NORSAR
14.03.2006/ 20.57.02	75.070N, 53.050E	2.2	Located by NORSAR
30.03.2006/ 10.46.03	70.790N, 51.500E	2.3	Located by NORSAR

Table 6.1.2. Automatic on-line GBF results for three Novaya Zemlya events during March 2006.

NOVAYA ZEMLYA, RUSSIA

Origin time	Lat	Lon	Azres	Timres	Wres	Nphase	Ntot	Nsta	Netmag
2006-064:23.17.35.0	76.80	66.04	8.04	0.56	2.57	3	11	2	2.65

Sta	Dist	Az	Ph	Time	Tres	Azim	Ares	Vel	Snr	Amp	Freq	Fkq	Arid	Mag
SPI	1176.3	72.5	p	23.20.02.4		77.4	4.9	8.4	119.9	1823.9	11.90	2	482426	
SPI	1176.3	72.5	p	23.20.04.6		73.9	1.4	7.8	14.8	368.4	5.73	1	482427	
SPI	1176.3	72.5	p	23.20.08.6		78.4	5.9	8.0	9.9	1944.8	9.82	3	482428	
SPI	1176.3	72.5	p	23.20.13.8		83.5	11.0	8.2	5.9	507.9	5.36	1	482429	
SPI	1176.3	72.5	Sn	23.21.56.4	0.0	66.5	-6.0	4.8	27.2	279.8	4.58	2	482431	2.49
SPI	1176.3	72.5	s	23.21.59.9		69.9	-2.6	4.2	9.8	671.4	5.06	3	482438	2.78
SPI	1176.3	72.5	s	23.22.02.5		74.5	2.0	5.0	6.9	1388.2	8.90	3	482440	
ARC	1497.3	39.9	Pn	23.20.43.4	-1.5	57.5	17.6	9.6	4.8	38.0	6.25	2	482275	
ARC	1497.3	39.9	p	23.20.47.5		47.0	7.1	10.4	6.5	44.4	7.00	1	482276	
ARC	1497.3	39.9	Sn	23.23.03.8	-0.1	39.4	-0.5	3.5	9.0	44.9	3.46	3	482289	2.42
ARC	1497.3	39.9	s	23.23.09.3		59.0	19.1	5.0	7.2	62.0	3.72	3	482292	2.53

NOVAYA ZEMLYA, RUSSIA

Origin time	Lat	Lon	Azres	Timres	Wres	Nphase	Ntot	Nsta	Netmag
2006-073:20.56.46.0	74.72	57.94	9.10	0.50	2.77	3	7	2	2.23

Sta	Dist	Az	Ph	Time	Tres	Azim	Ares	Vel	Snr	Amp	Freq	Fkq	Arid	Mag
SPI	1126.7	88.5	Pn	20.59.10.6	-0.3	96.1	7.6	8.4	18.5	435.7	9.54	3	519913	
SPI	1126.7	88.5	p	20.59.12.9		101.3	12.8	8.0	8.6	492.4	10.38	3	519915	
SPI	1126.7	88.5	p	20.59.15.4		98.0	9.5	9.1	7.7	450.3	9.73	3	519916	
SPI	1126.7	88.5	p	20.59.18.3		97.4	8.9	8.4	5.9	337.2	9.57	3	519919	
ARC	1232.8	47.7	Pn	20.59.24.4	0.6	57.5	9.8	10.6	5.4	47.1	5.65	2	519914	
ARC	1232.8	47.7	Sn	21.01.20.0	0.6	57.5	9.8	4.7	4.4	57.2	6.19	3	519921	2.07
ARC	1232.8	47.7	s	21.01.22.3		55.8	8.1	5.4	5.5	58.5	4.36	2	519923	2.23

BARENTS SEA

Origin time	Lat	Lon	Azres	Timres	Wres	Nphase	Ntot	Nsta	Netmag
2006-089:10.46.43.0	70.61	42.57	8.59	0.80	2.95	4	13	2	2.30

Sta	Dist	Az	Ph	Time	Tres	Azim	Ares	Vel	Snr	Amp	Freq	Fkq	Arid	Mag
ARC	659.1	71.6	Pn	10.48.11.0	-0.1	75.7	4.1	8.6	18.3	70.1	5.08	1	35736	
ARC	659.1	71.6	p	10.48.16.5		72.2	0.6	9.1	5.7	64.5	6.63	2	35737	
ARC	659.1	71.6	p	10.48.21.7		72.9	1.3	8.8	5.3	71.8	3.35	1	35738	
ARC	659.1	71.6	p	10.48.27.0		76.0	4.4	8.4	3.8	51.5	4.73	1	35742	
ARC	659.1	71.6	Sn	10.49.17.0	1.3	47.4	-24.2	4.7	3.8	375.4	1.00	1	35752	1.65
ARC	659.1	71.6	Lg	10.49.50.2	-1.0	73.8	2.2	5.3	12.4	305.6	3.91	1	35753	2.00
ARC	659.1	71.6	s	10.49.53.6		83.3	11.7	3.2	10.8	407.1	3.07	1	35754	2.23
ARC	659.1	71.6	s	10.49.57.1		78.3	6.7	3.1	4.8	163.6	3.71	3	35755	
ARC	659.1	71.6	s	10.50.06.0		75.9	4.3	3.9	4.0	249.0	2.50	1	35756	
SPI	1136.4	123.8	p	10.48.54.5		104.4	-19.4	8.3	6.7	167.9	4.78	2	35882	
SPI	1136.4	123.8	Sn	10.50.55.2	-0.8	120.0	-3.8	5.5	4.8	126.2	5.46	3	35886	1.99
SPI	1136.4	123.8	s	10.50.58.5		113.2	-10.6	5.0	7.1	229.6	5.95	2	35887	
SPI	1136.4	123.8	s	10.51.02.6		102.7	-21.1	5.4	5.4	193.4	4.39	1	35888	2.36

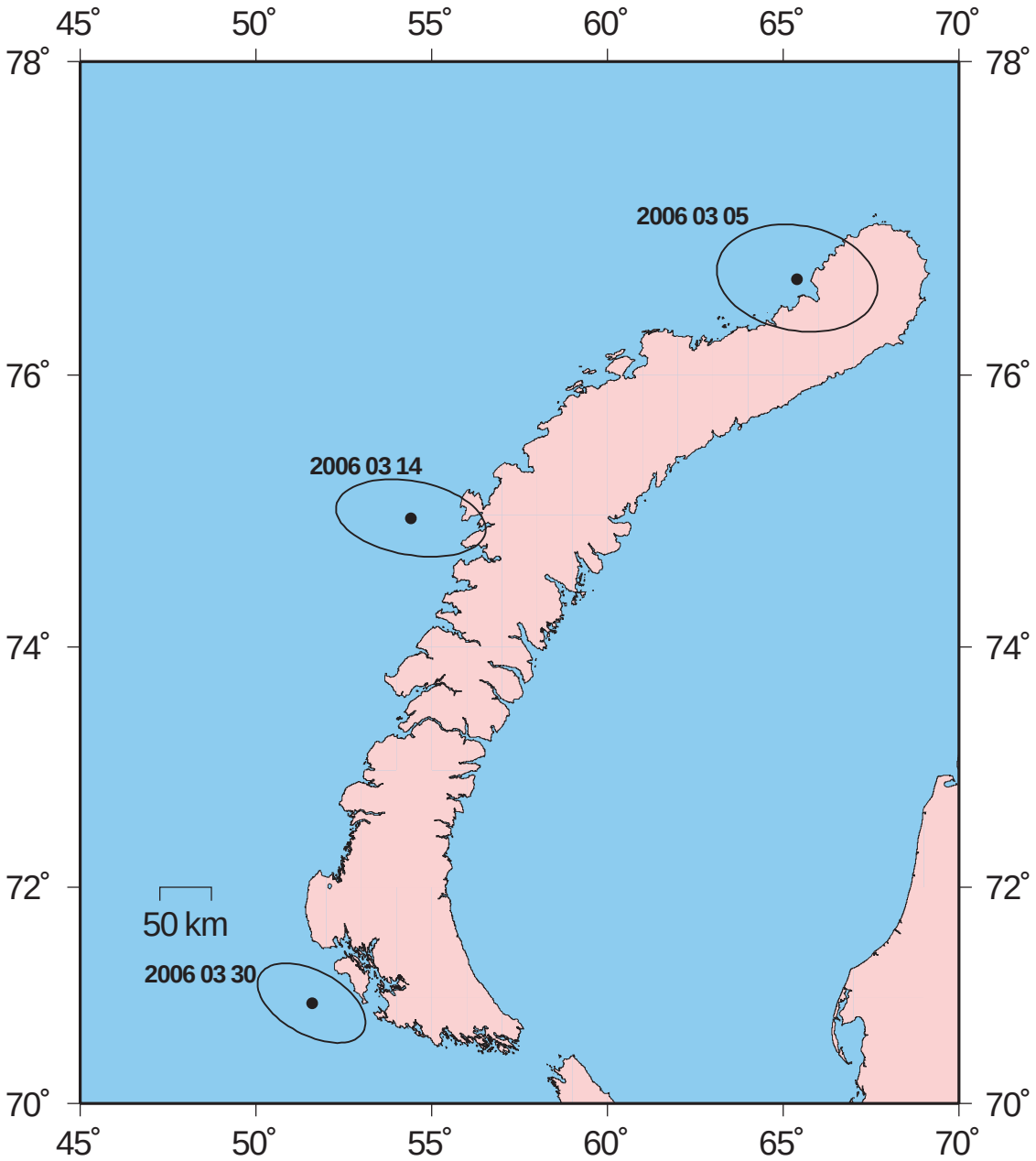

Fig. 6.1.1. Map of Novaya Zemlya showing the location of three seismic events during March 2006 as discussed in the text, together with their 90% confidence ellipses.

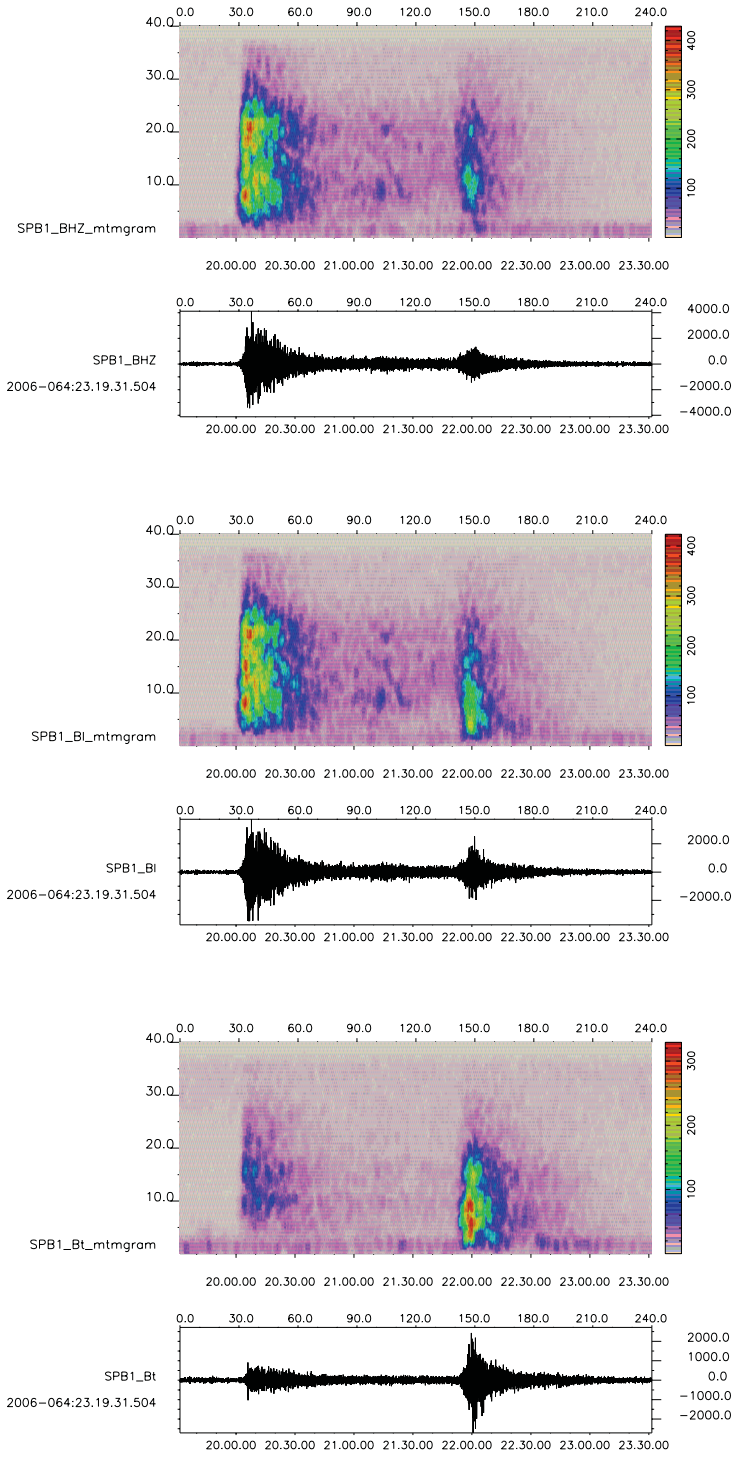

Fig. 6.1.2. Spectrograms for the Spitsbergen B1 seismometer for the Novaya Zemlya event on 5 March 2006. Top: vertical component; middle: longitudinal rotation; bottom: transverse rotation. The waveform traces are filtered with a 2 Hz high-pass filter. See text for details.

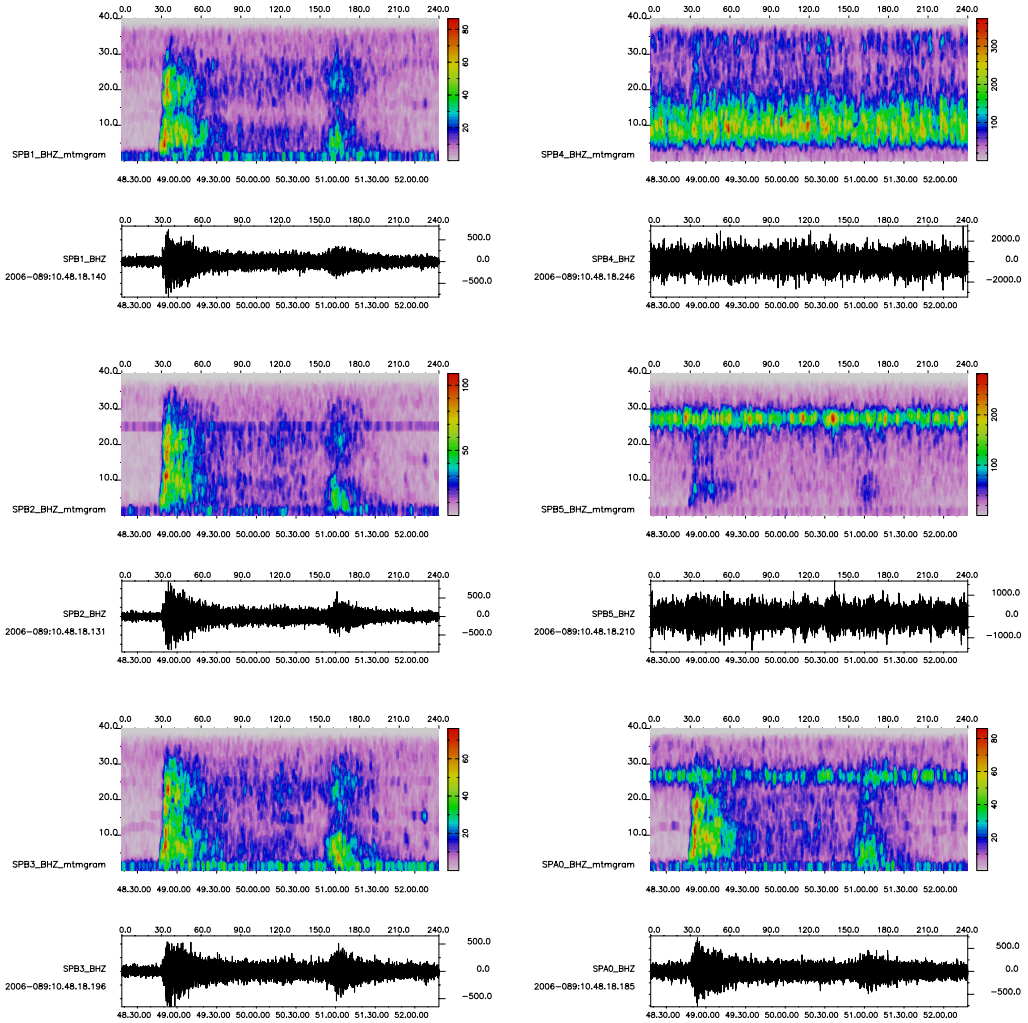

Fig. 6.1.3. *Spectrograms for the Spitsbergen A0 and B-ring seismometers (vertical components) for the Novaya Zemlya event on 30 March 2006. The waveform traces are filtered with a 2 Hz high-pass filter. See text for details.*

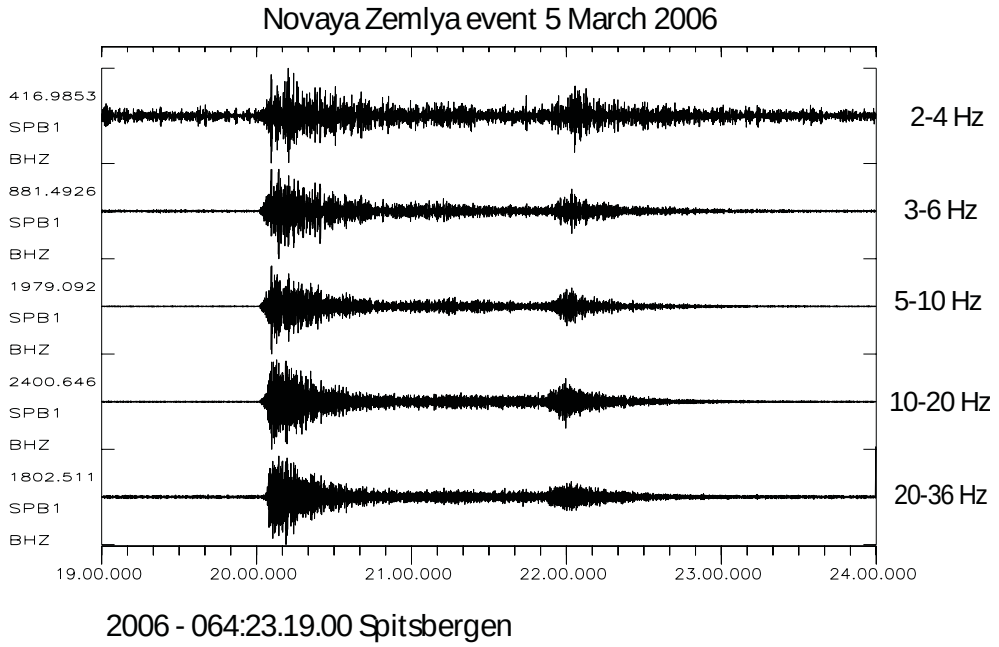

Fig. 6.1.4. ***Spitsbergen seismometer B1 recording for the 5 March 2006 Novaya Zemlya event, filtered in various passbands . Note the strong SNR even at the highest frequencies (20-36 Hz).***

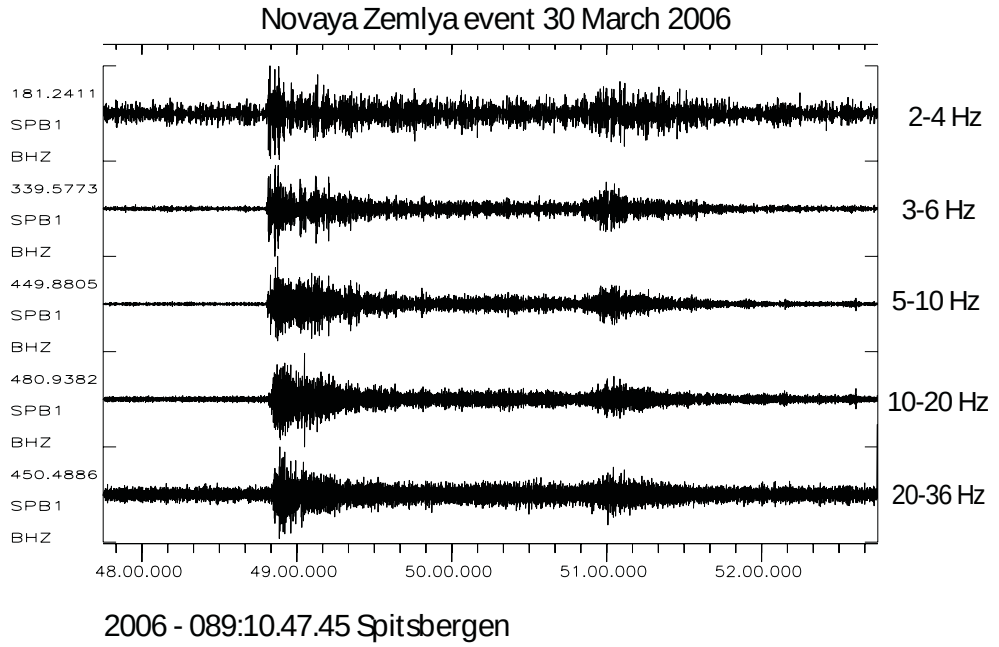

Fig. 6.1.5. ***Spitsbergen seismometer B1 recording for the 5 March 2006 Novaya Zemlya event, filtered in various passbands. Although the SNR is less than for the 5 March event, there is still significant signal energy in all of the frequency bands.***

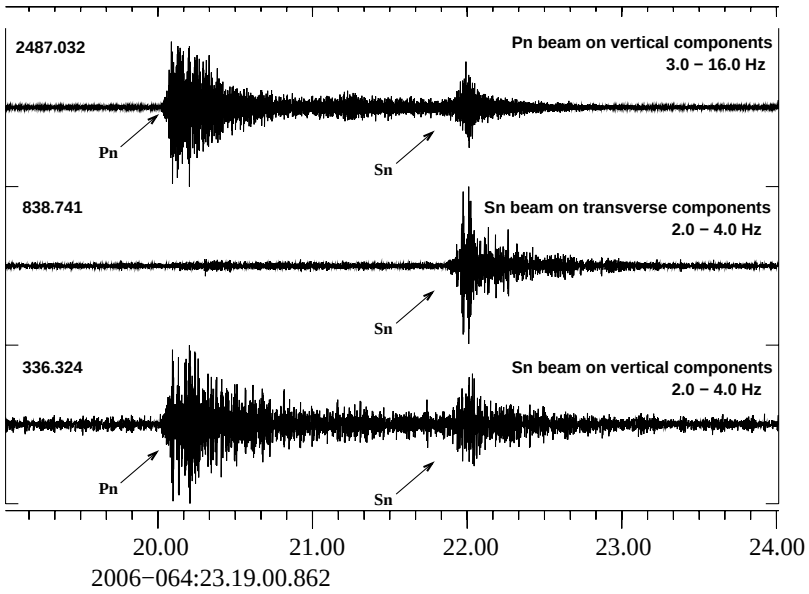

Fig. 6.1.6. Spitsbergen array waveforms for the 5 March 2006 Novaya Zemlya event. Note the greatly improved SNR gain for the Sn phase shown in middle trace, which represents the beams of the transverse components of the six three-component seismometers in the array.

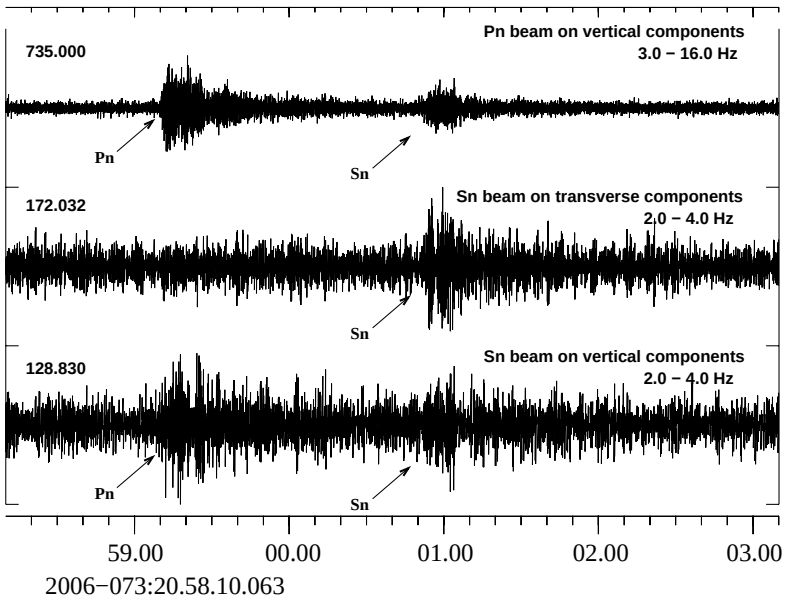

Fig. 6.1.7. Spitsbergen array waveforms for the 14 March 2006 Novaya Zemlya event.

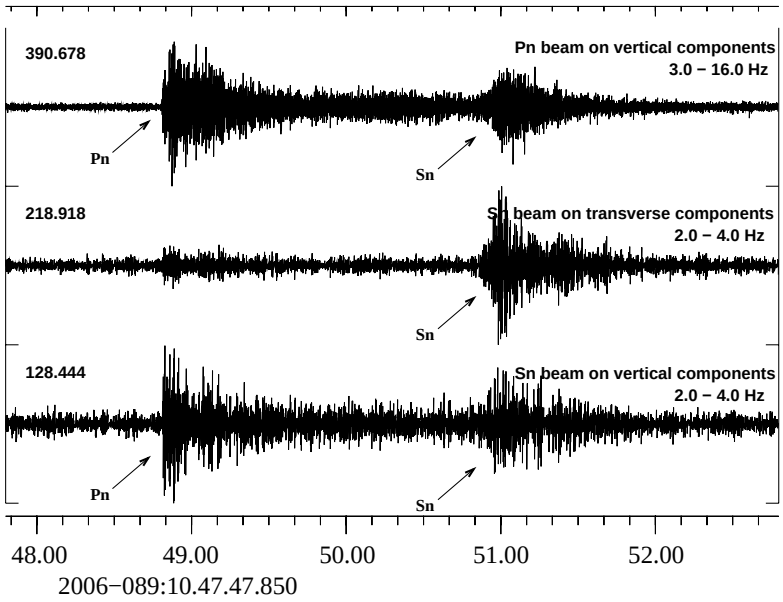

Fig. 6.1.8. *Spitsbergen array waveforms for the 30 March 2006 Novaya Zemlya event.*

6.2 Infrasound observations of two recent meteor impacts in Norway

6.2.1 Introduction

During the summer of 2006, a large number of people observed sound and light phenomena from two meteor impacts in Norway. The first impact was on 7 June at about 00:07 GMT in northern Norway (Finnmark) and the second impact was on 14 July at about 08:18 GMT in southern Norway (Oslo Fjord area). The observations indicate that the first event was larger than the second. Fragments of the meteors have up to now only been found for the second event in Rygge and Moss (see e.g., Aftenposten, 17 & 18 July 2006).

After NORSAR was informed by interested or frightened people about their meteor observations, a detailed data analysis was started to search for infrasonic or seismic signals of these explosive events in the atmosphere. In both cases, we were able to find such signals and to define a location of the probable explosions. This contribution reports on these preliminary results.

6.2.2 The impact of 7 June 2006

Observations on the ARCES seismic array

As known from former studies, the seismic sensors of the ARCES array are quite sensitive to infrasound signals (Ringdal & Schweitzer, 2005; Ringdal & Gibbons, 2006; Schweitzer et al., 2006). The meteor itself most probably exploded in the atmosphere at approximately 10 to 20 km above the ground. Until now, no fragments were found. The explosion was heard over a large area of northern Norway, and although the sky was quite bright due to the midnight sun, the explosion was also observed visually, and pictures are available from its smoky trace (e.g., Aftenposten, 9 June 2006).

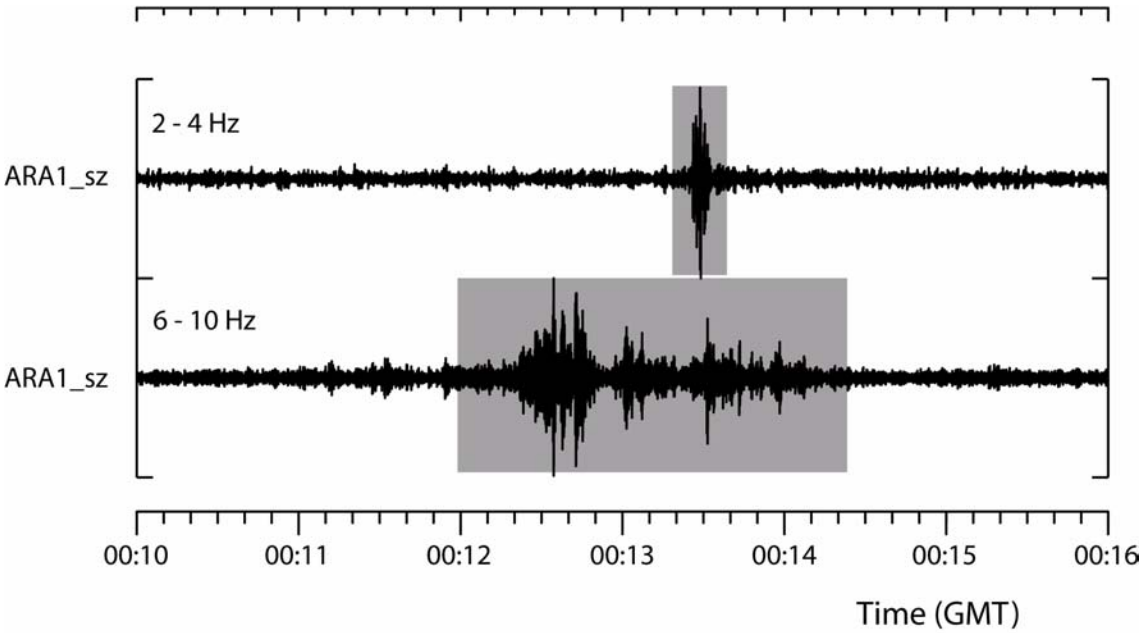

Fig. 6.2.1. The two different signals observed at the ARCES site A1. The upper trace shows the infrasound signal of the meteor explosion on 7 June 2006 and the lower trace higher frequency Rg waves observed at the same time.

The ARCES array is located east of the presumed explosion and, some minutes after the reported explosion time, a strong signal was recorded crossing the array from west to east with an apparent velocity of about 330 m/s. The upper trace in Fig. 6.2.1 shows this signal at the ARCES array site ARA1 after Butterworth bandpass filtering between 2 and 4 Hz. The lower trace in Fig. 6.2.1 shows a higher frequency signal (filtered between 6 and 10 Hz) that reached the array during the same time window from the west but with varying backazimuth (BAZ) and an apparent velocity of about 2.5 km/s, which is typical for Rg phases. In a first interpretation it was assumed that these signals were generated by the same source but the varying BAZ of the Rg-type energy was impossible to explain with the single explosion of a meteor.

To investigate these two signals in more detail, vespagrams were calculated in different frequency ranges and for different apparent velocities. The left panel of Fig. 6.2.2 shows a vespagram for a 20 minute long time window and a constant BAZ of 260 degrees. Two different signals are clearly visible: one with an apparent slowness of about 0.4 s/km (the Rg signal) followed by a signal with an apparent slowness of about 3 s/km (the infrasound signal). The right hand panel of Fig. 6.2.2 shows the time dependence of the infrasound signal (i.e., for energy with a constant apparent slowness of 3 s/km) with respect to the observed BAZ. The vespagram shows that the infrasound signal was generated during one single event and that its BAZ is quite stable at about 259 degrees.

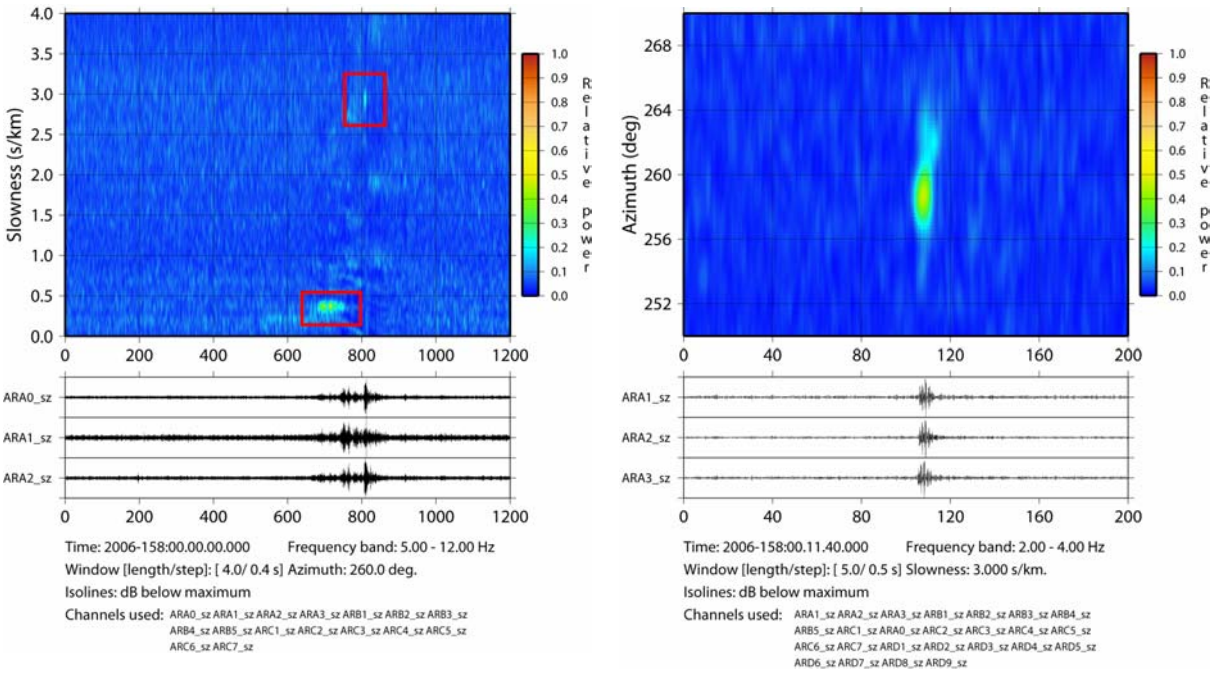

Fig. 6.2.2. Vespagrams of the data recorded at ARCES, see text for details.

Fig. 6.2.3 shows on the left the vespagram of the Rg signal recorded with the infrasound signal. In this case the constant apparent velocity was 2.5 km/s. As can be seen, the Rg signal starts earlier and ends later than the infrasound signal, which would be visible at about 200 s after the start of the vespagram. The spread of the BAZ values is quite remarkable and can only be explained by a moving source, active for more than 3 minutes. However, detailed calculations of theoretical travel time differences between the infrasound signal and an eventually ground coupled Rg energy could not be matched with the observations, and in addition the quite high signal frequency of the Rg energy indicates that the source may be located quite close to the

array. Some hours later a similar signal could be observed and its vespagram is shown on the right panel of Fig. 6.2.3. It is obvious that the two vespagrams are almost the mirror of each other: once the source moves from north to south (left) and once from south to north (right). Already in earlier times it was observed that heavy vehicles driving on a road at about 1 km west of the array can be seen on seismograms whenever they crossed significant bumps in the road. One can project the observed BAZ range of about 195 to 265 degrees onto this road, which give a road length of about 5 km. Driving with an assumed velocity of 90 km/h, a car will need about 200 s to drive these 5 km. Therefore, it is clear that the Rg signal observed in parallel with the infrasound signal from the meteor explosion was caused by a heavy vehicle driving on this road.

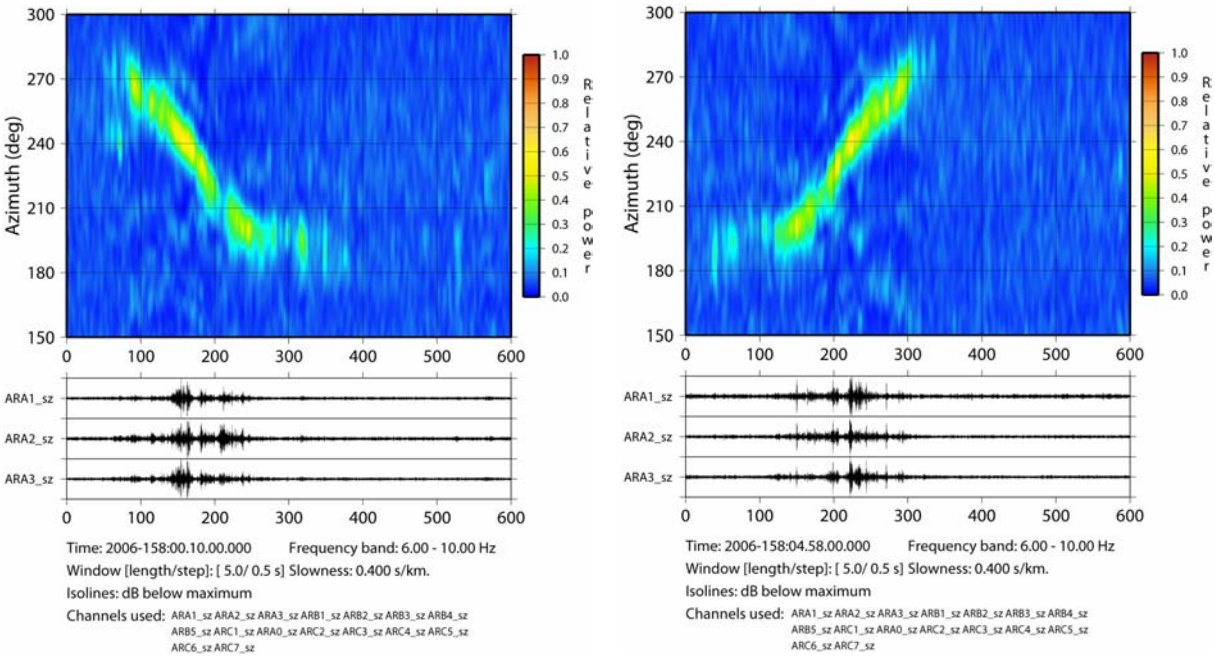

Fig. 6.2.3. Vespagram of the Rg signal as recorded at ARCES in parallel to the infrasound signal on the left and on the right a similar Rg signal recorded approximately 5 hours later.

Observations at the Apatity infrasound array

Many infrasound signals observed at ARCES are also detected by the infrasound array collocated with the Apatity seismic array on the Kola peninsula (Ringdal & Schweitzer, 2005; Ringdal & Gibbons, 2006). Therefore, we searched the infrasound data recorded at Apatity for a signal from this meteor explosion. Unfortunately, the infrasound data were quite noisy during the expected arrival time window and no clear signal is visible on the records. Fig. 6.2.4 shows on the left side the search vespagram for the BAZ range of 180 to 360 degrees during one hour after the event. On this vespagram two signals become visible (blue box) indicating coherent energy arriving the array from a BAZ of about 300 degrees. On the right side of Fig. 6.2.4 a more detailed vespagram is shown for the time and BAZ range around the detected signals.

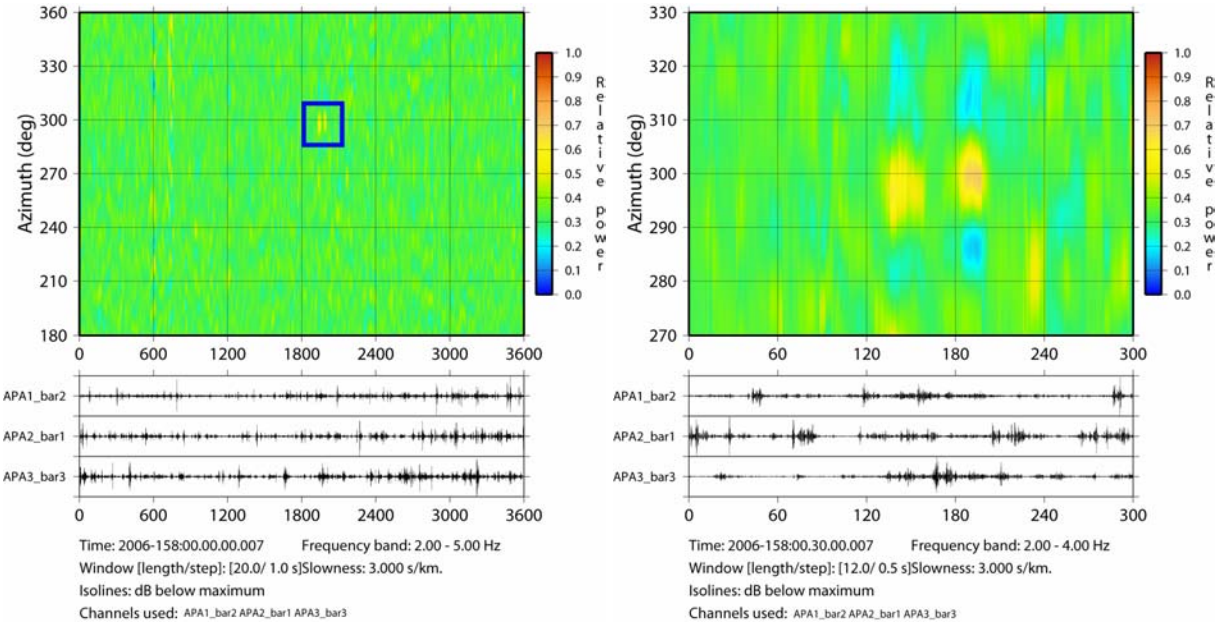

Fig. 6.2.4. Vespagrams showing the signals of the meteor explosion recorded with the Apatity infrasound array. The figure shows to the left the search vespagram with the two detected signals (blue box) and on the right a more detailed vespagram around these signals, respectively.

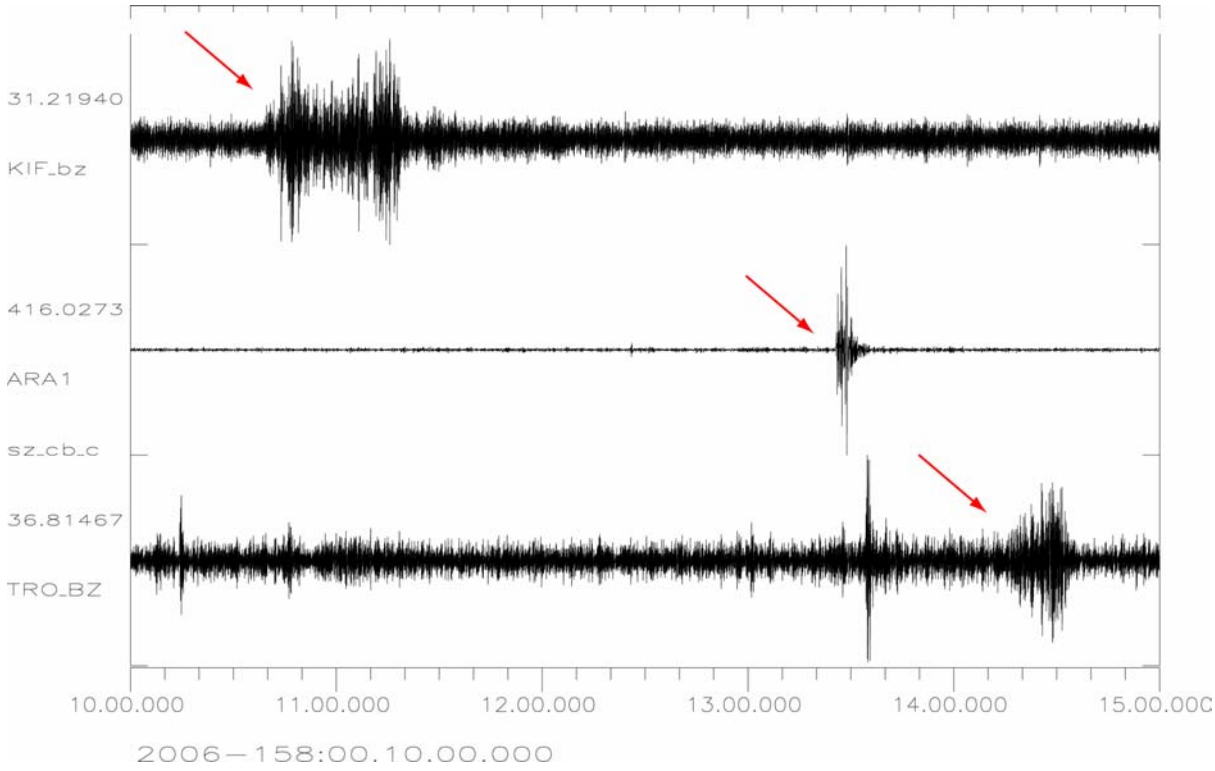

Fig. 6.2.5. Seismograms of the infrasound signal (red arrows) as recorded at the 3C stations KIF and TRO and with the ARCES array (ARA1, array beam). The data were Butterworth bandpass filtered between 2 and 5 Hz (ARA1), 5 and 10 Hz (TRO), and 8 and 16 Hz (KIF).

Additional observations at other stations

The two seismic broadband 3C stations KIF and TRO and the short period station KTK are located in the vicinity of the presumed location of the meteor explosion. We retrieved all available data from these stations and could identify signals at both broadband stations, which can be associated with the meteor event; KTK had unfortunately not triggered during the time period of interest.

In Sweden, a network of infrasound arrays is operated by the Swedish Institute of Space Physics. Some of theses arrays observed the event and signals could be analyzed. We received the measured BAZ values as parameter data from the infrasound arrays Jämtön and Lycksele (Ludwik Liszka, pers. communication).

Also the infrasound arrays in the Netherlands observed infrasound signals for which the observed BAZs, arrival times and apparent velocities fit with the meteor event (Läslo Evers, pers. communication).

Source parameters of the 7 June 2006 meteor explosion

Combining all observations and using them as input to a traditional event location program (HYPOSAT (Schweitzer, 2001)) a presumed location of the meteor explosion could be determined. To locate the event, the BAZ observations from the arrays (ARCES, Apatity, Jämtön, and Lycksele) could be used. The observations at the arrays in the Netherlands were too weak and the estimated onset parameters were too uncertain to be used for locating the event (Laslo Evers, pers. communication). The atmosphere as propagation medium of the infrasound waves was modelled by a simple halfspace with a constant velocity of 0.33 km/s. With this model the onset times of the infrasound signals at nearby stations (KIF, TRO, and ARCES) could also be used to locate the event (see Table 6.3.1).

Table 6.3.1. List of parameter data used to locate the meteor explosion of 7 June 2006

Station	Arrival Time	dt	BAZ	dBAZ
KIF	00:10:39.7	0.5	46.3	5.0
ARCES	00:13:25.8	0.2	259.16	0.3
TRO	00:14:16.5	0.5	48.9	5.0
Apatity	00:32:15.0	2.0	295.0	3.0
Apatity	00:33:01.5	1.0	299.32	2.0
Jämtön	?		1.08	2.0
Jämtön	?		0.96	2.0
Jämtön	?		351.01	2.0
Lycksele	?		13.6	2.0
Lycksele	?		12.82	2.0
Lycksele	?		12.39	2.0

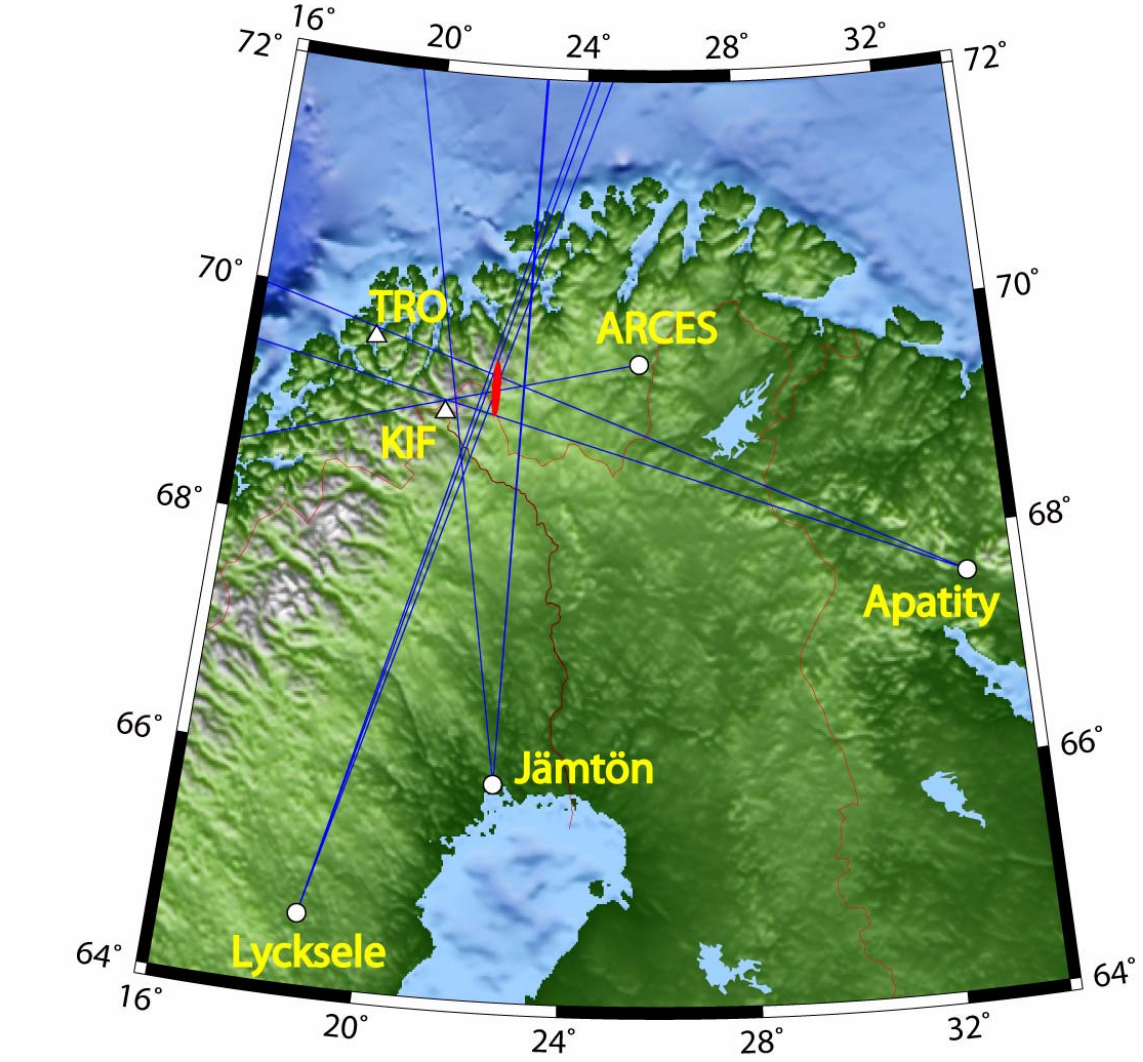

Fig. 6.2.6. Map with arrays (circles) and 3C stations (triangles) which observed the meteor explosion in northern Norway. The blue lines show the BAZ directions of the observed signals and the red ellipse shows the source region (+/- one standard deviation) calculated from these BAZ observations.

Table 6.3.2. List of locations for the meteor explosion above northern Norway on 7 June 2006

Location	Latitude	Longitude	Source Time
BAZ observations only, no height	69.28 +/- 0.23	22.17 +/- 0.09	-
BAZ and onset times, height fixed at 7 km	69.26 +/- 0.01	22.11 +/- 0.01	00:07:05.9 +/- 0.7
Closest people observing the event	69.279	22.383	-

However, our location is biased by the unknown 3D velocity structure of the atmosphere and the unmodelled influence of wind on the observed BAZ values. Two of our location results are listed in Table 6.3.2: one result for a location based on the BAZ observations only with its cor-

responding uncertainty of +/- one standard deviation and one result for a location based on the BAZ observations and the onset times at KIF, ARCES, and TRO. For the latter location the height was fixed at 7 km, which gives the smallest residuals in the chosen halfspace model with a constant velocity of 0.33 km/s. In addition, Table 6.3.2 also lists the position of two persons reporting that they observed the meteor explosion on the sky directly above them. Their position was slightly east of the presumed source region. Despite intensive search, remains of the meteor have yet to be found (Knut Jørgen Røed Ødegaard, pers. communication). A map showing the observing stations together with the presumed source region based on the BAZ observations only (in red) is shown in Fig. 6.2.6.

The observed infrasound signals are related to the size of the meteor explosion. Following ReVelle (1975; 1997), the explosion size of a meteor can be calculated with the formula

$$\log\left(\frac{E}{2}\right) = 3.34 \cdot \log(P) - 2.58$$

where E is the explosion yield in kilotons TNT equivalent and P the dominant period of the infrasound signal. The signal at ARCES has a dominant period of about 1 s and at KIF of about 0.6 s. From this the yield can be calculated as 5.3 tons for ARCES and as 1 ton for KIF. How significant the difference is in yield between the two measurements cannot be decided because contrary to ARCES the seismometer at KIF is installed in a small cabin, which may filter out parts of the infrasound signal and thereby change the observable dominant period.

6.2.3 The impact of 14 July 2006

About five weeks later another meteor was observed during its impact and explosion. This time the observations came from the border region between southern Norway and Sweden. The explosion of the meteor was heard in Rygge and at least 2 fragments were found on ground in the Rygge - Moss area. After we were informed about this new event, data from nearby located seismic stations were searched for corresponding signals. No related signal could be found in records of the broadband station KONO and of the Hagfors array in Southern Sweden. Moreover, on the traces of the short period sensors of the large NORSAR array, a signal was detected crossing the array from south to north with sound velocity. Fig. 6.2.7 shows a seismogram section of all available short period traces of the NORSAR array. The seismograms are plotted with respect to the estimated event location. The infrasound wave can clearly be identified. Unfortunately the signal itself is quite incoherent so that no standard tool to analyze array data could be applied.

To measure the onset time of the infrasound energy, all traces were transformed into short-term-average (STA) traces using a 2 s long moving window with 0.25 s steps. On 28 of the transformed traces the time of the maximum STA value was measured as ‘onset’ time of the infrasound signal. Fig. 6.2.8 shows a section of these STA traces. The measured ‘onset’ times were used as input parameter for HYPOSAT, which again used a halfspace model with a constant velocity of 0.33 km/s.

Using such approximate onset time readings, a very simple velocity model and only observations from one main direction makes the resulting location of the event quite inaccurate. As already mentioned some meteorite fragments were found after the event (Aftenposten, 17 & 18 July 2006, Knut Jørgen Røed Ødegaard, pers. communication). Fig. 6.2.9 shows a map with the location of the event, its corresponding error ellipse, and two of the sites where meteorite fragments were collected. However, the location of the infrasound signal is sufficiently precise

to be connected with the observed meteor explosion and the area where its fragments were found.

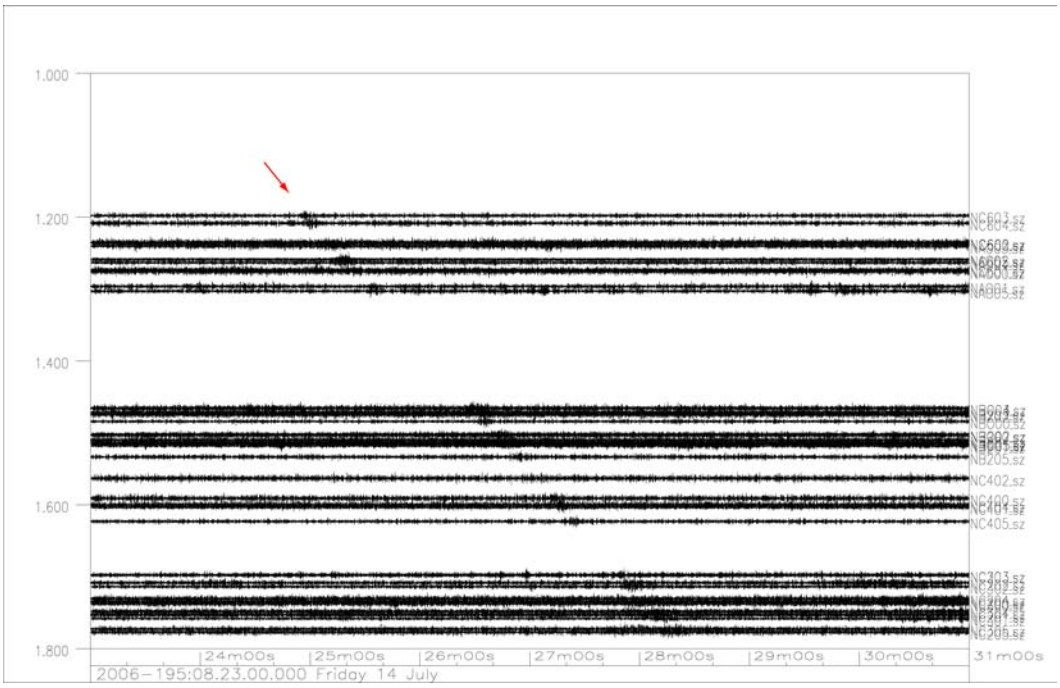

Fig. 6.2.7. Seismogram section with the observed infrasound signal (see red arrow). The data for the short period sensors of the large NORSAR array are 3 - 7 Hz bandpass filtered and plotted with respect to the estimated location of the explosion of the meteor. The vertical axis shows the distance in degrees.

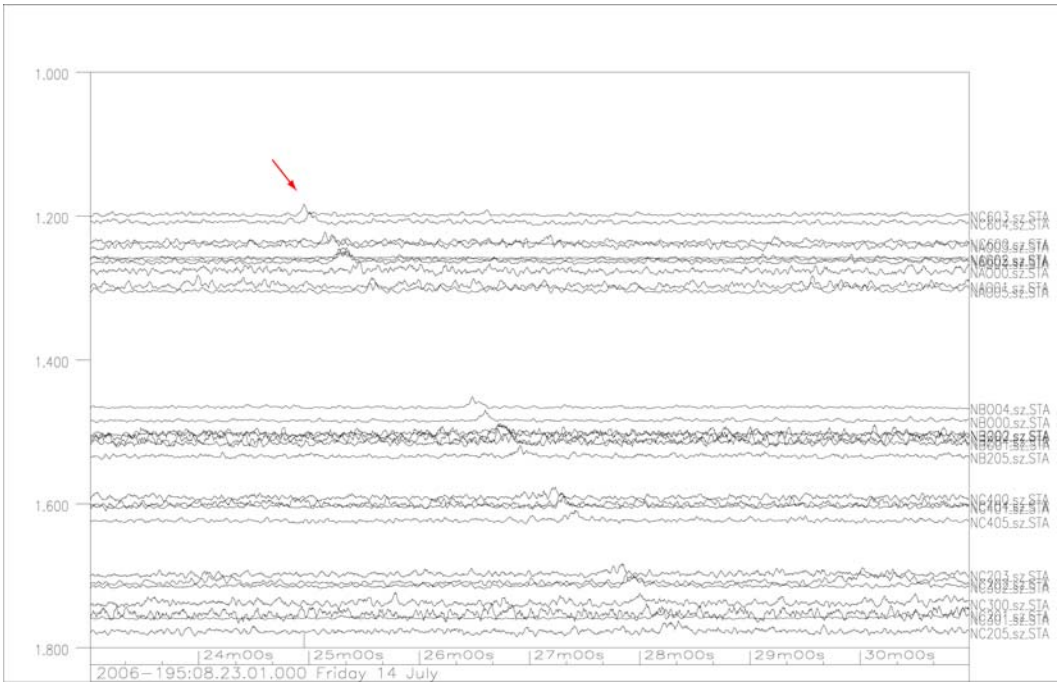

Fig. 6.2.8. Seismogram section as in Fig. 6.2.7, here for the STA traces used to locate the meteor explosion on 14 July 2006.

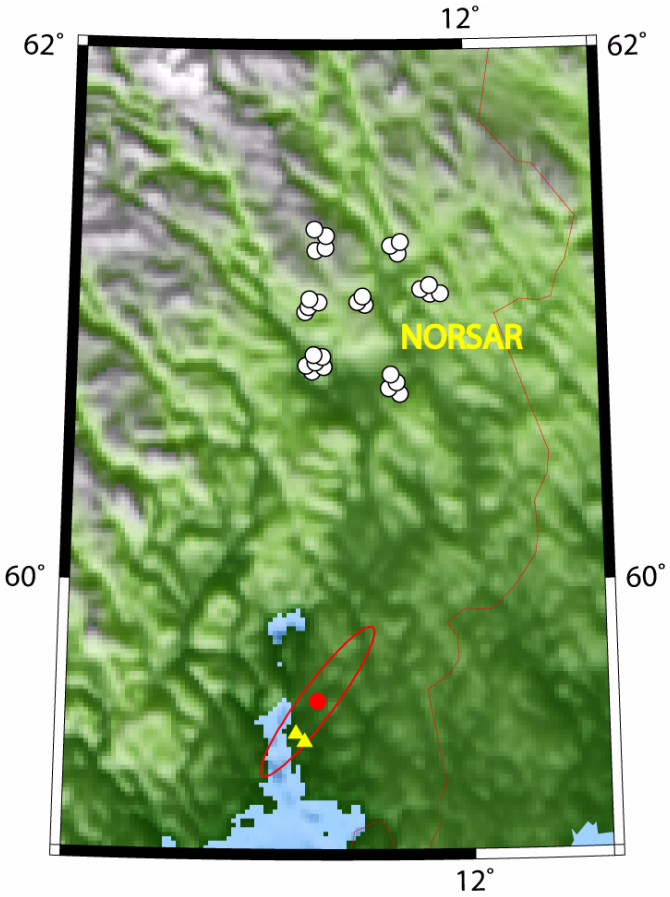

Fig. 6.2.9. Map of the estimated location of the 14 July 2006 meteor explosion in red, estimated using data recorded at the shown NORSAR sites. The yellow triangles show sites where meteorite fragments had been found.

Acknowledgements

Part of this work were supported by the USA SMDC contract W9113M-05-C-0224. The data from the Apatity infrasound array were made available by the Kola Regional Seismological Center (KRSC) in Apatity, from the seismic station KIF of the Finish National Seismic Network operated by the University of Helsinki, and from the seismic station TRO of the Norwegian National Seismic Network operated by the University of Bergen. We thank Ludwik Liszka (Swedish Institute od Space Physics, Umeå) for providing us with the backazimuth observations at the Swedish infrasound arrays Jämtön and Lycksele and Läslo Evers (KNMI, De Bilt), who provided us with observations from two infrasound arrays in The Netherlands. We also thank Knut Jørgen Røed Ødegaard (Institute of Astrophysics, University of Oslo) for stimulating discussions about meteors and meteorites and providing us with helpful information about the actual cases.

Johannes Schweitzer
Tormod Kværna

References

Aftenposten, 9 June 2006: http://www.aftenposten.no/viten/article1345940.ece

Aftenposten 17 July 2006: http://www.aftenposten.no/viten/article1389622.ece

Aftenposten, 18 July 2006: http://www.aftenposten.no/viten/article1390933.ece

ReVelle, D.O. (1975). Studies of sounds from meteors. Sky and Telescope **49,** (2), 87-91

ReVelle, D.O. (1997). Historical detection of atmospheric impacts by large bolides using acoustic-gravity waves. Ann. New York Acad. Sci. **822**, 284-302.

Ringdal, F. & S. Gibbons (2006). Seismic/infrasonic processing: case study of explosions in north Finland. Semiannual Technical Summary, 1 July – 31 December 2005, NORSAR Scientific Report **1-2006**, 54-68.

Ringdal, F. & J. Schweitzer (2005). Combined seismic/infrasonic processing: a case study of explosions in NW Russia. Semiannual Technical Summary, 1 January – 30 June 2005, NORSAR Sci. Rep. **2-2005**, 49-60.

Schweitzer, J., F. Ringdal, T. Kværna, V. Asming & Y. Vinogradov (2006). Infrasound data processing using Apatity and ARCES array data. Semiannual Technical Summary, 1 July – 31 December 2005, NORSAR Scientific Report **1-2006**, 42-53.

Schweitzer, J. (2001). HYPOSAT - an enhanced routine to locate seismic events. PAGEOPH **158**, 277-289.

6.3 Improvements to SPITS regional S-phase detection; coherent beamforming of rotated horizontal components

Sponsored by US Army Space and Missile Defence Command, Contract No. W9113M-05-C-0224

6.3.1 Introduction

During the refurbishment of the SPITS array in 2004, the number of three-component sites was increased from one to six, as proposed by Schweitzer & Kværna (2002). This new array configuration opened for the possibility to redefine and tune the automatic data processing processing recipes of the SPITS array, including redefinition of the detection beam deployment, procedures for fk-analysis and the rules for fully automatic single array event location. This contribution describes the details of the new beam deployment, and presents some examples of the improvements achieved.

6.3.2 The new beam set

The refurbishment of the SPITS array included installation of new broadband sensors with a transfer function which is flat versus acceleration and having a sampling rate of 80 Hz (Fyen, 2004; Fyen 2005). Because of the relatively small aperture of the array (see Figure 6.3.1), array processing tools are effective only for higher frequencies. Therefore, the lower frequencies are removed, and as a first step of the new detection processing all data are prefiltered with a wide 6th order Butterworth bandpass filter between 0.4 and 30 Hz.

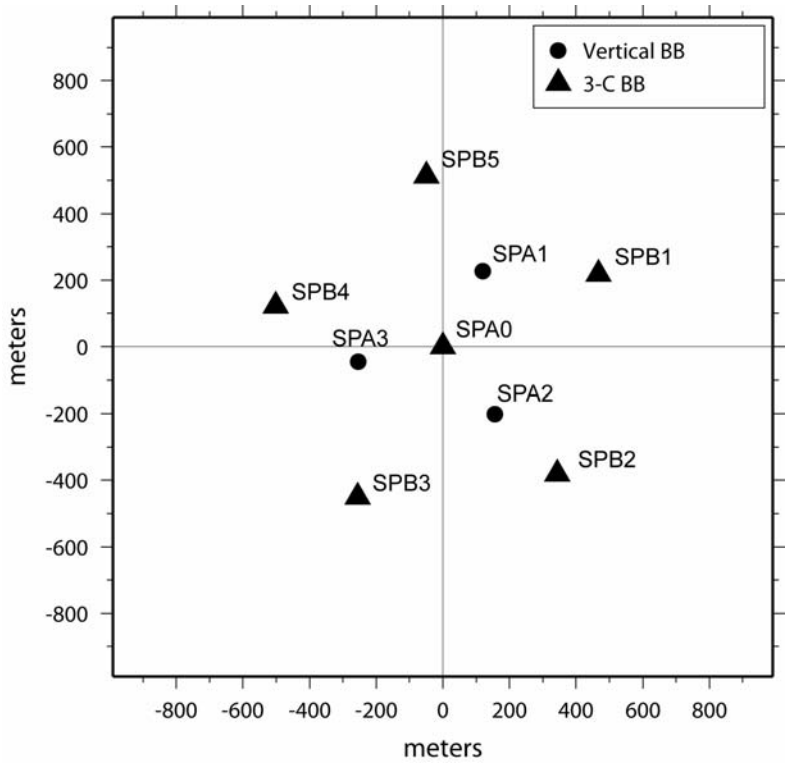

Fig. 6.3.1. Sensor configuration of the upgraded SPITS array. The three sensors of the A-ring are vertical component only, whereas the center instrument SPA0 and the five B-ring sensors are three-component.

Together with the higher sensitivity of the new sensors for higher frequencies, the most important change in the SPITS instrumentation was the installation of five additional 3C sensors. With this change, the array now consists of six sites with horizontal components (SPA0, SPB1, SPB2, SPB3, SPB4, and SPB5), which allows us to run array processing tools also on these components. Based on the observation that regional S-phases at the SPITS array usually have the highest SNR on the horizontal components, the design study for the refurbishment of the SPITS array of Schweitzer and Kværna (2002) proposed the installation of additional 3C sensors. The benefit from having additional 3C sensors are further confirmed by Ringdal and Gibbons (2006) who demonstrated large Sn-phase SNR improvements when using transverse beams for detection of three recent events near Novaya Zemlya.

When using the horizontal components for S-phase detection, it is preferable to decompose the energy into SH and SV components. This is because explosion-type sources are expected to radiate S energy mostly of SV type, whereas many earthquakes (however, depending on the radiation pattern) may dominantly radiate SH energy. Therefore, all horizontal beams are coherently stacked for radial and transverse components after rotating the original north-south and east-west components with respect to the actual backazimuth (BAZ) of the beam. Details about the new beam set are given in Table 6.3.2. A total of 999 beams are defined, out of which 221 are radial component, and 222 are transverse component coherent horizontal beams. The higher sampling rate of the upgraded SPITS array also made it possible to include a high frequency 12-24 Hz filter in the detection processing.

The beam deployment of the old SPITS array (Schweitzer, 1998) included 257 beams, and after the 2004 refurbishment, an initial attempt was made to improve the S-phase detection by introduction of so-called incoherent beams. Each of the incoherent beams were calculated from all 12 horizontal N-S and E-W channels, which first were bandpass filtered, rectified through short-term-average (STA) calculations, and finally the STA traces were stacked without time shifts (incoherent beamforming). Incoherent horizontal beams were introduced in four different frequency bands, i.e., 1.5-3.5 Hz, 3.0-5.0 Hz, 5.0-10.0 Hz and 6.0-12.0 Hz.

6.3.3 Initial assessment of the new SPITS detection processing

Following the implementation of horizontal coherent beams in the new detection process, corresponding modifications had to be included for the subsequent automatic f-k analysis. We have now run the new SPITS processing setup for 58 consecutive days for the time period 19 February 2006 (day-of-year (DOY) 050) to 17 April 2006 (DOY 107). This resulted in an average of 2945 detections per day, which is about twice as many as the number of detections found when using the old processing recipe (average of 1655 per day).

For this same time period we have run automatic multi-array phase association and event location using the Generalized Beamforming (GBF) approach (Ringdal and Kværna, 1989; Kværna et al., 1999). Focusing on the Barents Sea area, north of 70^{o} latitude, we have searched for events where the SPITS and the ARCES arrays both have defining P- and S-phase detections. The criterion that both P- and S-phases are automatically found at two arrays is quite strong, in the sense that such events are quite unlikely to be caused by false phase associations and that the corresponding event locations are usually quite good. Figure 6.3.2 shows the location of the 36 events of this type found during the actual time period. For reference, we show in Figure 6.3.3 the location of similar type events found from processing using the old SPITS detection recipe for the same time period (17 events). A striking improvement is attributed to the three

recent events near Novaya Zemlya (Ringdal and Gibbons, 2006), where S-phase signals at SPITS are now detected on the horizontal coherent beams and associated with the P- and S-phases at ARCES and the P-phase at SPITS.

Table 6.3.1 shows details about the three Novaya Zemlya events as defined by the GBF process. We find that the seismic phases of the two first events are correctly associated as Pn and Sn at SPITS and ARCES. However, for the third event, in the attempt to maximize the number of associated phases, the GBF process incorrectly attribute an Sn-coda detection at ARCES to Lg. This again results in erroneous association of ARCES Sn and SPITS Pn, and a location error of almost 190 km relative to the analyst location result presented by Ringdal and Gibbons (2006). The ARCES Lg is typically absent, or very weak, for regional events located in the Barents Sea. In order to avoid future phase association errors of the type demonstrated above, we plan to fully implement regionalized criteria for the propagation of different phases at different stations in the GBF processing setup (e.g., no Lg at ARCES for regional events in the Barents Sea).

It is also apparent from Figs. 6.3.2 and 6.3.3 that more S-phases from the events in the western Barents Sea and along the mid-Atlantic Ridge are now detected at the SPITS array. Examples of the benefit from using coherent beamforming of rotated horizontal components for S-phase detection are shown in Figs. 6.3.4 and 6.3.5, in terms of SPITS Sn beams for two events located at regional distances from SPITS.

Following this initial assessment of the new SPITS detection processing, we will continue to analyze the processing results. Of particular interest will be to evaluate the SNR improvements and the stability of the S-phase f-k estimates (apparent velocity and back-azimuth) when using the horizontal components. Other factors like the density in slowness space of the coherent Sn beams, detection threshold setting and false alarm rate also need to be investigated. We are now in the process of running both the old and new processing setup in parallel, and, provided that no major problems are found, we plan to put the new setup into regular operations in the near future.

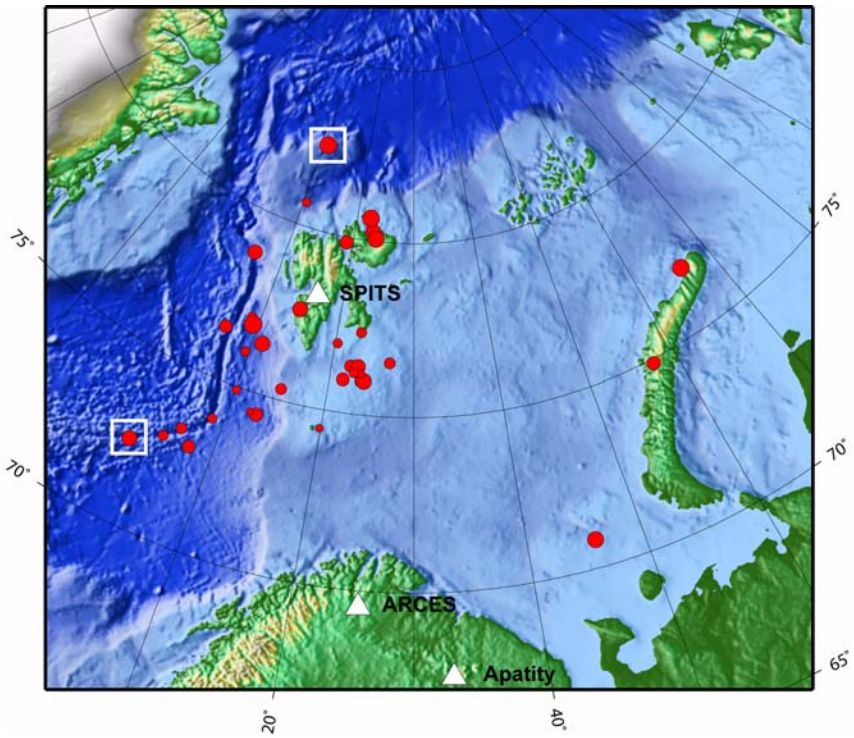

Fig. 6.3.2. GBF locations for events north of 70^o latitude for the time period 19 February to 17 April 2006. Shown are events with defining P- and S-phases both at SPITS and ARCES. The new SPITS processing results have been used as input to the phase association process. SPITS beams for the two events marked by white squares are shown in Figs 6.3.4 and 6.3.5.

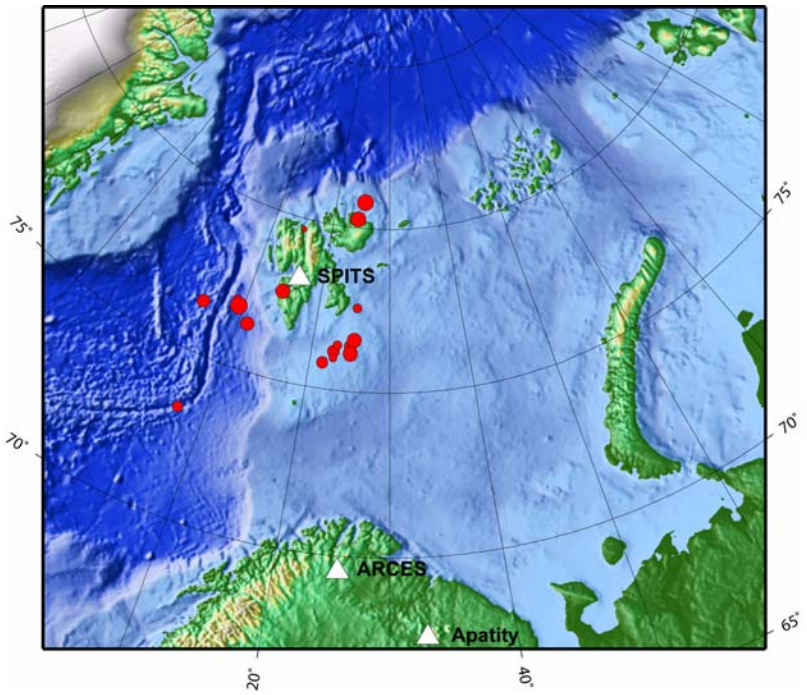

Fig. 6.3.3. GBF locations for events north of 70^o latitude for the time period 19 February to 17 April 2006. Shown are events with defining P- and S-phases both at SPITS and ARCES. The old SPITS processing results, created without coherent horizontal beams, have been used as input to the phase association process.

Table 6.3.1. Automatic on-line GBF results for the three Novaya Zemlya events using the new SPITS detection recipe

NOVAYA ZEMLYA, RUSSIA

Origin time	Lat	Lon	Azres	Timres	Wres	Nphase	Ntot	Nsta	Netmag
2006-064:23.17.34.0	76.80	66.04	6.46	0.97	2.58	4	11	2	2.63

Sta	Dist	Az	Ph	Time	Tres	Azim	Ares	Vel	Snr	Amp	Freq	Fkq	Arid	Mag
SPI	1176.3	72.5	Pn	23.20.03.6	-1.3	76.1	3.6	8.2	130.2	1590.9	7.25	2	225715	
SPI	1176.3	72.5	p	23.20.11.7		79.9	7.4	6.5	10.5	1130.4	7.09	2	225735	
SPI	1176.3	72.5	p	23.20.15.8		81.4	8.9	7.8	5.0	340.8	5.00	1	225740	
SPI	1176.3	72.5	p	23.20.18.0		84.7	12.2	8.2	5.7	452.0	5.52	1	225745	
SPI	1176.3	72.5	Sn	23.21.56.5	1.2	76.7	4.2	4.7	23.0	731.1	5.60	3	225760	2.73
SPI	1176.3	72.5	s	23.22.02.7		83.0	10.5	4.6	3.4	1551.0	9.11	3	225770	
SPI	1176.3	72.5	s	23.22.04.8		72.3	-0.2	4.3	5.7	379.0	5.42	3	225775	
ARC	1497.3	39.9	Pn	23.20.43.4	-0.5	57.5	17.6	9.6	4.8	38.0	6.25	2	482275	
ARC	1497.3	39.9	p	23.20.47.5		47.0	7.1	10.4	6.5	44.4	7.00	1	482276	
ARC	1497.3	39.9	Sn	23.23.03.8	0.9	39.4	-0.5	3.5	9.0	44.9	3.46	3	482289	2.42
ARC	1497.3	39.9	s	23.23.09.3		59.0	19.1	5.0	7.2	62.0	3.72	3	482292	2.53

NOVAYA ZEMLYA, RUSSIA

Origin time	Lat	Lon	Azres	Timres	Wres	Nphase	Ntot	Nsta	Netmag
2006-073:20.56.49.0	74.87	57.40	7.99	0.78	2.78	4	10	2	2.19

Sta	Dist	Az	Ph	Time	Tres	Azim	Ares	Vel	Snr	Amp	Freq	Fkq	Arid	Mag
SPI	1104.0	88.3	Pn	20.59.10.5	-0.7	94.7	6.4	8.4	21.1	329.5	10.68	3	346615	
SPI	1104.0	88.3	p	20.59.15.4		95.2	6.9	8.2	11.0	453.1	9.75	3	346620	
SPI	1104.0	88.3	p	20.59.17.9		101.4	13.1	8.4	9.1	508.1	11.12	3	346625	
SPI	1104.0	88.3	p	20.59.20.3		90.4	2.1	7.7	6.9	377.8	6.24	1	346630	
SPI	1104.0	88.3	p	20.59.22.5		84.8	-3.5	8.6	4.2	267.0	6.58	1	346640	
SPI	1104.0	88.3	Sn	21.00.56.5	1.3	92.4	4.1	4.7	6.4	388.6	10.20	3	346650	1.73
SPI	1104.0	88.3	s	21.01.03.2		81.1	-7.2	5.0	3.9	142.5	3.86	3	346660	2.14
ARC	1220.8	46.8	Pn	20.59.24.4	-1.0	57.5	10.7	10.6	5.4	47.1	5.65	2	519914	
ARC	1220.8	46.8	Sn	21.01.20.0	0.2	57.5	10.7	4.7	4.4	57.2	6.19	3	519921	2.07
ARC	1220.8	46.8	s	21.01.22.3		55.8	9.0	5.4	5.5	58.5	4.36	2	519923	2.23

BARENTS SEA

Origin time	Lat	Lon	Azres	Timres	Wres	Nphase	Ntot	Nsta	Netmag
2006-089:10.46.26.0	70.80	45.91	11.21	4.38	7.18	5	16	2	2.56

Sta	Dist	Az	Ph	Time	Tres	Azim	Ares	Vel	Snr	Amp	Freq	Fkq	Arid	Mag
ARC	782.8	70.1	Pn	10.48.11.0	1.8	75.7	5.6	8.6	18.3	70.1	5.08	1	35736	
ARC	782.8	70.1	p	10.48.16.5		72.2	2.1	9.1	5.7	64.5	6.63	2	35737	
ARC	782.8	70.1	p	10.48.21.7		72.9	2.8	8.8	5.3	71.8	3.35	1	35738	
ARC	782.8	70.1	p	10.48.27.0		76.0	5.9	8.4	3.8	51.5	4.73	1	35742	
ARC	782.8	70.1	Sn	10.49.17.0	-7.7	47.4	-22.7	4.7	3.8	375.4	1.00	1	35752	1.95
ARC	782.8	70.1	s	10.49.50.2		73.8	3.7	5.3	12.4	305.6	3.91	1	35753	
ARC	782.8	70.1	s	10.49.53.6		83.3	13.2	3.2	10.8	407.1	3.07	1	35754	2.63
ARC	782.8	70.1	s	10.49.57.1		78.3	8.2	3.1	4.8	163.6	3.71	3	35755	
ARC	782.8	70.1	Lg	10.50.06.0	-3.5	75.9	5.8	3.9	4.0	249.0	2.50	1	35756	2.31
SPI	1183.8	118.1	p	10.48.48.5		111.9	-6.2	7.8	31.9	225.9	4.16	1	571905	
SPI	1183.8	118.1	Pn	10.48.56.4	-1.4	100.9	-17.2	8.2	7.5	187.5	6.08	2	571920	
SPI	1183.8	118.1	p	10.49.02.0		104.0	-14.1	9.1	5.4	289.2	10.14	2	571930	
SPI	1183.8	118.1	Sn	10.50.56.4	7.4	113.3	-4.8	4.4	12.8	256.4	5.22	3	571940	2.34
SPI	1183.8	118.1	s	10.50.58.5		112.8	-5.3	4.7	15.5	506.5	6.18	3	571955	2.49
SPI	1183.8	118.1	s	10.51.02.6		103.6	-14.5	4.4	8.8	212.1	4.32	3	571960	
SPI	1183.8	118.1	s	10.51.05.3		103.8	-14.3	4.7	3.6	189.3	5.17	3	571965	

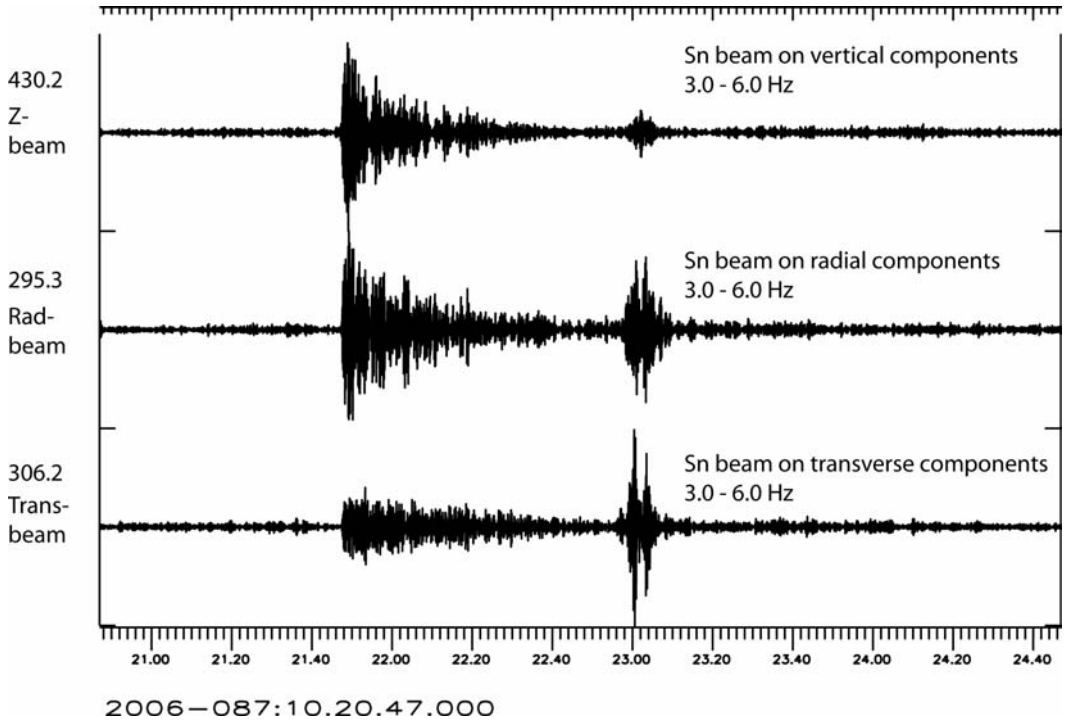

Fig. 6.3.4. SPITS Sn beams for an event on the Mohn's Ridge, located about 750 km south-west of SPITS. The automatic GBF event location is marked by a white square in Figure 6.3.2.

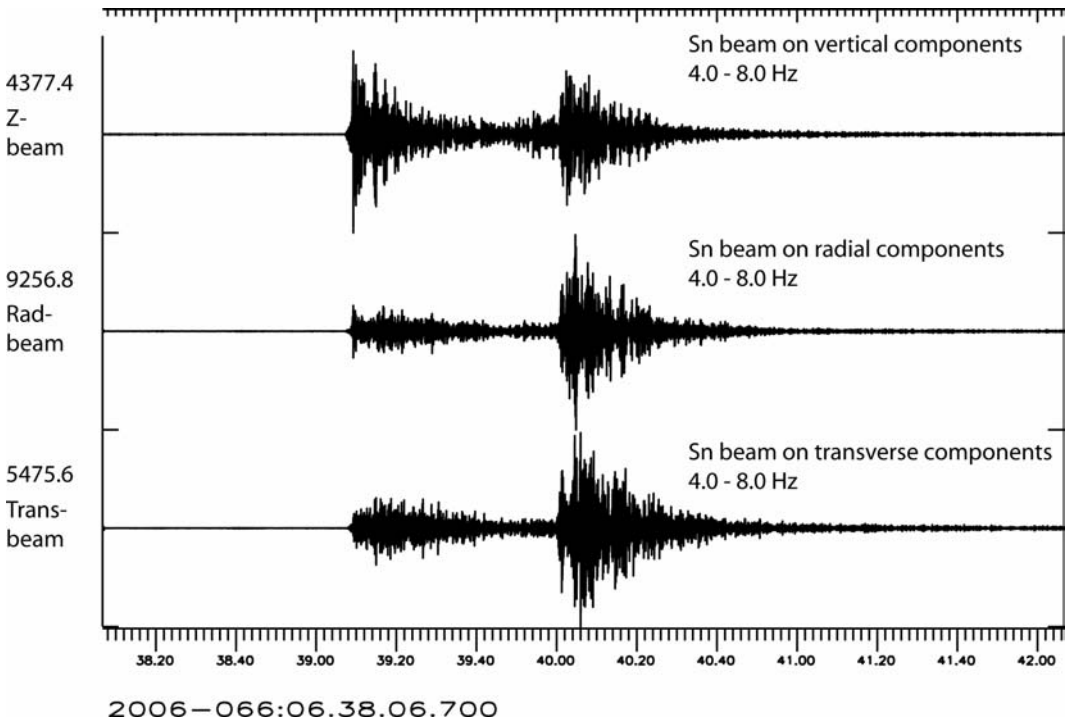

Fig. 6.3.5. SPITS Sn beams for an event north of Svalbard, located about 490 km from SPITS. The automatic GBF event location is marked by a white square in Figure 6.3.2.

References

Fyen, J. (2004). Selection of seismometers for Spitsbergen array refurbishment. In: NORSAR Semiannual Tech. Summ. 1 July - 31 December 2003, NORSAR Sci. Rep. **1-2004**, 26-31.

Fyen, J. (2005). Spitsbergen array refurbishment. In: NORSAR Semiannual Tech. Summ. 1 July - 31 December 2004, NORSAR Sci. Rep. **1-2005**, 24-33.

Kværna, T., J. Schweitzer, L. Taylor and F. Ringdal (1999). Monitoring of the European Arctic using Regional Generalized Beamforming. In: NORSAR Semiannual Tech. Summ. 1 October 1998 - 31 March 1999, NORSAR Sci. Rep. **2-98/99**.

Ringdal, F. and T. Kværna (1989). A multi-channel processing approach to real time network detection, phase association and threshold monitoring, *Bull. Seism. Soc. Am.*, **79**, pp 1927-1940.

Ringdal, F. and S. Gibbons (2006). Processing of low-magnitude seismic events near Novaya Zemlya. In: NORSAR Semiannual Tech. Summ. 1 January - 30 June 2006, NORSAR Sci. Rep. **2-2006** (this volume).

Schweitzer, J. (1998). Tuning the automatic data processing for the Spitsbergen array (SPITS). In: NORSAR Semiannual Tech. Summ. 1 April - 30 September1998, NORSAR Sci. Rep. **1-98/99**, 110-125.

Schweitzer, J. & T. Kværna (2002). Design study for the refurbishment of the SPITS Array (AS72). In: NORSAR Semiannual Tech. Summ. 1 January - 30 June 2002, NORSAR Sci. Rep. **2-2002**, 65-77.

Johannes Schweitzer
Tormod Kværna

Table 6.3.2. The new beam set for the SPITS array.
THR is the SNR threshold used to define a detection,
ALL means all nine vertical components of the SPITS array (SPA0, SPA1, SPA2, SPB1, SPB2, SPB3, SPB4, and SPB5).
TEL means the vertical components of the center instrument and the B-ring (SPA0, SPB1, SPB2, SPB3, SPB4, and SPB5.
RAD means all radial components of the 3C sites (SPA0, SPB1, SPB2, SPB3, SPB4, and SPB5).
TRA means all transverse components of the 3C sites (SPA0, SPB1, SPB2, SPB3, SPB4, and SPB5).

BEAM NAME	APPARENT VELOCITY [km/s]	BACK-AZIMUTH [°]	Filter		THR	Sensors used
			bandwidth [Hz]	order		
S001	99999.9	0.0	0.8 - 2.0	4	4.5	TEL
S002	99999.9	0.0	0.8 - 2.0	4	4.5	ALL
S003 - S006	20.0	0 90 180 270	0.8 - 2.0	4	4.5	TEL
S007 - S010	15.0	45 135 225 315	0.8 - 2.0	4	4.5	TEL
S011	99999.9	0.0	0.9 - 3.5	3	4.5	TEL
S012	99999.9	0.0	0.9 - 3.5	3	4.5	ALL
S013 - S016	20.0	0 90 180 270	0.9 - 3.5	3	4.5	TEL
S017 - S020	15.0	45 135 225 315	0.9 - 3.5	3	4.5	TEL
S021	99999.9	0.0	1.0 - 3.0	3	4.5	TEL
S022	99999.9	0.0	1.0 - 3.0	3	4.5	ALL
S023 - S026	20.0	0 90 180 270	1.0 - 3.0	3	4.5	TEL
S027 - S030	15.0	45 135 225 315	1.0 - 3.0	3	4.5	TEL
S031	99999.9	0.0	1.0 - 4.0	3	4.5	TEL
S032	99999.9	0.0	1.0 - 4.0	3	4.5	ALL
S033 - S036	20.0	0 90 180 270	1.0 - 4.0	3	4.5	TEL
S037 - S040	15.0	45 135 225 315	1.0 - 4.0	3	4.5	TEL
S041	99999.9	0.0	2.0 - 4.0	3	4.0	TEL
S042	99999.9	0.0	2.0 - 4.0	3	4.0	ALL
S043 - S046	20.0	0 90 180 270	2.0 - 4.0	3	4.0	TEL
S047 - S050	15.0	45 135 225 315	2.0 - 4.0	3	4.0	TEL
S051	99999.9	0.0	2.5 - 4.5	3	4.0	TEL
S052	99999.9	0.0	2.5 - 4.5	3	4.0	ALL
S053 - S056	20.0	0 90 180 270	2.5 - 4.5	3	4.0	TEL
S057 - S060	15.0	45 135 225 315	2.5 - 4.5	3	4.0	TEL
SA01 - SA04	10.0	0 90 180 270	1.0 - 3.0	3	4.5	TEL
SA05 - SA08	9.0	45 135 225 315	1.0 - 3.0	3	4.5	ALL
SA09 - SA12	10.0	0 90 180 270	3.0 - 5.0	3	4.0	TEL
SA13 - SA16	9.0	45 135 225 315	3.0 - 5.0	3	4.0	ALL

BEAM NAME	APPARENT VELOCITY [km/s]	BACK-AZIMUTH [°]	Filter		THR	Sensors used
			bandwidth [Hz]	order		
SA17 - SA20	10.0	0 90 180 270	5.0 - 10.0	3	4.0	TEL
SA21 - SA24	9.0	45 135 225 315	5.0 - 10.0	3	4.0	ALL
SA25 - SA28	10.0	0 90 180 270	8.0 - 15.0	4	4.0	TEL
SA29 - SA32	9.0	45 135 225 315	8.0 - 15.0	4	4.0	ALL
SB01 - SB04	8.0	0 90 180 270	1.5 - 3.5	3	4.0	TEL
SB05 - SB08	7.0	45 135 225 315	1.5 - 3.5	3	4.0	ALL
SB09 - SB12	8.0	0 90 180 270	3.0 - 6.0	3	4.0	TEL
SB13 - SB16	7.0	45 135 225 315	3.0 - 6.0	3	4.0	ALL
SB17 - SB20	8.0	0 90 180 270	4.0 - 8.0	3	4.0	TEL
SB21 - SB24	7.0	45 135 225 315	4.0 - 8.0	3	4.0	ALL
SB25 - SB28	8.0	0 90 180 270	6.0 - 12.0	3	4.0	TEL
SB29 - SB32	7.0	45 135 225 315	6.0 - 12.0	3	4.0	ALL
SB33 - SB36	8.0	0 90 180 270	12.0 - 24.0	3	4.0	TEL
SB36 - SB40	7.0	45 135 225 315	12.0 - 24.0	3	4.0	ALL
SC01 - SC04	6.0	0 90 180 270	2.0 - 4.0	3	4.0	TEL
SC05 - SC08	6.0	45 135 225 315	2.0 - 4.0	3	4.0	ALL
SC09 - SC12	6.0	0 90 180 270	3.0 - 6.0	3	4.0	TEL
SC13 - SC16	6.0	45 135 225 315	3.0 - 6.0	3	4.0	ALL
SC17 - SC20	6.0	0 90 180 270	5.0 - 10.0	3	4.0	TEL
SC21 - SC24	6.0	45 135 225 315	5.0 - 10.0	3	4.0	ALL
SC25 - SC28	6.0	0 90 180 270	8.0 - 15.0	4	4.0	TEL
SC29 - SC32	6.0	45 135 225 315	8.0 - 15.0	4	4.0	ALL
SC36 - SC40	6.0	0 90 180 270	12.0 - 24.0	3	4.0	TEL
SC36 - SC40	6.0	45 135 225 315	12.0 - 24.0	3	4.0	ALL
SD01 - SD12	5.5	0 30 60 90 120 150 180 210 240 270 300 330	1.0 - 3.0	3	4.0	ALL
SD13 - SD24	5.5	0 30 60 90 120 150 180 210 240 270 300 330	3.0 -5.0	3	4.0	ALL
SD25 - SD36	5.5	0 30 60 90 120 150 180 210 240 270 300 330	4.0 -8.0	3	4.0	ALL
SD37 - SD48	5.5	0 30 60 90 120 150 180 210 240 270 300 330	6.0 -12.0	3	4.0	ALL
SD49 - SD60	5.5	0 30 60 90 120 150 180 210 240 270 300 330	12. 0 -24.0	3	4.0	ALL
SE01 - SE12	5.0	0 30 60 90 120 150 180 210 240 270 300 330	1.0 - 3.0	3	4.0	ALL
SE13 - SE24	5.0	0 30 60 90 120 150 180 210 240 270 300 330	2.5 - 4.5	3	4.0	ALL
SE25 - SE36	5.0	0 30 60 90 120 150 180 210 240 270 300 330	4.0 -8.0	3	4.0	ALL
SE37 - SE48	5.0	0 30 60 90 120 150 180 210 240 270 300 330	6.0 -12.0	3	4.0	ALL
SF01 - SF12	4.5	0 30 60 90 120 150 180 210 240 270 300 330	1.0 - 4.0	3	4.0	ALL

BEAM NAME	APPARENT VELOCITY [km/s]	BACK-AZIMUTH [°]	Filter		THR	Sensors used
			bandwidth [Hz]	order		
SF13 - SF24	4.5	0 30 60 90 120 150 180 210 240 270 300 330	3.0 - 5.0	3	4.0	ALL
SF25 - SF36	4.5	0 30 60 90 120 150 180 210 240 270 300 330	5.0 -10.0	3	4.0	ALL
SF37 - SF48	4.5	0 30 60 90 120 150 180 210 240 270 300 330	8.0 -15.0	4	4.0	ALL
SG01 - SG12	4.0	0 30 60 90 120 150 180 210 240 270 300 330	1.0 - 4.0	3	4.0	ALL
SG13 - SG24	4.0	0 30 60 90 120 150 180 210 240 270 300 330	4.0 - 8.0	3	4.0	ALL
SG25 - SG36	4.0	0 30 60 90 120 150 180 210 240 270 300 330	6.0 -12.0	3	4.0	ALL
SH01 - SH12	3.5	0 30 60 90 120 150 180 210 240 270 300 330	1.5 - 3.5	3	4.0	ALL
SH13 - SH24	3.5	0 30 60 90 120 150 180 210 240 270 300 330	3.0 - 6.0	3	4.0	ALL
SH25 - SH36	3.5	0 30 60 90 120 150 180 210 240 270 300 330	5.0 -12.0	3	4.0	ALL
SI01 - SI12	3.0	0 30 60 90 120 150 180 210 240 270 300 330	1.0 - 3.0	3	4.0	ALL
SI13 - SI24	3.0	0 30 60 90 120 150 180 210 240 270 300 330	3.0 - 5.0	3	4.0	ALL
SI25 - SI36	3.0	0 30 60 90 120 150 180 210 240 270 300 330	4.0 - 8.0	3	4.0	ALL
SJ01 - SJ12	2.5	0 30 60 90 120 150 180 210 240 270 300 330	1.0 - 3.0	3	4.0	ALL
SJ13 - SI24	2.5	0 30 60 90 120 150 180 210 240 270 300 330	2.0 - 4.0	3	4.0	ALL
SJ25 - SJ36	2.5	0 30 60 90 120 150 180 210 240 270 300 330	3.0 - 6.0	3	4.0	ALL
SK01 - SK12	2.0	0 30 60 90 120 150 180 210 240 270 300 330	1.0 - 4.0	3	4.0	ALL
SK13 - SK24	2.0	0 30 60 90 120 150 180 210 240 270 300 330	3.0 - 4.0	3	4.0	ALL
SK25 - SK36	2.0	0 30 60 90 120 150 180 210 240 270 300 330	4.0 - 8.0	3	4.0	ALL
SL01 - SL12	1.7	0 30 60 90 120 150 180 210 240 270 300 330	1.0 - 4.0	3	4.0	ALL
SL13 - SL24	1.7	0 30 60 90 120 150 180 210 240 270 300 330	3.0 - 5.0	3	4.0	ALL
SL25 - SL36	1.7	0 30 60 90 120 150 180 210 240 270 300 330	4.0 - 8.0	3	4.0	ALL
S101 - S112	5.0	0 30 60 90 120 150 180 210 240 270 300 330	1.0 - 3.0	3	4.0	RAD
S113 - S124	5.0	0 30 60 90 120 150 180 210 240 270 300 330	2.5 - 4.5	3	4.0	RAD
S125 - S136	5.0	0 30 60 90 120 150 180 210 240 270 300 330	4.0 - 8.0	3	4.0	RAD
S137 - S148	4.0	0 30 60 90 120 150 180 210 240 270 300 330	1.0 - 4.0	3	4.0	RAD
S149 - S160	4.0	0 30 60 90 120 150 180 210 240 270 300 330	4.0 - 8.0	3	4.0	RAD
S161 - S172	4.0	0 30 60 90 120 150 180 210 240 270 300 330	6.0 - 12.0	3	4.0	RAD
S172 - S184	3.5	0 30 60 90 120 150 180 210 240 270 300 330	1.5 - 3.5	3	4.0	RAD
S185 - S196	3.5	0 30 60 90 120 150 180 210 240 270 300 330	3.0 - 5.0	3	4.0	RAD
S197 - S208	3.5	0 30 60 90 120 150 180 210 240 270 300 330	5.0 - 10.0	3	4.0	RAD
S209 - S220	3.0	0 30 60 90 120 150 180 210 240 270 300 330	1.0 - 3.0	3	4.0	RAD
S221 - S232	3.0	0 30 60 90 120 150 180 210 240 270 300 330	2.5 - 4.5	3	4.0	RAD
S233 - S244	3.0	0 30 60 90 120 150 180 210 240 270 300 330	4.0 - 8.0	3	4.0	RAD

BEAM NAME	APPARENT VELOCITY [km/s]	BACK-AZIMUTH [°]	Filter		THR	Sensors used
			bandwidth [Hz]	order		
S245 - S256	2.5	0 30 60 90 120 150 180 210 240 270 300 330	1.0 - 3.0	3	4.0	RAD
S257 - S268	2.5	0 30 60 90 120 150 180 210 240 270 300 330	2.0 - 4.0	3	4.0	RAD
S269 - S280	2.5	0 30 60 90 120 150 180 210 240 270 300 330	3.0 - 6.0	3	4.0	RAD
S281 - S292	2.0	0 30 60 90 120 150 180 210 240 270 300 330	1.0 - 4.0	3	4.0	RAD
S293 - S304	2.0	0 30 60 90 120 150 180 210 240 270 300 330	3.0 - 6.0	3	4.0	RAD
S305 - S316	2.0	0 30 60 90 120 150 180 210 240 270 300 330	4.0 - 8.0	3	4.0	RAD
S501 - S112	5.0	0 30 60 90 120 150 180 210 240 270 300 330	1.0 - 3.0	3	4.0	TRA
S513 - S124	5.0	0 30 60 90 120 150 180 210 240 270 300 330	2.5 - 4.5	3	4.0	TRA
S525 - S136	5.0	0 30 60 90 120 150 180 210 240 270 300 330	4.0 - 8.0	3	4.0	TRA
S137 - S148	4.0	0 30 60 90 120 150 180 210 240 270 300 330	1.0 - 4.0	3	4.0	TRA
S549 - S160	4.0	0 30 60 90 120 150 180 210 240 270 300 330	4.0 - 8.0	3	4.0	TRA
S561 - S172	4.0	0 30 60 90 120 150 180 210 240 270 300 330	6.0 - 12.0	3	4.0	TRA
S572 - S184	3.5	0 30 60 90 120 150 180 210 240 270 300 330	1.5 - 3.5	3	4.0	TRA
S585 - S196	3.5	0 30 60 90 120 150 180 210 240 270 300 330	3.0 - 5.0	3	4.0	TRA
S597 - S608	3.5	0 30 60 90 120 150 180 210 240 270 300 330	5.0 - 10.0	3	4.0	TRA
S609 - S620	3.0	0 30 60 90 120 150 180 210 240 270 300 330	1.0 - 3.0	3	4.0	TRA
S621 - S632	3.0	0 30 60 90 120 150 180 210 240 270 300 330	2.5 - 4.5	3	4.0	TRA
S633 - S644	3.0	0 30 60 90 120 150 180 210 240 270 300 330	4.0 - 8.0	3	4.0	TRA
S645 - S656	2.5	0 30 60 90 120 150 180 210 240 270 300 330	1.0 - 3.0	3	4.0	TRA
S657 - S668	2.5	0 30 60 90 120 150 180 210 240 270 300 330	2.0 - 4.0	3	4.0	TRA
S669 - S680	2.5	0 30 60 90 120 150 180 210 240 270 300 330	3.0 - 6.0	3	4.0	TRA
S681 - S692	2.0	0 30 60 90 120 150 180 210 240 270 300 330	1.0 - 4.0	3	4.0	TRA
S693 - S704	2.0	0 30 60 90 120 150 180 210 240 270 300 330	3.0 - 6.0	3	4.0	TRA
S705 - S716	2.0	0 30 60 90 120 150 180 210 240 270 300 330	4.0 - 8.0	3	4.0	TRA
SN01	8.4	97.6	1.0 - 4.0	3	3.7	ALL
SN02	8.4	97.6	3.0 - 5.0	3	3.7	ALL
SN03	8.4	97.6	4.0 - 8.0	3	3.7	ALL
SN04	8.4	97.6	6.0 - 12.0	3	3.7	ALL
SN05	8.4	97.6	8.0 - 15.0	4	3.7	ALL
SN06	8.4	97.6	12.0 - 24.0	3	3.7	ALL
SN07	4.7	97.6	1.0 - 4.0	3	3.7	ALL
SN08	4.7	97.6	3.0 - 5.0	3	3.7	ALL

BEAM NAME	APPARENT VELOCITY [km/s]	BACK-AZIMUTH [°]	Filter		THR	Sensors used
			bandwidth [Hz]	order		
SN09	4.7	97.6	4.0 - 8.0	3	3.7	ALL
SN10	4.7	97.6	6.0 - 12.0	3	3.7	ALL
SN11	4.7	97.6	8.0 - 15.0	4	3.7	ALL
SN12	4.7	97.6	12.0 - 24.0	3	3.7	ALL
SN13	4.7	97.6	1.0 - 3.0	3	3.7	TRA
SN14	4.7	97.6	2.5 - 4.5	3	3.7	TRA
SN15	4.7	97.6	4.0 - 8.0	3	3.7	TRA
SN16	4.7	97.6	6.0 - 12.0	3	3.7	TRA
SN17	4.7	97.6	12.0 - 24.0	3	3.7	TRA
SN18	4.7	97.6	1.0 - 3.0	3	3.7	RAD
SN19	4.7	97.6	2.5 - 4.5	3	3.7	RAD
SN20	4.7	97.6	4.0 - 8.0	3	3.7	RAD
SN21	4.7	97.6	6.0 - 12.0	3	3.7	RAD
SN22	4.7	97.6	12.0 - 24.0	4	3.7	RAD

6.4 The exploitation of repeating seismic events to measure and correct erroneous timing at the KBS station, Spitsbergen, during February and March 2006

6.4.1 Introduction

The IRIS/GEOFON/AWI seismic station KBS is situated near to Ny Ålesund, King's Bay, on the arctic island of Spitsbergen (Figure 6.4.1). The location is important in the context of nuclear explosion monitoring due to the relative proximity of the Russian island of Novaya Zemlya which was the site of numerous Soviet-era nuclear tests, the last known event being on October 24, 1990. Also on Spitsbergen, a highly sensitive small-aperture seismic array, SPITS, became operational in 1992 and is now a designated Auxiliary Seismic Array (AS72) of the International Monitoring System (IMS) of the Comprehensive nuclear Test-Ban-Treaty Organization (CTBTO). However, the KBS station is still of great importance given both the high quality of the continuous seismic data and the availability of the historical data recorded at that site. Crucially, all the known nuclear tests preceded the installation of the SPITS array whereas many were recorded at the KBS site providing an essential basis for comparison (see, for example, Hartse 1998).

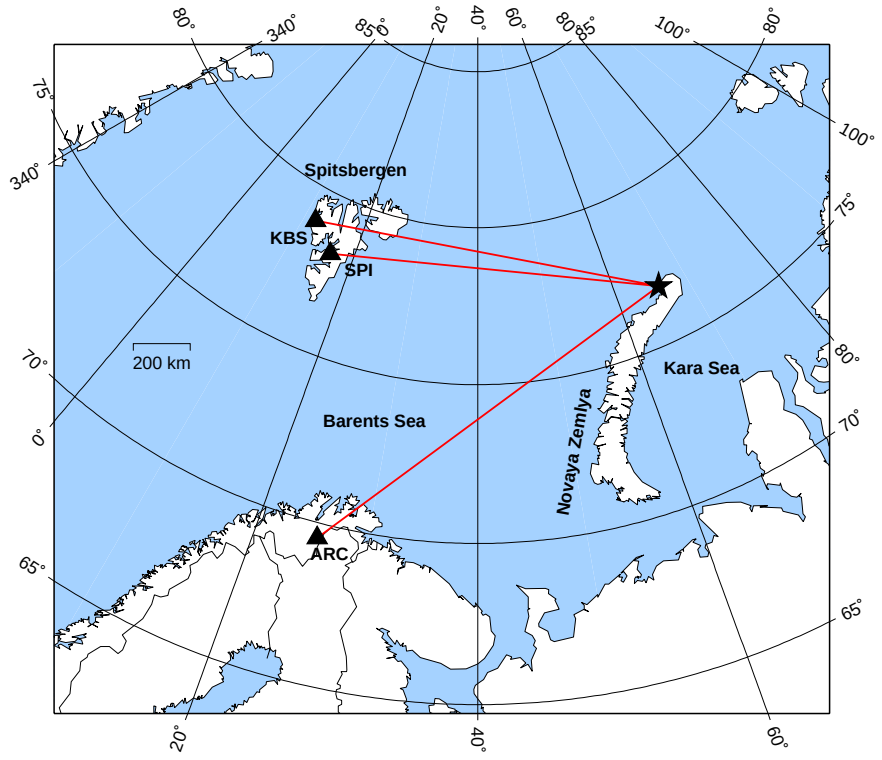

Fig. 6.4.1. Location of the IRIS/GEOFON/AWI station KBS, the IMS auxiliary seismic array SPITS, and the island of Spitsbergen in relation to Novaya Zemlya, the Barents Sea, the Kara Sea, and the IMS primary seismic array station ARCES. The black star at the northern tip of Novaya Zemlya indicates the fully-automatic location estimate for the March 5, 2006, event using the GBF algorithm (Ringdal and Kværna, 1989). Note that this location estimate is a trial epicenter location on a predetermined grid.

On March 5, 2006, an event on or close to Novaya Zemlya was detected using automatic phase determinations at the ARCES and SPITS seismic arrays. The fully-automatic Generalized Beamforming (GBF) phase-association and event location procedure (described by Ringdal and Kværna, 1989) provided the event with coordinates 76.80^{o} N, 66.04^{o} E, an origin time 2006-064:23.17.35.0, and a network magnitude estimate of 2.65[1]. Seismic events occurring in the vicinity of Novaya Zemlya are few and far between and consequently always examined very closely (see, for example, Ringdal, 1997; Richards and Kim, 1997; Bowers et al., 2001; Bowers, 2002). Although the event was reasonably well recorded by the ARCES array, and very well recorded by the SPITS array, it is desirable to utilize all available recordings in order to apply the best possible constraints on the event location and source type. P- and S- arrivals from this event are seen clearly on the KBS data.

Using *Pn* and *Sn* arrivals from SPITS and ARCES, with both arrival time, slowness, and back-azimuth estimates, an analyst location of the event was obtained with a well-constrained hypocenter and small traveltime and azimuth residuals. Location attempts which include the phase picks from KBS correspond to far larger error ellipses and time-residuals. The routine employed to locate the event was the HYPOSAT program (Schweitzer, 2001a) which is equipped with features that allow such discrepancies to be investigated. Most usefully, a flag can be set such that, for specified stations, the absolute arrival times are ignored and only the S-P traveltime difference is used in the inversion. Using absolute arrival times from SPITS and ARCES, but only the difference t_S - t_P for KBS, a well constrained location estimate was obtained with large but self-consistent time-residuals for both P- and S- arrivals at KBS. It was first at this time that analysts and researchers at NORSAR became aware of a possible timing disparity at KBS. Following contact with GEOFON staff at GFZ-Potsdam, it transpired that in February 2006 a technical malfunction had occurred at the KBS station such that high quality broadband seismic data continued to be recorded and transmitted, albeit with an incorrect and varying time-stamp. The fault had been identified rapidly, replacement parts were dispatched, and the station was repaired on March 22, 2006. In the meantime, we are in possession of a recording of an event of interest, without an authentic time-stamp, and we would like to evaluate whether or not it is possible to measure (and therefore correct) the timing anomaly in order that phase readings from the data can be used in any subsequent event locations.

Problems of instrument synchronization present formidable challenges to a seismologist attempting to obtain accurate location estimates for seismic events. Koch and Stammler (2003) realized that many poor parameter estimates using the IMS seismic array GERESS in Germany were the result of one or several channels being unsynchronized. They developed an ingenious system for the detection and measurement of timing anomalies whereby the continuous and highly coherent microseismic background noise was correlated between the different sites of the array. They point out that such a procedure is not possible for a single-site station, such as KBS. A different approach is required.

There is a source of seismicity close to both the KBS and SPITS stations from which subsequent seismic events have been demonstrated to produce very similar signals. The mining-induced seismicity is generated at the Barentsburg coal mine, approximately 50 km from SPITS and 120 km from KBS. Gibbons and Ringdal (2005, 2006) describe how the signal from a single rockburst at Barentsburg could be used as a waveform template to detect many far weaker subsequent rockbursts using multichannel waveform correlation. The continuous corre-

1. See http://www.norsar.no/NDC/bulletins/gbf/2006/GBF06064.html

lation coefficient traces between the master-event waveform template and the incoming data at each of the seismometer sites were demonstrated by Gibbons and Ringdal (2006) to be coherent over an arbitrary array or network even when the actual waveforms are not: provided that the two events considered are essentially co-located. If the correlation maxima from two co-located events are not aligned at two different stations, this is essentially a guaranteed indicator of a timing irregularity. This is demonstrated pictorially in Figure 6.4.2. The clear disadvantage of this method, compared with that of Koch and Stammler (2003), is that it requires the occurrence of fortuitous seismic events. Gibbons and Ringdal (2005) showed that a vast number of similar signals were generated by events at Barentsburg between January and August 2004; it is by no means guaranteed that the same regularity of repeating events will be observed in February and March 2006. Whereas the goal of Gibbons and Ringdal (2005, 2006) was to detect events with as low a magnitude as possible, our goal now is to detect events as similar as possible. We require that all events used occurred very close to each other such that differences in traveltimes can be neglected. We have the additional constraint that the events must be large enough to be well recorded at both SPITS and the more distant KBS station.

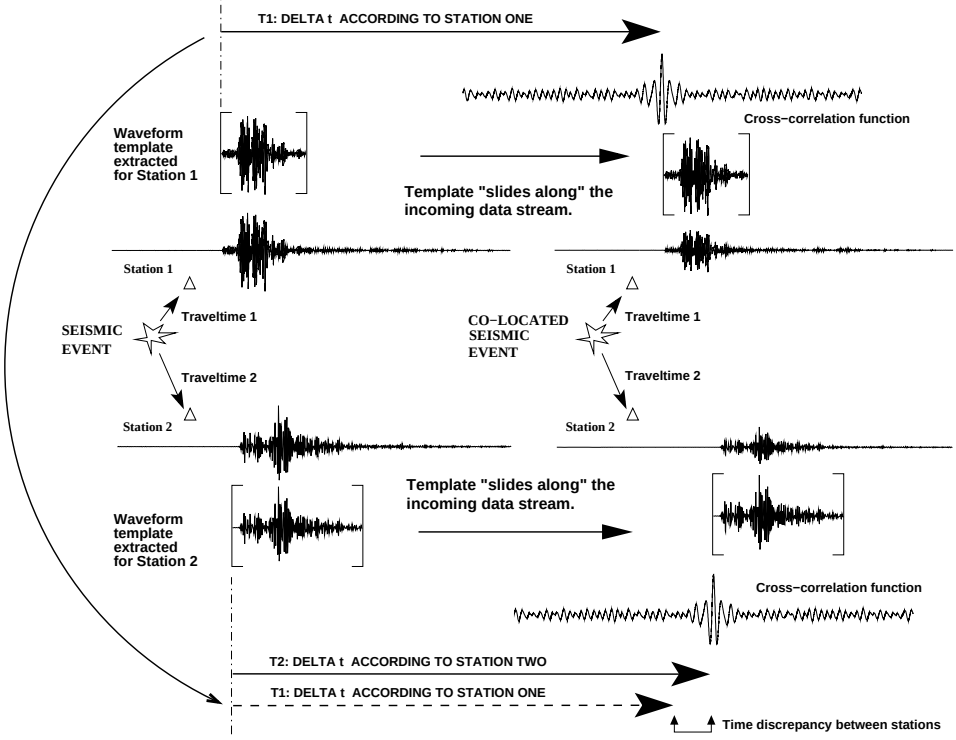

Fig. 6.4.2. A schematic illustration of how two successive events from almost identical seismic sources can be exploited to reveal anomalies in the timing at a given station. Assuming that no measurable changes occur to the velocity structure between source and receivers, seismic waves from two co-located events will take the same length of time to reach any given sensor. The cross-correlation function for a given signal at a given station measures how similar the subsequent portion of the seismogram is to the waveform template. The time separating the start of the template and the maximum of the cross-correlation function should equal the time separating the two event origin times for all stations. Any discrepancy in the separation times measured at two different stations, which is not attributable to source differences or a poor SNR, must be the result of a timing anomaly at one, or both, of the instruments.

It transpired that a large number of events at Barentsburg did indeed produce similar signals during the period of interest. In the following section, I will describe the observations of the March 5, 2006, event on Novaya Zemlya and I will proceed by discussing the results of various

attempts to locate the event. I will then present an overview of the timing anomaly at the KBS station as is discernible using the repeating events from the Barentsburg mine. I will conclude by making a few suggestions about strategies we ought to consider for known timing discrepancies at seismic stations.

6.4.2 Observations of the March 5, 2006, Novaya Zemlya event

Of the recordings of this event which are available to the international seismological community, by far the best is that from the SPITS array (Figure 6.4.3). The array was upgraded in the summer of 2004, with 3-component instruments being installed at 6 of the 9 seismometer sites. This has made an enormous improvement to the signal-to-noise ratio (SNR), and therefore the detection capability, for S-phases since beamforming is now possible using the horizontal components. Both the *Pn* and *Sn* phases are dominated by quite high frequencies and, due to the characteristic high amplitude microseismic background noise in the 1-2 Hz band, the best SNR for both phases is observed above 3 Hz. The *Lg*-phase is characteristically absent. (The blockage of *Lg* propagation by sediments in the Barents Sea Basin and elsewhere is discussed in depth by Baumgardt, 2001.)

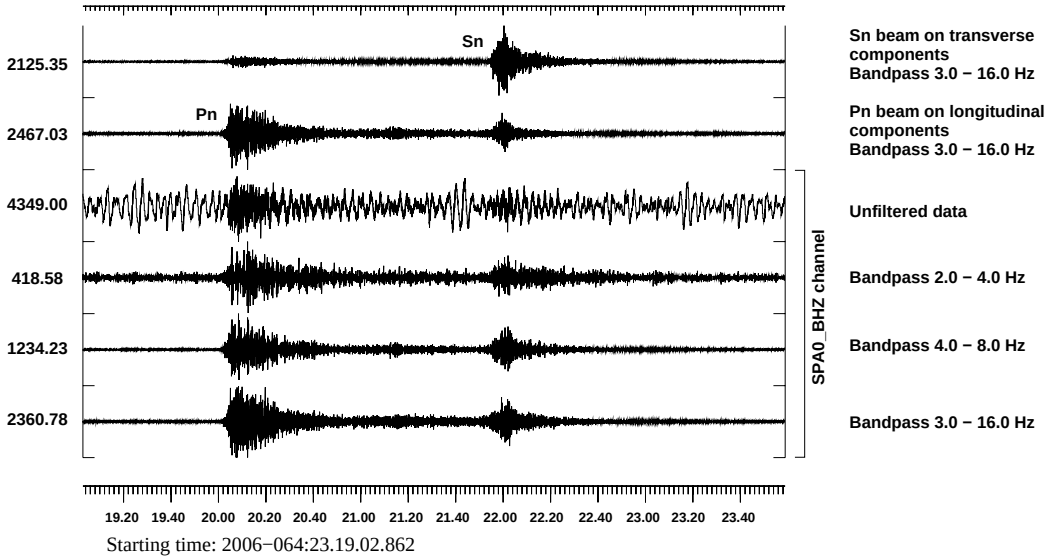

Fig. 6.4.3. Waveform data from the SPITS array for the March 5, 2006, Novaya Zemlya event. The longitudinal and transverse channels are rotated from the 3-component instruments assuming a backazimuth of 80^o and an incidence angle of 45^o. The Pn- and Sn- beams are formed assuming apparent velocities of 8.5 kms^{-1} and 4.5 kms^{-1} with elevation corrections imposed assuming P- and S- velocities of 4.75 kms^{-1} and 3.0 kms^{-1}.

Figure 6.4.4 shows waveforms from ARCES for the March 5, 2006, event. The SNR is substantially worse at ARCES than at SPITS in spite of the fact that the ARCES array is not much further from the assumed event location. (The last event on Novaya Zemlya prior to 2006 to be detected by the NORSAR-operated seismic arrays was on October 8, 2003, quite close to the presumed location of the March 5, 2006, event[2]. This event registered a reasonable SNR on SPITS but failed to produce a detection at ARCES.) Due to the diminished signal to noise ratio, the accuracy with which the phase onset times can be read is significantly poorer. However,

2. See http://www.norsar.no/NDC/bulletins/regional/2003/10/5705.html

considering the SNR, directional estimates for both *Pn* and *Sn* using broadband f-k analysis are surprisingly well-determined and robust.

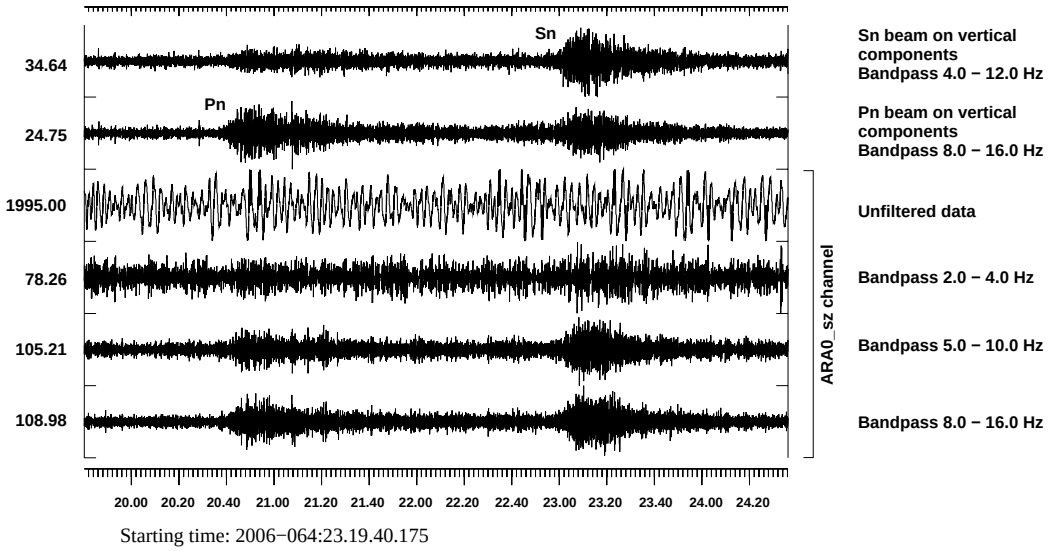

Fig. 6.4.4. Waveform data from the ARCES array for the March 5, 2006, Novaya Zemlya event. Since ARCES has 25 vertical component sensors and only 4 3-component sensors, the SNR gain is often better on the vertical component beams even though the signal is stronger on the horizontal components.

The KBS recording of the Novaya Zemlya event is displayed in Figure 6.4.5. The SNR is poorer than for the single channels at SPITS, possibly a result of higher background noise (particularly at the lower frequencies). However, the *Pn* and *Sn* arrivals are at least as discernible as at the ARCES array. The absence of recordings at distinct sites precludes the determination of direction using f-k analysis, although a reasonably stable backazimuth and incidence angle for the P-arrival may be estimated using polarization analysis. An excellent introduction to both methods of direction estimation is provided in Chapter 23 of Kennett (2002).

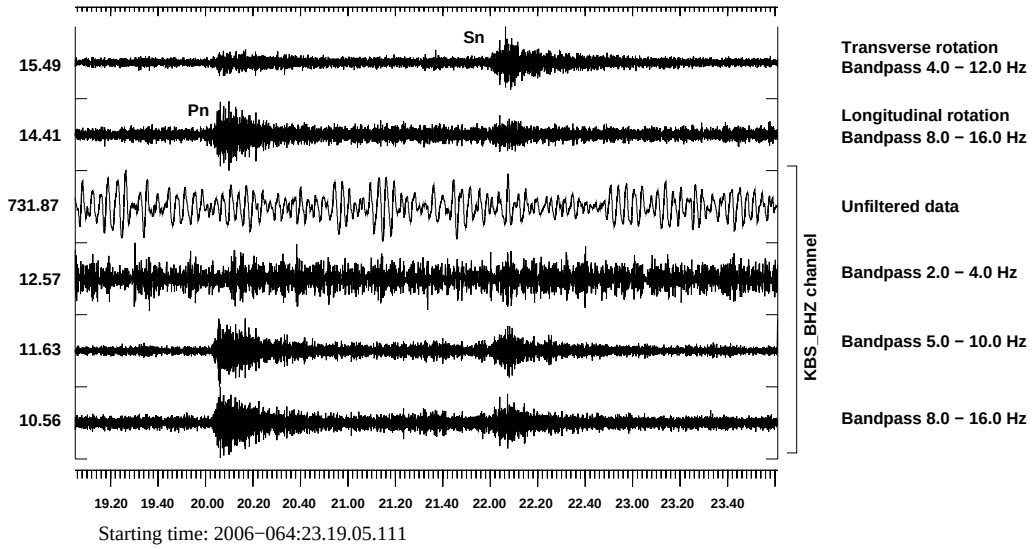

Fig. 6.4.5. Waveform data from the KBS 3-component station for the March 5, 2006, Novaya Zemlya event. With channels from only a single site, we are unable to perform beamforming. However, we are able to improve the SNR for the Sn phase by rotating the horizontal components.

The results of all of the phase arrival determinations are displayed in Table 6.4.1. In principle, all of these time picks and slowness/azimuth estimates can be input into a location routine (such as HYPOSAT) to obtain an event location estimate. We discuss a number of attempts to locate the event in the following section.

Table 6.4.1. Phase determinations for the March 5, 2006, Novaya Zemlya seismic event estimated for the central sites of the SPITS and ARCES arrays and the KBS 3-component station. Azimuth and apparent velocity are measured using broadband f-k analysis for all phases at the array stations and using 3-component polarization analysis for the Pn-phase at KBS.

Station	Phase	Arrival time	Estimated error (s)	Backazimuth (^{O})	Apparent velocity (km/s)
SPA0	Pn	23.20.00.863	±0.5	76.4 ± 5.0	7.79 ± 1.0
SPA0	Sn	23.21.53.416	±1.2	82.5± 10.0	4.60 ± 1.0
ARA0	Pn	23.20.38.414	±1.5	55.1± 7.0	9.65 ± 1.0
ARA0	Sn	23.22.57.704	±2.0	51.0± 8.0	4.98 ± 1.0
KBS	Pn	23.20.01.526	±1.5	73.0±12.0	7.40 ± 2.0
KBS	Sn	23.21.59.289	±2.0	Not available	Not available

6.4.3 Location estimates for the March 5, 2006, Novaya Zemlya event

Whilst the phase picks and parameter estimates listed in Table 6.4.1 are not the only observations of this Novaya Zemlya event, they are by far the best that researchers at NORSAR have access to. Other phase picks from more distant stations are unlikely to lead to a more accurate location estimate. All location estimates discussed here are consequently limited to the information provided in Table 6.4.1. The routine used to locate the event is the HYPOSAT program (Schweitzer, 2001a) and the 1-dimensional velocity model used is the *barey* model, as tabulated in Hicks et al. (2004). A number of different location attempts are tabulated in Table 6.4.2 and mapped out in Figure 6.4.6. The location estimates differ only by the use of different subsets of the arrivals listed in Table 6.4.1, and by the use or otherwise of the option in the HYPOSAT program which allows the inclusion of only the travel time difference (t_S-t_P) in the location inversion for a given station, rather than the absolute arrival times t_P and t_S.

The most natural approach when locating a seismic event is to constrain the location by using as many high quality onset estimates as possible. Solution A in Table 6.4.2 includes all of the phase arrival determinations listed in Table 6.4.1 with both absolute arrival times and travel-time differences being used in the inversion. This location estimate lies approximately 50 km West of the GBF solution and has an origin time within one second of the GBF estimate. However, the RMS time-residual of 3.65 seconds is completely unacceptable and immediately alerts an analyst to the possibility of a qualitative error in the list of phase determinations.

Table 6.4.2. Summary of location estimates for the March 5, 2006, Novaya Zemlya event using HYPOSAT and various subsets of the phase determinations listed in Table 6.4.1. Table cells which contain only a dash (-) indicate that the value in question was not used in the inversion. An asterisk (*) against a time residual indicates that only the S-P traveltime difference was used in the inversion, and not the actual phase arrival times. The depth is fixed to zero for all estimates. Note that no RMS time residuals are given for the single station location estimates since, with only two defining phases, the times can essentially be fitted exactly with the dimensions of the error ellipse being determined by the time uncertainty and azimuth values. Note that RMS time residuals are provided for solutions F and G but that these values are misleadingly low since the differential time constraint for the second station is far weaker than the absolute time constraint.

Location estimate	A	B	C	D	E	F	G	H
Latitude	76.8390	76.6528	76.1376	73.7171	77.2153	74.0465	76.2267	76.6613
Longitude	64.4691	64.4518	63.1573	65.1605	64.3826	65.2217	63.4022	64.4094
Origin time: seconds after 2006-064:23.17.00.000	34.299	34.313	33.736	36.558	31.998	36.310	33.732	34.281
Origin time uncertainty (s)	4.388	2.470	1.622	7.762	4.722	7.178	1.592	2.135
RMS onset time residual	3.656	0.469	N/A	N/A	1.200	0.084	0.001	0.432
Err. ellipse major axis (km)	38.66	21.06	83.58	209.72	38.92	186.64	77.26	18.50
Err. ellipse minor axis (km)	36.23	20.11	18.47	63.47	25.02	56.91	18.28	17.81
Err. ellipse azimuth	85.7	99.3	26.6	2.3	98.4	2.4	26.5	95.4
Err. ellipse area (km^2)	4400.0	1330.9	4849.78	41818.0	3059.4	33371.0	4436.08	1034.75
SPITS Pn time residual (s)	2.946	-0.333	N/A	-	-	-	0.000	-0.352
SPITS Sn time residual (s)	4.088	-0.144	N/A	-	-	-	-0.001	-0.031
ARCES Pn time residual (s)	2.244	0.801	-	N/A	1.552	0.058	-	0.715
ARCES Sn time residual (s)	0.656	-0.324	-	N/A	-0.777	-0.103	-	-0.332
KBS Pn time residual (s)	-4.872	-	-	-	-1.505	-35.348*	-8.592*	-8.360*
KBS Sn time residual (s)	-5.062	-	-	-	0.692	-55.898*	-10.521*	-9.516*
SPITS Pn azimuth residual	3.04	2.13	-1.22	-	-	-	-0.62	2.14
SPITS Sn azimuth residual	9.14	8.23	4.88	-	-	-	5.48	8.24
ARCES Pn azimuth residual	15.72	14.92	-	1.78	17.36	3.25	-	14.97
ARCES Sn azimuth residual	11.62	10.82	-	-2.32	13.26	-0.85	-	10.87
KBS Pn azimuth residual	-1.21	-	-	-	0.39	-10.94	-4.59	-2.02

The first exploratory step is to repeat the location procedure but only using phase arrivals from the array stations (i.e. ignoring the KBS phase determinations). This solution is labelled B and, whilst located quite close to the previous estimate, has a far smaller RMS onset time residual. The time residuals for the SPITS and ARCES arrays are all smaller than one second without the inclusion of the KBS station. This however does not prove that the KBS phase picks are to blame for the poor fit of solution A; other combinations need to be tried in order to eliminate other sources of error.

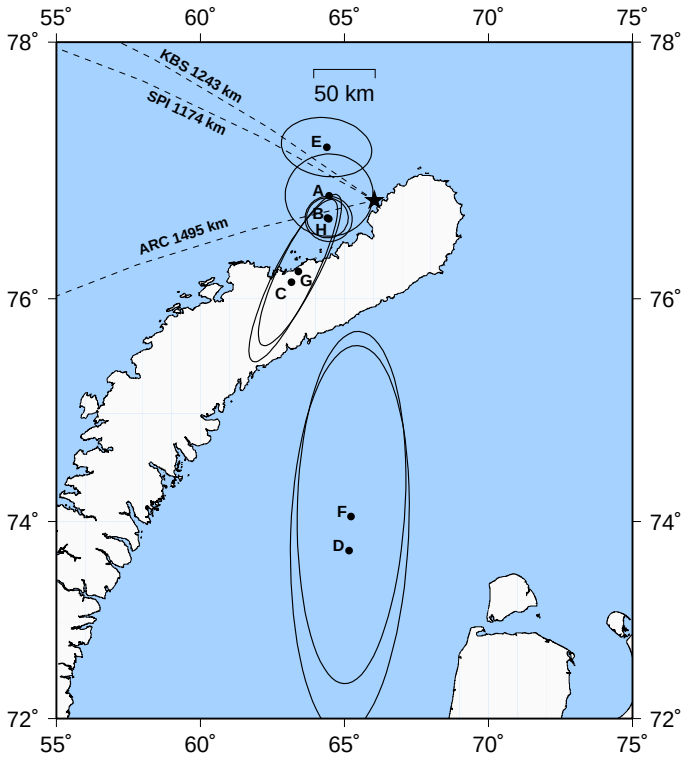

Fig. 6.4.6. Location estimates and associated error ellipses for the March 5, 2006, Novaya Zemlya event. The letters adjacent to each of the epicenter locations correspond to the solutions listed in Table 6.4.2. The asterisk indicates the GBF fully-automatic location for the event and the dashed lines indicate the great circles joining this location to the marked stations

A single array location, using only *Pn* and *Sn* from SPITS, is labelled C in Table 6.4.2. The corresponding error-ellipse is elongated perpendicular to the great circle linking the epicenter solution and the array. This reflects the fact that the epicentral distance can be determined to fit the two arrival times perfectly and the minor axis of the error-ellipse only reflects the uncertainty in the arrival time estimates; the major axis of the error-ellipse accounts for both the uncertainty in the azimuth estimates and the conflict inherent in the azimuth estimates for the two phases. The corresponding single array solution for ARCES (labelled D) has a somewhat larger error-ellipse as a result of the larger parameter uncertainties but, more worryingly, exhibits a large offset from all the solutions so far obtained which include phases from the stations on Spitsbergen. This is because the solution is dominated by the backazimuth estimates obtained using broadband f-k analysis, and these indicate an apparent direction of arrival which is quite different to that anticipated geographically. Whilst very accurate single array solutions can be obtained (see, for example, Gibbons et al., 2005) we cannot use azimuth estimates from regional arrays uncritically, especially when these values are paramount in determining the location. We must follow the counsel of Schweitzer (2001b) and apply a slowness correction based upon calibration studies prior to locating the event.

In solution E, the *Pn* and *Sn* phase determinations from the KBS station are added to the ARCES phases (whilst ignoring SPITS) bringing the location estimate back to the North East tip of Novaya Zemlya. The solution is equivalent to B, except with KBS phase readings in place of those from SPITS. The RMS time residuals, the origin time uncertainty, and the corresponding error ellipse are all far larger for solution E than for solution B, indicating that phase

determinations from SPITS fit the solution better. Solution F has an almost identical input to that for solution E except that HYPOSAT is now instructed to consider only the S-P traveltime difference for the KBS station. The phase determinations from ARCES now completely dominate the solution and location estimate F is little different from that in D. A location attempt using phase readings (with both absolute and differential times) from SPITS and KBS only is not possible; the inversion fails. This indicates that an inconsistency between the absolute arrival times recorded for SPITS and those recorded for KBS is pivotal to the location failure. Again, instructing HYPOSAT to ignore the absolute arrival times for KBS allows for a solution (labelled G) which falls close to the SPITS-only solution (C) but which indicates quite consistent traveltime residuals of approximately -9 seconds for both *Pn* and *Sn* from KBS.

A final solution, H, is proposed whereby phase readings from all three stations are included but with only the S-P traveltime difference (and the *Pn* azimuth estimate) for the KBS station. This location estimate is almost identical to estimate B which ignored the KBS station completely. Solution H corresponds to the smallest time-residuals and the smallest error ellipse. The *Pn* and *Sn* traveltime residuals from the KBS station are consistent in the sense that, if a timing error of approximately 9 seconds at KBS were to be assumed, all constituent phase arrival times would correspond to an error less than one second. In the following section, we investigate a strategy for measuring a timing error at the KBS station.

6.4.4 Overview of the KBS timing error based upon correlation analysis of repeating events at the Barentsburg coal mine

Scientists at NORSAR and at the Kola Regional Seismological Center (KRSC) in Apatity, Russia, have observed mining-induced seismicity at the Barentsburg coal mine over many years (see, for example, Kremenetskaya et al., 2001). Following a fatal rockburst on July 26, 2004, a special effort was launched to detect with a high level of confidence all seismic events which had occurred in the immediate vicinity of this event. It was decided that the most effective method was to extract a waveform template from the July 26 event and to identify subsequent (or previous) events by running a multi-channel matched filter detector on continuous SPITS data (see Gibbons and Ringdal; 2005, 2006). This procedure identified over 1500 Barentsburg events within an eight month period in 2004, approximately an order of magnitude more events than could be detected using traditional STA/LTA detectors. Provided that the source mechanisms for the different events do not vary too much, the signal recorded at a given station is like a fingerprint for a given source location. Since correlation detectors work by comparing a sample waveform with a given segment of arriving data, they are exquisitely sensitive detectors for events from a specific source location which are seldom triggered by signals from different locations.

Not only is the correlation detector for the July 26, 2004, Barentsburg event still running on incoming SPITS data, but the pool of master-events has been expanded continually to include an ever greater number of waveform templates. Every signal identified by the correlation detector is subjected to an automatic post-processing system which measures the SNR on the P- and S- arrivals anticipated for events at Barentsburg. If this indicates a high-SNR event from our site of interest, the event is marked for analyst review. An event detected because of sufficient similarity to a current Barentsburg master event, but which is dissimilar enough to indicate a source at a slightly different location within the mine, is earmarked for possible inclusion as a new master event. In this way, a pool of over 100 master event signals has now been accumulated which are all correlated in quasi real-time with the latest SPITS array data. It is not yet

known what proportion of seismicity at the mine is covered by the given master event pool, or the degree of degeneracy which exists within the event pool with respect to the detectability of new events.

We assume an origin location of 77.9375° N and 14.0703° E for events at Barentsburg. If an event at this site occurs with an origin time, t_0, the barey velocity model predicts a first arrival at SPITS at a time $t_0 + 8.55$ seconds and a first arrival at KBS at a time $t_0 + 18.41$ s. It must however be emphasized that neither the precise location of the event nor the velocity model assumed is important. As illustrated in Figure 6.4.2, the only measurement made is the time separating the start of the waveform template and the maximum of the correlation coefficient function. As a result, the only real prerequisite is that the two events being compared are essentially co-located; if this is not the case, the measured time difference will include a component due to traveltime differences which may not be possible to quantify.

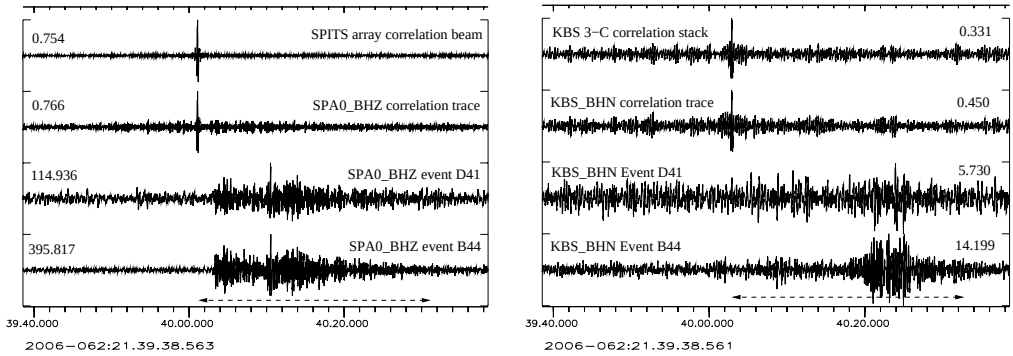

Fig. 6.4.7. Correlation between a master event with assumed origin time 2006-037:23.14.08.413 and a detected event with assumed origin time 2006-062:21.39.53.563 on the SPITS array (left) and on the KBS 3-component station (right). For each panel, the lowermost trace is the master event waveform for a single channel (with the template duration indicated by the arrow), the second trace up is the detected waveform for the same channel aligned according to the maximum correlation coefficient, the third trace up is the corresponding single channel correlation coefficient trace, and the top channel is the correlation coefficient beam. The SPITS waveform template begins at a time 2006-037:23.14.15.96250 and the interpolated correlation coefficient maximum at SPITS occurs at a time 2006-062:21.40.01.11667. The KBS waveform template begins at a time 2006-037:23.14.25.82310 and the interpolated correlation coefficient maximum at KBS occurs at a time 2006-062:21.40.02.93727. All waveforms were bandpass filtered between 3.0 and 6.0 Hz prior to resampling, and all correlation coefficient maxima times were estimated using spline interpolation. Note that the correlation maxima can be very well-defined even when the signal SNR is low.

For each master event used, waveform templates were prepared for both the SPITS and KBS stations. For each channel (3 components for KBS and up to 21 components on the SPITS array) a long segment of waveform data was bandpass filtered between 3.0 and 6.0 Hz, resampled to 200 samples per second, and a 30.0 second long window was cut starting at the assumed first arrival time. Due to the distances involved, a 30.0 second long segment includes both P- and S- phases for both receiver sites. Master Events were restricted to periods in which no known timing problems occurred. This is easier said than done since it has been demonstrated that single channels on the SPITS array have displayed synchronization problems analogous to those demonstrated by Koch and Stammler (2003) on the GERESS array. In order to identify any master events which are subject to single channel synchronization errors, all master events were cross-correlated with all other master events and, for each event-pair, the alignment of the correlation coefficient traces was verified using the Multi-Channel Cross-Correlation (MCCC) and Least Squares method of VanDecar and Crosson (1990). This method

is employed by Gibbons et al. (2006) to identify and measure synchronization problems between sites on the NORSAR and SPITS arrays. Figure 6.4.7 shows the detection of a Barentsburg event using a template from a master event at both KBS and SPITS.

If t always denotes a UTC time then we can define a correction function $C_{KBS}(t)$ which allows the apparent time according to the KBS station to be calculated using

$$t_{KBS}^{app} = t - C_{KBS}(t)$$

The time separating the origin times of the two events is equal to the time separating the start of the waveform template and the maximum correlation coefficient for all stations.

Assuming that the SPITS array recorded both master and detected events with the correct time, and that the KBS station recorded the master event with the correct time, we can calculate $C_{KBS}(t)$ using

$$C_{KBS}(t) = \left[t_{KBS}^{ccm} - t_{KBS}^{wft}\right] - \left[t_{SPI}^{ccm} - t_{SPI}^{wft}\right]$$

where t_x^{wft} is the start of the waveform template for station x and t_x^{ccm} is the apparent time of the maximum of the correlation coefficient maximum for station x. For the example displayed in Figure 6.4.7, replacing the terms in the formula above with the times quoted in the figure caption gives a $C_{KBS}(t)$ value of 8.040 seconds. Since this implies that the time stamp indicated by the KBS station was 8.040 seconds earlier than the actual UTC time, this would be consistent with the time-residuals obtained for the March 5 Novaya Zemlya event. There were no usable, well-correlating, Barentsburg events on March 5 (Julian day 064). If we repeat the procedure for the first Barentsburg event following the Novaya Zemlya event (using the same master event), we obtain a $C_{KBS}(t)$ value of 8.089 seconds. The similarity of these time correction estimates provides the basis for a cautious optimism that a similar correction would apply at the time of the March 5 event. The following Barentsburg event results in a $C_{KBS}(t)$ value of -19.108 seconds, when the same master event is used. This is a substantial apparent leap in time which demands closer scrutiny.

We must be aware of the fact that the values for $C_{KBS}(t)$ vary slightly depending upon which master event is used. This is due to the fact that signals from subsequent events are not identical and any waveform dissimilarity will always lead to a degree of ambiguity in the time of best correlation. Whether the signal dissimilarity is due to reduced SNR, a difference in event location, or most likely a combination of both, the correlation coefficient will provide a reasonable indication of the quality of a $C_{KBS}(t)$ estimate and we need to evaluate the variability observed for a large number of master events. Figure 6.4.8 shows $C_{KBS}(t)$ evaluated at the times of a number of Barentsburg events as a function of the correlation coefficient. In the right hand panel, where both master and detected events occurred after the station was repaired, the time-correction term estimates clearly tend towards a zero mean value, with a standard deviation which increases as the correlation coefficient decreases. In the left hand panel, where the detected events occurred during the period of uncertain timing, not only is $C_{KBS}(t)$ clearly non-zero for these events, it also appears to be increasing steadily with time. The time-correction term evaluated on March 6, 2006, is approximately 0.2 seconds greater than that measured on February 26. One conclusion which can be drawn from Figure 6.4.8 is that it is essential to

have as many reference events as possible in order to maximize the likelihood of including a master event which correlates well with the detected event.

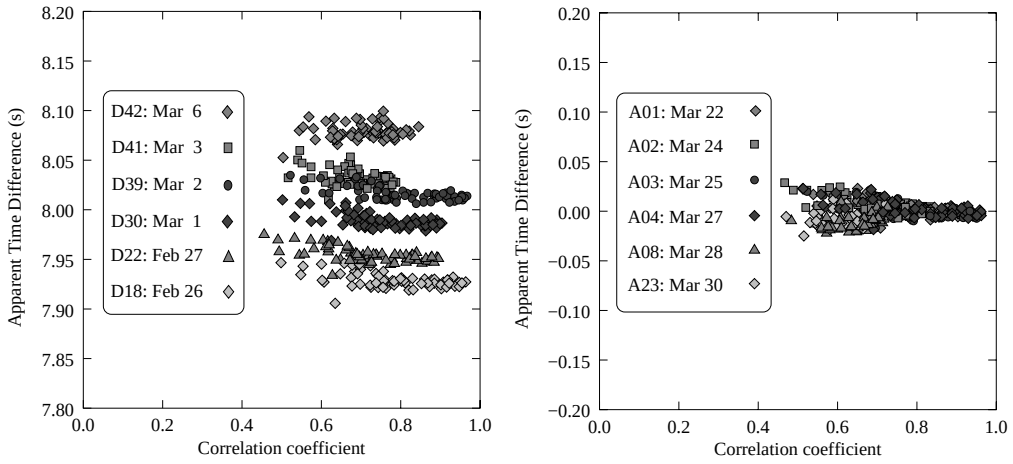

Fig. 6.4.8. Variability of the time-correction function $C_{KBS}(t)$ for a number of detected Barentsburg events. Each point indicates the time-difference calculated for the indicated event using a certain master event with the SPITS array correlation coefficient displayed on the x-axis. All master events are taken from March 22, 2006, or later after the KBS station was repaired. The detected events in the left hand panel all occurred during the time-period without an authentic time-stamp and the events in the right hand panel occurred after the station was repaired. All autocorrelations are trivial and have not been included in the right hand panel.

Figure 6.4.9 shows the time-correction term evaluated for every instant at which we have a repeating event from the Barentsburg mine. There are four clear time intervals, separated by data gaps, over which the time according to KBS is associated with a steady drift and a different offset term of up to 20 seconds. The drift appears to be the same for each interval, indicating that it is probably associated with the digitizer. Under normal operation, this drift is corrected at regular intervals. The times of the data gaps were observed easily by differentiating long segments of waveform data. Whilst there are several periods of several days in which no Barentsburg events were detected, each new occurrence of Barentsburg events appears to be consistent with the pattern previously observed.

6.4.5 Conclusions and Discussion

A timing error at the KBS station between February 17, 2006, and March 22, 2006, resulted from a temporary technical fault. The operators of the station were alerted to the problem rapidly and took the necessary corrective steps. Scientists at NORSAR only became aware of a synchronization problem when attempting to locate an interesting seismic event using KBS phase determinations. Successive, strategic attempts to locate the event using a fixed set of phase determinations indicated that anomalous P- and S- arrival times at KBS were almost certainly to blame for the large residuals in the location estimates. It was demonstrated that if both P- and S- phases had arrived at KBS approximately 8 seconds later than indicated on the seismograms, the phase determinations would be consistent with P- and S- arrivals from the SPITS and ARCES seismic arrays. Mining-induced seismicity at the Barentsburg coal mine, close to the SPITS and KBS stations, results in signals at both sites which are very similar from event to event. Many such events occurred during the period in which the timing at KBS was erroneous. The frequency of these repeating events was sufficiently high during this period for the KBS timing error to be measured by comparing the time separating the correlating patterns in the

subsequent waveforms at the two different stations. Based upon numerous waveform correlation calculations, we can state with a high level of confidence that the time-stamp on the KBS data at the time of the March 5, 2006, seismic event at Novaya Zemlya was approximately 8.07 seconds earlier than real-time. The corrected arrival time estimates allow for a very well-defined location estimate for the Novaya Zemlya event.

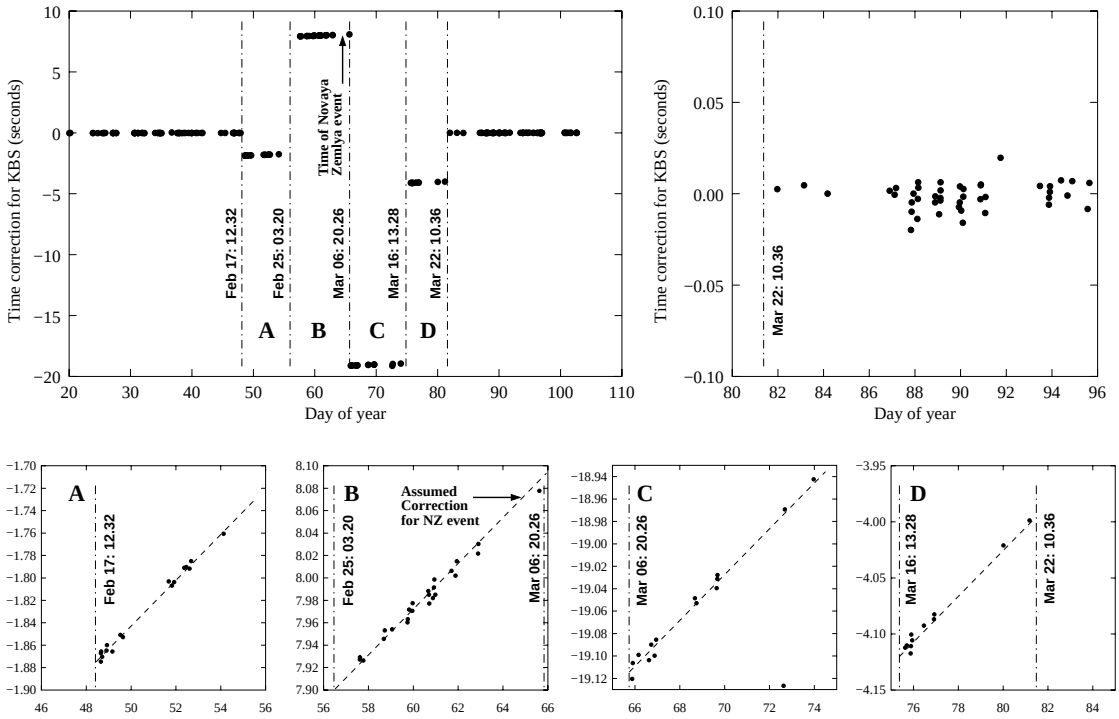

Fig. 6.4.9. The largest panel shows variation of CKBS(t) with time for all Barentsburg events in the interval shown. Each of the vertical dashed lines indicates the time at which a data gap is observed. The remaining panels each show a zoom-in of the indicated time-windows. The four unlabeled plots for windows A, B, C, and D are all drawn to the same scale and the diagonal lines are fitted by eye to the scatter plots and have the same gradient in each panel.

At least five gaps appear in the KBS data stream between February 22 and March 22, 2006. In between each of these discontinuities, the apparent time-stamp on KBS data appears to drift by approximately 0.021 seconds (i.e. slightly less than one sample) per day. Whilst this drift is small, this amounts to 0.2 seconds over 10 days which is measured clearly in these correlation calculations. Whilst scatter is observed in the data due to failings of our identical-event assumption, the uncertainty is far smaller than the uncertainty associated with phase onset time readings.

Whilst it is desirable to simply eliminate such timing errors, the fact is that they do occur and we must become better equipped to detect, identify, document, and (if possible) correct them. With regard to the detection and identification of timing errors, both station operators and observatory analysts have an important role to play. In the example presented here, the station operators were aware that the time-stamp for a given station over a given period could not be relied upon but had no mechanism by which to make current and future users of the data aware of the fact. One solution would of course be to simply cease to archive data which were known to be subject to a time uncertainty. However, waveform data is precious and, once lost, cannot be replaced. It may be possible to calculate a high-level-of-confidence timing correction at a later date (as we have done here) in which case, with careful processing, the data can be used as

if no error existed. It may be deemed impossible to correct for a given timing error. In such a case, we need to accept that the data cannot be used for location purposes (or used to a limited degree only) but we may be able to extract other useful information from the data (for instance spectral properties for source discrimination).

The observatory analyst has a responsibility to react to phase determinations that would appear to preclude a well-determined solution. In the current example, the removal of the KBS station led immediately to dramatically reduced residuals; the temptation in such circumstances is to accept the first solution with small residuals without questioning why the inversion fails with all data present. In the CTBT context, where accurate locations for small seismic events are sought using a fairly sparse global network of 3-component stations and arrays, large residuals (particularly in azimuth) can be observed frequently due to insufficient calibration studies. Location routines generally attempt to minimize some form of residual norm; uncertainties should be weighted appropriately and deviations due to demonstrable and calibrated geophysical anomalies should be corrected for prior to the inversion. An unidentified case of erroneous timing provides an additional deviation which is not corrected for or weighted accordingly in the input, but which may be capitalized on by the inversion routine to produce a plausible but erroneous location estimate. Had the Novaya Zemlya event occurred at a time when the KBS offset was 2 seconds rather than 8 seconds, the erroneous timing could have been completely absorbed by the phase-pick uncertainties in our location estimate. However, the world of earthquake location procedures is changing rapidly as has been reviewed recently by Richards et al. (2006), with highly accurate cross-correlation relative times becoming increasingly important. Never before has it been so important to have complete control on instrumental timing. (A differential traveltime measurement in a double difference location calculation will in general determine the spatial separation of event hypocenters; it is essential to ensure that such measurements are not the result of instrumental anomalies.)

Whilst the rockbursts at the Barentsburg mine are a convenient source of repeating signals for our timing verification, they are by no means unique and there are most likely such sources in the vicinity of many seismic stations. Their identification could provide us with a wide range of means with which to verify or control instrumental timing. There are probably many more on the island of Spitsbergen; they have simply yet to be identified. In situations where seismologists discover sources of repeating seismic signals, I would advocate the documentation and publication of these sources (preferably with reference to specific events and with details about the signal repetition) such that the signals can subsequently be exploited to verify instrumental timing.

The time-stamp on seismograms, once made, is irreversible. It has to be this way since data is downloaded by different users at different times and stored in different formats; the circulation of waveform data with a multitude of different time-stamps would lead to chaos. I would like to throw down the gauntlet to the seismological community to reach a consensus on a standardized information center for seismic stations. My suggestion would comprise a single website with an information retrieval page whereby a user would input a station name and a UTC epoch time and could expect to receive a status report for the specified channel at that time. Such a report could contain the information “status not known”, “station not in operation”, “timing certified OK”, “questionable time stamp”, or “8.0674 seconds to be added to time-stamp to provide true UTC”. It would provide the necessary mechanism for station operators to provide information of known uncertainties and for analysts to raise questions of data authenticity. The single site would be preferable since an institute-based system would be de facto

very heterogeneous and seismologists often have many different sources of the same seismic data. It would remain to be seen how such a project would be administrated or financed. Is there a need for such an information repository?

6.4.6 Acknowledgements

NORSAR obtains data from the KBS station via GEOFON at GeoForschungsZentrum, Potsdam, Germany and gratefully acknowledges the GEOFON Program of GFZ Potsdam.

I would like to thank Dr. Winfried Hanka at GFZ Potsdam for providing me with status reports on the KBS station during this period and for confirming the time when the station was repaired. I am also grateful to Dr. Johannes Schweitzer for useful discussions.

Maps were created using GMT software (Wessel and Smith, 1995).

An edited version of this report has been accepted for publication in Seismological Research Letters.

S. J. Gibbons

References

Baumgardt, D. R. (2001). Sedimentary Basins and the Blockage of Lg Wave Propagation in the Continents, *Pure Appl. Geophys.*, **158**, 1207-1250.

Bowers, D. (2002). Was the 16 August 1997 Seismic Disturbance near Novaya Zemlya an Earthquake?, *Bull. Seism. Soc. Am.*, **92**, 2400-2409.

Bowers, D., Marshall, P. D. and Douglas, A. (2001). The level of deterrence provided by data from the SPITS seismometer array to possible violations of the Comprehensive Test Ban in the Novaya Zemlya region, *Geophys. J. Int.*, **146**, 425-438.

Gibbons, S. J., Bøttger-Sørensen, M., Harris, D. B. and Ringdal F. (2006). The detection and location of low magnitude earthquakes in Northern Norway using multi-channel waveform correlation. *Manuscript submitted to Phys. Earth Planet. Inter. Under review.*

Gibbons, S. J., Kværna, T. and Ringdal, F. (2005). Monitoring of seismic events from a specific source region using a single regional array: a case study. *J. Seismol.*, **9**, 277-294.

Gibbons, S. J. and Ringdal, F. (2005). "The detection of rockbursts at the Barentsburg coal mine, Spitsbergen, using waveform correlation on SPITS array data", In *NORSAR Scientific Report: Semiannual Technical Summary No. 1 - 2005*. NORSAR, Kjeller, Norway. 35-48.

Gibbons, S. J. and Ringdal, F. (2006). The detection of low magnitude seismic events using array-based waveform correlation, *Geophys. J. Int.*, **165**, 149-166.

Hartse, H. (1998). The 16 August 1997 Novaya Zemlya Seismic Event as Viewed From GSN Stations KEV and KBS, *Seism. Res. Lett.*, **69**, 206-215.

Hicks, E. C., Kværna, T., Mykkeltveit, S., Schweitzer, J. and Ringdal, F. (2004). Travel-times and Attenuation Relations for Regional Phases in the Barents Sea Region, *Pure Appl. Geophys.*, **161**, 1-19.

Kennett, B. L. N. (2002). The Seismic Wavefield. Volume II: Interpretations of Seismograms on Regional and Global Scales, Cambridge University Press, Cambridge, United Kingdom.

Koch, K. and Stammler, K. (2003). Detection and Elimination of Time Synchronization Problems for the GERESS Array by Correlating Microseismic Noise, *Seism. Res. Lett.*, **74**, 803-816.

Kremenetskaya, E., Baranov, S., Filatov, F., Asming, V. E., and Ringdal, F. (2001). "Study of seismic activity near the Barentsburg mine (Spitsbergen)", In *NORSAR Scientific Report: Semiannual Technical Summary No. 1 - 2001*. NORSAR, Kjeller, Norway. 114-121.

Richards, P. G. and Kim, W. Y. (1997). Testing the nuclear test-ban treaty, *Nature*, **389**, 781-782.

Richards, P. G., Waldhauser, F., Schaff, D. and Kim, W.-Y. (2006). The Applicability of Modern Methods of Earthquake Location, *Pure Appl. Geophys.*, **163**, 351-372.

Ringdal, F. (1997). Study of low-magnitude seismic events near the Novaya Zemlya nuclear test site, *Bull. Seism. Soc. Am.*, **87**, 1563-1575.

Ringdal, F. and Kværna, T. (1989). A multi-channel processing approach to real time network detection, phase association, and threshold monitoring, *Bull. Seism. Soc. Am.*, **79**, 1927-1940.

Schweitzer, J. (2001a). HYPOSAT - An enhanced routine to locate seismic events, *Pure Appl. Geophys.*, **158**, 277-289.

Schweitzer, J. (2001b). Slowness Corrections - One Way to Improve IDC Products, *Pure Appl. Geophys.*, **158**, 375-396.

VanDecar, J. C. and Crosson, R. S. (1990). Determination of teleseismic relative phase arrival times using multi-channel cross-correlation and least squares, *Bull. Seism. Soc. Am.*, **80**, 150-169.

Wessel, P. and Smith, W. H. F. (1995). New version of the Generic Mapping Tools, *EOS Trans. Am. Geophys. Union*, **76**, 329.